CONSTRUCTION OF RECOMBINANT HUMAN RHINOVIRUS 85 GENOMES.

By

James David Lees B.Sc.(Hons)

School of Biomedical Sciences

University of St. Andrews.

A thesis submitted in partial fulfillment

of the requirements for the

degree of Master of Philosophy.

January 2002.

DECLARATIONS

I, James David Lees, hereby certify that this thesis, which is approximately 21,000 words in length, has been written by me, that is the record of work carried out by me and that it has not been submitted in any previous application for a higher degree.

Date 11/11/02 Signature of Candidate

I was admitted as a research student in October 2000 and as a candidate for the degree of Master of Philosophy in October 2000; the higher study for which this is a record was carried out in the University of St. Andrews between 2000 and 2002.

Date 11/11/02 Signature of Candidate

I hereby certify that the candidate has fulfilled the conditions of the Resolution and Regulations appropriate for the degree of Master of Philosophy in the University of St. Andrews and that the candidate is qualified to submit this thesis in application for that degree.

Date ..... Signature of Supervisor .....

In submitting this thesis to the University of St. Andrews I understand that I am giving permission for it to be made available for use in accordance with the regulations of the University Library for the time being in force, subject to any copyright vested in the work not being affected thereby. I also understand that the title and abstract will be published, and that a copy of the work may be made and supplied to any *bona fide* library or research worker.

Date 11/11/02 Signature of Candidate

ACKNOWLEDGEMENTS

I would like to thank Dr. Martin Ryan for his excellent supervision and unstinting encouragement throughout the course of this degree.

Thanks also go to my friend and lab mate Dr. Garry Luke, whose excellent advice in the lab coupled with his down-to-earth sense of humor helped smooth out many of the bumps along the way.

Finally and most importantly, I wish to thank my mother and father, without whose unwavering support this degree would never have reached completion.

ABSTRACT

The intention of this project was to generate and characterize specific plasmid constructs and recombinant Human Rhinovirus 85 (HRV85) genomes in order to facilitate a study which would enhance the current state of knowledge regarding the replicative, translational and encapsidation properties of the virus. To this end, four plasmid constructs were produced, i.e.; pJL3, pJMP1del, pHRV85-T7, and pHRV85R.

Plasmid pJL3 consisted of the gene encoding T7 RNA polymerase (T7 RNA POL) fused, to the 5′ terminus of cDNA sequences encoding the 2A region of HRV85. The plasmid was designed to examine whether (and if so, to what level) the self-processing capabilities of HRV85-2A protease ($2A^{pro}$) might be retained when coupled to the T7 RNA POL gene sequences as a substitute for the P1 capsid coding region of HRV85 as in the *wt* virus. It was found that $2A^{pro}$ retained it's ability to cleave at it's own N-terminus, however, the cleavage efficiency witnessed was found to be at a much lower level than that seen in wild type HRV85.

One possible explanation for the reduced cleavage efficiency of $2A^{pro}$ when used in *in vitro* transcription/translation systems, is that the chelating agent EGTA (Ethylene glycol-bis (β-aminoethyl ether) N,N,N',N',- Tetraacetic acid), used to remove excess calcium ions from the coupled systems, will also deplete the level of zinc ions present (pers. Comm. L. Sheppeard, Sigma-Aldrich). This is detrimental to $2A^{pro}$ function, as correct folding of $2A^{pro}$ is dependent upon a single zinc ion within the $2A^{pro}$ structure (Sommergruber *et al.*, 1994b; Voss *et al.*, 1995).

In plasmid pJMP1del, the entire P1 capsid-coding region of HRV85 was deleted in order to produce a construct which would define whether replication competency is dependent upon these sequences.

Analogous to pJMP1del, the P1 capsid-coding region of HRV85 was deleted from recombinant plasmid pHRV85-T7, however, in pHRV85-T7 the P1 sequences were exchanged for those encoding the T7 RNA POL. The main objective for this construct was to characterize the expression levels of T7 RNA POL when directed by the HRV85 genome.

Plasmid pHRV85R consists of a moderately truncated cDNA form of the HRV85 genome, which, following transfection, could not give rise to any RNA replication. This was achieved by the deletion of 669 nucleotides which comprised; most of the 5′ NCR, and also sequences encoding the N-terminal region of P1. pHRV85R was created to serve as a negative control for the nucleic acid hybridization analysis of RNA replication since an HRV85 specific probe would hybridize to the input cDNA/RNA transcripts in the absence of any RNA replication.

Of special relevance to the study of plasmids pHRV85-T7 and pJMP1del was the precise location within the HRV85 genome of the *cis*-acting replication element (CRE). This stable stem-loop secondary structure is essential to replication, and therefore, if found to reside within the P1 capsid-coding region HRV85, clearly, neither pHRV85-T7 (P1 sequences replaced by gene for T7 RNA POL), nor pJMP1del (P1 sequences deleted) would retain replication competency. In this eventuality however, it is acceptable to presume that the HRV85 CRE could be mapped by systematic reinsertion of a series of P1 sequences into pJMP1del. Once located, the sequences containing the CRE could be specifically incorporated to return replication competency to the modified genomes.

CONTENTS

LIST OF FIGURES

LIST OF TABLES

ABBREVIATIONS

αα	Amino acid
ACTH	Adrenocorticotropic hormone
AFGP	Antifreeze glycoproteins
AIDS	Acquired immune deficiency syndrome
ATP	Adenosine triphosphate
BA	6-benzylaminopurine
BFP	Blue fluorescent protein
BSA	Bovine serum albumin
C	Carboxy
CBC	Cap-binding complex
CaMV	*Cauliflower mosaic virus*
CAT	Chloramphenicol acetyl transferase
cDNA	Complementary deoxyribonucleic acid
CMPV	*Cowpea mosaic virus*
CRE	*cis*-acting replication element
CREB	cAMP-responsive element binding protein
dH_20	Distilled water
DMSO	Dimethyl sulphoxide
dNTP	Deoxynucleotide triphosphate
dsRNA	Double-stranded ribonucleic acid
eBFP	Enhanced blue fluorescent protein
E. Coli	*Escherichia coli*
EDTA	Disodium ethylenediaminetetra acetate
EGFP	Enhanced green fluorescent protein
EGTA	Ethylene glycol-bis(β-aminoethyl ether) N,N,N',N', tetraacetic acid
eIF	Eukaryotic initiation factor
EMCV	*Encephalomyocarditis virus*
ERAV	*Equine rhinitis A virus*

ERBV	*Equine rhinitis B virus*
ERV	*Equine rhinovirus*
FMDV	*Foot-and-mouth disease virus*
GAG	Group-specific antigen
GDP	Guanosine diphosphate
GFP	Green fluorescent protein
GTP	Guanosine triphosphate
GUS	β-glucuronidase
HAV	*Hepatitis A virus*
HCV	*Hepatitis C virus*
HpeV	*Human parechovirus*
HRP	*Horseradish peroxidase*
HRV	*Human rhinovirus*
HIV	*Human immunodeficiency virus*
HSV	*Herpes simplex virus*
ICAM-1	Intercellular adhesion molecule-1
IL-12	Interleukin-12
IPTG	Isopropylthio-β-D-galactoside
IRES	Internal ribosome entry site
kb	kilobase
kDa	Kilo daltons
LB	Luria-Bertani medium
LDLR	Low-density lipoprotein receptor
LMP	Low melting point
MCS	Multiple cloning site
MLV	*Murine leukaemia virus*
mRNA	Messenger ribonucleic acid
N	Amino
NCR	Non-coding region
OL-PCR	Overlap-polymerase chain reaction
ORF	Open reading frame

PAGE	Polyacrylamide gel electrophoresis
PBS	Phosphate buffered saline
PCR	Polymerase chain reaction
POL	Polymerase
PV	*Poliovirus*
PVR	*Poliovirus* receptor
RNA	Ribonucleic acid
rRNA	Ribosomal ribonucleic acid
RRL	Rabbit reticulocyte lysate
SDS	Sodium dodecyl sulphate
SGPB	*Streptomyces griseus* proteinase B
ssRNA	Single-stranded ribonucleic acid
TAE	Tris-acetate/EDTA electrophoresis buffer
Taq POL	*Thermus aquaticus* polymerase
TE	Tris-EDTA buffer
TEMED	N,N,N',N'-tetramethylenediamine
TEV	*Tobacco etch virus*
TMEV	*Theiler's murine encephalomyelitis*
TnT	Transcription and Translation
TRIS	2-amino-2-(hyroxymethyl) propan-1,3-diol
tRNA	Transfer ribonucleic acid
UTR	Untranslated region
UMP	Uridine monophosphate
UV	Utraviolet
VPg	Genome-linked viral protein
vRNA	Viral ribonucleic acid
WGE	Wheatgerm Extract
wt	Wild-type
X-GAL	5-Bromo-4-Chloro-3-Indolyl-β-D-Galactoside

Abbreviations for amino acids

Alanine	Ala	**A**
Arginine	Arg	**R**
Asparagine	Asn	**N**
Aspartic acid	Asp	**D**
Cysteine	Cys	**C**
Glutamine	Glu	**Q**
Glutamic acid	Glu	**E**
Glycine	Gly	**G**
Histidine	His	**H**
Isoleucine	Ile	**I**
Leucine	Leu	**L**
Lysine	Lys	**K**
Methionine	Met	**M**
Phenylalanine	Phe	**F**
Proline	Pro	**P**
Serine	Ser	**S**
Threonine	Thr	**T**
Tryptophan	Trp	**W**
Tyrosine	Tyr	**Y**
Valine	Val	**V**

1.0. Introduction.

1.1. Picornaviridae - Overview. *Picornaviruses* are among the most diverse and oldest known viruses. There are more than 200 serotypes, with records of disease caused by these pathogens dating back to 1400 B.C. The name, "*Picornavirus*", means, "very small RNA virus", i.e. Pico (Greek = very small) RNA viruses (Melnick, 1974). The most recent revision of virus taxonomy comprises nine genera within the family *Picornaviridae*; *Enterovirus*, *Rhinovirus*, *Hepatovirus*, *Cardiovirus*, *Aphthovirus*, *Parechovirus*, *Erbovirus*, *Kobuvirus* and *Teschovirus*.

Of the above, only *Enteroviruses* and *Rhinoviruses* cause human disease. The *Enteroviruses* can be distinguished from the *Rhinoviruses* by the stability of the capsid at pH 3, the optimum temperature for growth, their mode of transmission and the diseases they cause. Reportedly 111 serotypes of human *Enterovirus* exist, including the *Polio-*, *Coxsackie-* and *Echoviruses*. The capsids of these viruses are very resistant to harsh environmental conditions (e.g. sewerage systems) and the conditions in the gastrointestinal tract, a property which facilitates their transmission by the faecal-oral route. The *Human Rhinoviruses* include at least 100 serotypes and are the major cause of the common cold. They are sensitive to acidic pH and replicate poorly at temperatures above 33°C. This sensitivity usually limits *Rhinoviruses* to causing upper respiratory tract infections (reviewed by Rueckert, 1996).

The *Picornaviral* genome consists of a single-stranded positive sense RNA molecule (Kitamura *et al.*, 1981; Racaniello and Baltimore, 1981), of between 7.2kb (e.g. *Human rhinovirus14* - HRV14) to 8.56kb (e.g. *Foot-and-mouth disease virus* - FMDV). The genomic RNA is infectious (characteristic of all positive sense RNA viruses) since the vRNA can act directly as mRNA to direct the translation of virus proteins. The genomic RNA is 10^6-fold less infectious than the intact particles. The infectivity is increased, however, if the RNA is introduced into cells by transfection. There are non-coding regions (NCRs) of differing length at both the 5′ and 3′ termini of the positive stranded RNA genome. The unusually long 5′ NCR (ranging 600 – 1200 residues across the genera), is important in translation, virulence, and possibly encapsidation (reviewed by Agol, 1991). The much shorter 3′ NCR region (50 – 100 bases) is important in

negative strand synthesis (Pilipenko *et al.*, 1996). The 5′ NCR contains a cloverleaf secondary structure known as the **IRES**, i.e. the **I**nternal **R**ibosome **E**ntry **S**ite (reviewed by Meerovitch and Sonenberg, 1993; Stewart and Semler, 1997) (see below). The rest of the genome encodes a single polyprotein of between 2100 – 2400 amino acids. Both ends of the genome are modified: the 5′ end by covalent attachment of a small protein, **VPg** (3B: ~23 amino acids), the 3′ end by polyadenylation.

Mature viral proteins are derived by progressive, post-translational cleavage of the polyprotein (figure 1.0) (discussed in section 1.5.). A non-cleaved full-length polyprotein is never produced since proteolytic processing events occur when the peptides are still nascent on the ribosomes ('primary' proteolytic cleavages). These cleavages are performed by virus-encoded proteinases that ultimately generate the end products (Palmenberg, 1987b). Mature proteins and their precursors are subdivided into four groups (**L, P1, P2, P3**) on the basis of structure, enzymatic function, and position of primary cleavages (refer to figure 1.0.). The leader or "L" protein is encoded by sequences in the genomes of *Cardio- and Aphtoviruses.* The P1 peptides are the capsid structural proteins, and the non-structural proteins required for virus replication are provided by the P2 and P3 regions of the polyprotein.

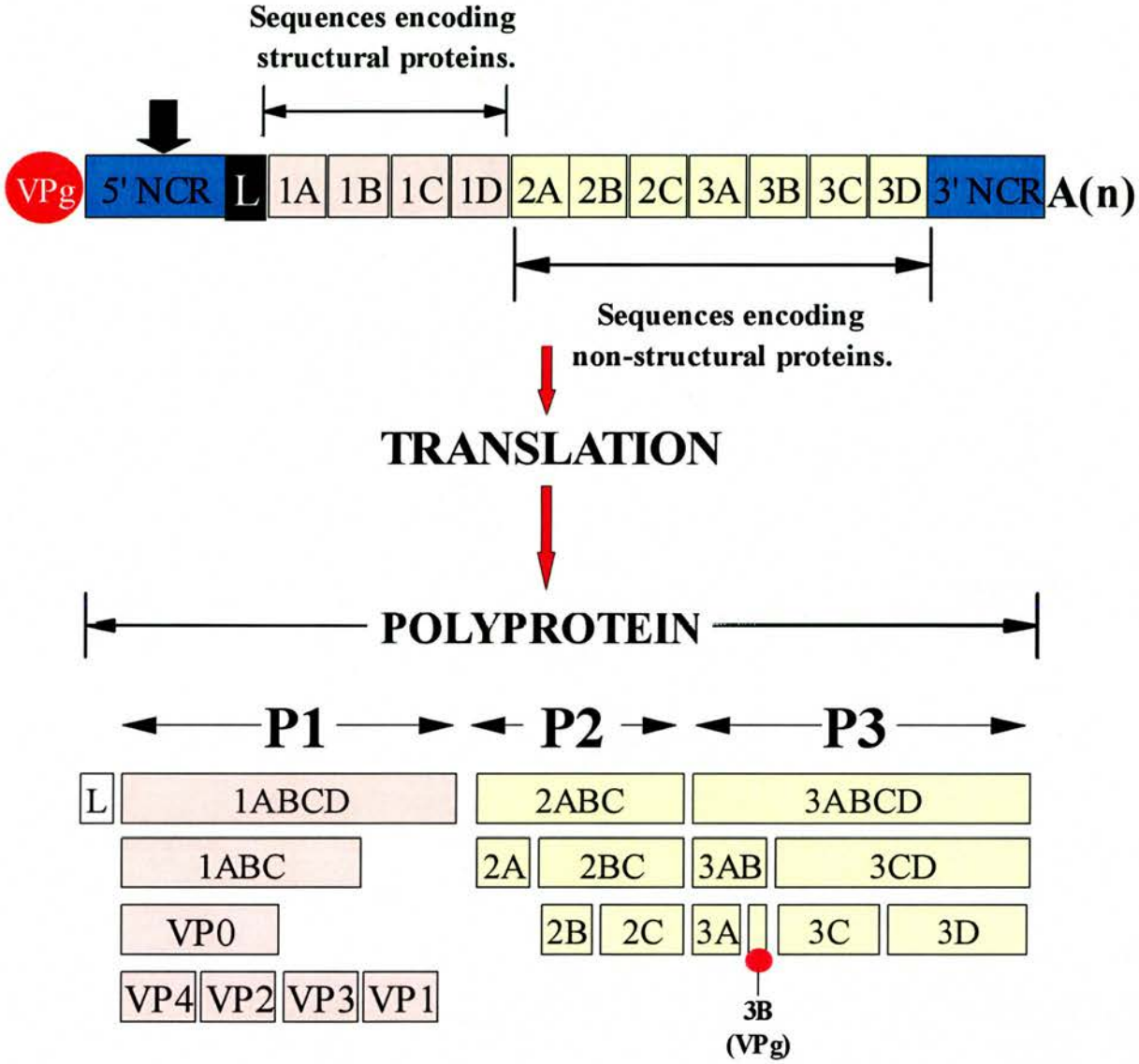

Figure 1.0. *Organization and expression of the Picornaviral RNA genome. The capsid proteins; 1A, 1B, 1C and 1D, are more familiarly identified as viral proteins; VP4, VP2, VP3 and VP1 respectively. The non-structural proteins required for virus growth and replication are supplied by the P2 and P3 regions of the polyprotein. The black arrow over the 5′NCR indicates the presence of the poly(C) tract found in members of the Cardio- and Aphthovirus genera. Members of the Cardio- and Aphthovirus genera also encode a Leader (L) protein at the N-terminus of the polyprotein.*

The specificity of the *Picornavirus* interaction for cellular receptors is a major determinant of their target tissue tropism and disease. The VP1 proteins at the vertices of each of the capsid pentameric units contains 'canyon' or 'pit' structures into which the receptor binds (Hogle *et al.*, 1985; Minor *et al.*, 1986).

Picornaviruses have been categorized into several receptor families. The receptors for *Poliovirus*es and *Rhinoviruses* have been identified as tissue-specific cellular adhesion molecules. These molecules are members of the immunoglobulin superfamily. Their primary function is to promote normal and immunological cell-to-cell interactions. At least 80% of the *Rhinoviruses* and several serotypes of *Coxsackievirus* recognize intercellular adhesion molecule 1 (ICAM-1), which is expressed on epithelial cells, fibroblasts, and endothelial cells (Greve *et al.*, 1989). *Poliovirus* (PV) binds to a molecule of similar structure and presumably similar function. The cell types upon which the *Poliovirus* receptor is expressed does not, however, correlate directly with the limited tissue specificity of the *Poliovirus*es.

The kinetics of *Picornavirus* replication are rapid, the cycle being completed in from 5 – 10 (typically 8) hours. Genomic RNA is translated directly by polysomes, but some 30mins after infection cellular protein synthesis declines sharply, almost to zero, this is called "shut off".

1.2. The 5′and 3′Non-Coding Regions. The protein coding region of the picornaviral genome is flanked on either end by non-coding regions (figure 1.0.) whose sequences tend to be strongly conserved and carry signals initiating translation near the 5′ end, and for initiation of RNA synthesis at the 3′ ends of the plus and minus strands respectively.

1.2.1. The 5′NCR. The 5′ NCR of the RNA is unusually long, in the range of 10% of the total genome length. It ranges in size from 614 bases in HRV14, to nearly 1200 bases in *Aphthoviruses*. *Aphthovirus* and *Encephalomyocarditis virus* RNAs contain a poly(C) tract located in the 5′ NCR upstream from the initiation site for translation (Chumakov and Agol, 1976). The size of the poly(C) tract is homogeneous within a given isolate of virus but varies in length in different virus isolates and so may, therefore, be a useful tool for identifying virus strains.

Already mentioned above, 5′ NCR contains the IRES (see figure 1.1. below for predicted folding patterns), internal ribosome entry site, or 'landing pad'. Cellular mRNA translation is initiated when ribosomes bind to the 5′ methylated cap, then scan along the mRNA to find the first AUG initiation codon. The IRES overcomes this and allows *Picornavirus* RNAs to continue to be translated after degradation of the 220kD component (eIF4G) of the cap-binding-complex (CBC), involved in binding the m^7G cap structure at the 5′ end of all eukaryotic mRNAs during initiation of translation.

1.2.2. The 3′NCR. The 3′ NCR is relatively short, ranging in length from 47 bases for HRV14 to 126 bases for EMC virus. Its function is unknown but may be important at some stage of replication because an 8-base insertion in this region of *Poliovirus* produces a temperature-sensitive phenotype (Sarnow *et al.*, 1986). Located at the 3′ end of the RNA is a poly(A) tract of heterogeneous length, ranging from 35 residues in EMCV (Palmenberg *et al.*, 1984) to 100 residues in *Aphthoviruses* (Carroll *et al.*, 1984). This heterogeneity is not eliminated by plaque-purifying virus stocks. However, the mean length of the heterogeneous tract is genetically determined (Yogo *et al.*, 1974). Picornaviral genomes do not possess a polyadenylation signal - which would specify a post-transcriptional addition of adenosyl residues to the 3′ NCR (Porter *et al.*, 1978). Instead, the poly(A) tract is believed to be transcribed from poly(U) sequences on the 5′ ends of negative RNA strands during replication (Spector and Baltimore, 1975b; Yogo *et al.*, 1974; Yogo and Wimmer, 1975). The poly(A) tract is proposed to be a requirement for virus infectivity, with RNA molecules containing short poly(A) tracts exhibiting lower specific infectivity (Sarnow, 1989; Spector and Baltimore, 1979).

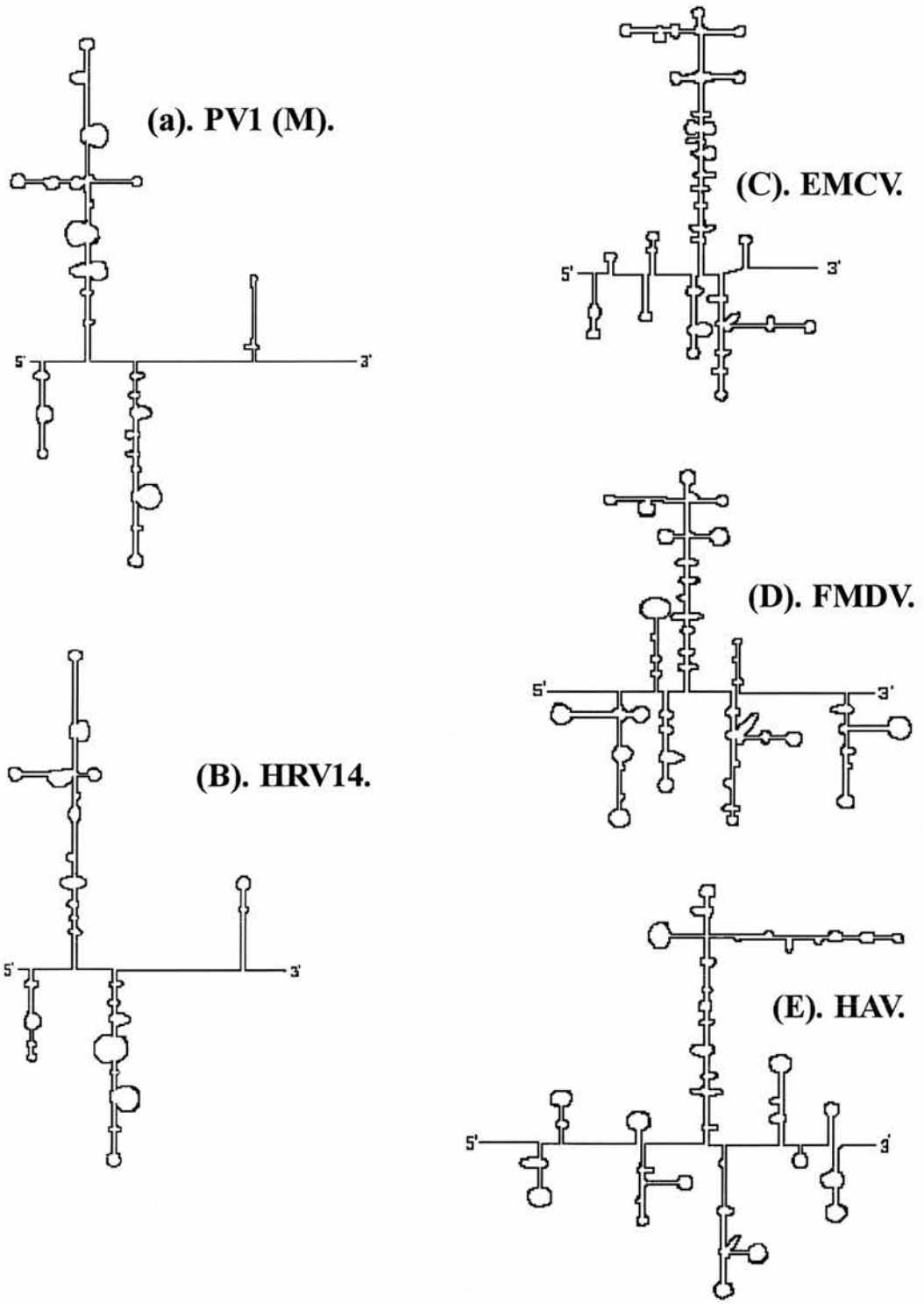

Figure 1.1. *Computer analysis, supported by site directed mutagenesis and enzymatic analysis, predicts the IRES folding patterns of: (a). Poliovirus type-1 (Skinner et al., 1989), (b). Human rhinovirus 14, (c). Encephalomyocarditis virus, (d). Foot-and-mouth disease virus and (e). Hepatitis A virus (Pilipenko et al., 1989).*

1.3. Structural Proteins.

1.3.1. Structure of the Virus Particles. The capsids consist of a densely packed icosahedral arrangement of sixty protomers (see figure 1.2.), each consisting of four polypeptides;. VP1 (1D), VP2 (1B), VP3 (1C), and VP4 (1A), all derived from the P1 precursor protein (figure 1.0.), with (pseudo) T=3 packing. The particle (figure 1.2.) is 27-30nm in diameter, while the length of the genome is ~ 2500nm. The genome is tightly packed into the capsid, together with sodium or potassium ions, or polyamines (in *Rhinoviruses*) to counteract the negative (-ve) charges on the phosphate groups of the viral RNA. There is great variety in the surface topography of different *Picornavirus* serotypes, i.e. human *Rhinoviruses* and *Enteroviruses* feature prominent canyons at the center of each pentameric unit in the shell, while *Cardiovirus*es and *Aphthoviruses* lack these canyons (Rossmann *et al.*, 1985).

It was proposed that the prominent cleft in the protomer of HRV14 might be a receptor binding site on the grounds that the canyon is too narrow (1.2-3.0 nm wide) to admit deep penetration of antibody molecules (Rossmann *et al.*, 1985; Rueckert *et al.*, 1986). The notion that this offers an advantage to the virus by permitting it to conserve its crucial cell attachment site in the face of antibody driven evolution, is supported by evidence that binding affinity to isolated cellular receptors can be changed by site-directed alteration of amino acid residues in the canyon floor (Colonno *et al.*, 1988) and by demonstration that drugs which selectively alter the topography of the canyon floor, also block attachment of HRV14 to HeLa cells (Heinz *et al.*, 1989) and to isolated receptors (Pevear *et al.*, 1989). That the receptor binding site is indeed located deep in the canyon, has now been confirmed by direct visualization, using image reconstruction of a complex between HRV16 and a soluble portion of ICAM-1 (Olson *et al.*, 1993).

The study of *Picornavirus* structures at the atomic level has provided an insight into many features relevant to icosahedral RNA viruses including surface architecture, virus antigenicity, determinants of virus host range and tissue tropism, and the role of surface conformational changes in virus assembly and uncoating.

X-ray crystalographic studies have revealed that capsid proteins of *Picornaviruses* possess a structural motif designated the RNA virus capsid (RVC) core (reviewed by

Rossmann and Johnson, 1989). This core is composed of an eight-stranded anti-parallel β-barrel which overall takes the shape of a triangular wedge, packing neatly into the icosahedral lattice of the viral capsid. The eight β-strands, labeled A-H, are connected by short loops which vary in both size and composition between viruses. Variations in the loops and termini confer each virus with distinctive morphology and antigenicity. For example, the FMDV genome encodes VP1 and VP2 proteins which are much shorter in relation to those of other *Picornaviruses* (Carroll *et al.*, 1984). However, it has been shown that these truncations do not affect the protein core structure, but mainly result in shortening of the loops joining the β-strands (Acharya *et al.*, 1989).

The conformations assumed by picornaviral capsid proteins during assembly and maturation of the virion provide a unique surface architecture through which the virus interacts with its environment. The determination of three-dimensional structures of *Picornaviruses* at the atomic level (see above) has demonstrated characteristic structural motifs which are accessible to the host immune system, and which are located predominantly on exposed loops and protrusions on the capsid surface. The antigenic determinants of *Picornaviruses* have been characterized using a wide variety of techniques (for reviews see; Minor, 1990; Usherwood and Nash, 1995).

HRV14 and PV are similar in that they have three major antigenic sites labeled NIm-I, -II, and –III on HRV14 and sites 1, 2, and 3 on PV. These antigenic sites are in similar positions on both viruses. NIm-I on HRV14 and site 1 on PV, are formed by residues from loops on the capsid protein VP1 (Blondel *et al.*, 1986; Evans *et al.*, 1983; Minor *et al.*, 1983; Rossmann *et al.*, 1985; Sherry *et al.*, 1986; Wiegers *et al.*, 1988). However, on HRV14 this site consists of two independent sites located a short distance apart on the virion surface, labeled NIm-Ia and NIm-Ib (Rossmann *et al.*, 1985; Sherry *et al.*, 1986). Residues from both VP1 and VP2 contribute to the second site NIm-II and site 2 (Diamond *et al.*, 1985; Minor *et al.*, 1986; Page *et al.*, 1988; Rossmann *et al.*, 1985; Sherry *et al.*, 1986; Wiegers *et al.*, 1990). Included in the site are residues from the VP2 "puff" in the E-F loop which projects from the two-fold axis of the capsid surface. The third antigenic site on both HRV14 (Rossmann *et al.*, 1985; Sherry *et al.*, 1986; Sherry and Rueckert, 1985) and PV (Diamond *et al.*, 1985; Minor *et al.*, 1986; Page *et al.*, 1988; Wiegers *et al.*, 1988; Wiegers and Dernick, 1992) are complex. NIm-III on HRV14

consists of residues from both VP3 and VP1, as is the situation observed for site 3 on PV type 3. This site on other PV serotypes comprises the same region of VP3, however, other residues are contributed by VP2. On PV type 1, site 3 consists of two independent sites designated 3a and 3b, which are situated close together on the capsid surface. A prominent feature located within site 3 of PV, is the VP3 "knob" exposed at the three-fold axis (Minor *et al.*, 1985; Patel *et al.*, 1993). Although all three serotypes of PV have comparable antigenic structures, paradoxically, the neutralizing antigenic site 1 in serotypes 2 and 3 is immunodominant (Minor *et al.*, 1985; 1986; Patel *et al.*, 1993), whereas, sites 2 and 3 are dominant in serotype 1 (Page *et al.*, 1988).

The generation of antibodies to internal epitopes of VP4 and VP1 proteins of PV, surprisingly resulted in neutralization of virus infectivity (Li *et al.*, 1994). The observed neutralization was thought to occur as a result of reversible exposure of these sequences at physiological temperatures, which temporarily exposed these regions, thereby enabling antibody binding to take place. Such results demonstrate that structures of viruses determined at the atomic level display surface proteins in a fixed configuration, and that as a result of environmental changes which occur during virus infection, the configuration of viral epitopes may also change.

1.3.2. Myristoylation of VP4. Myristic acid, also known as *n*-tetradecanoic acid, is covalently linked to N-terminal glycine residues on VP4, VP0 and P1 of most *Picornaviruses* (Chow *et al.*, 1987). The sequence; GXXXS/T (where X is any αα) has been suggested as the consensus sequence for myristoylation (Chow *et al.*, 1987; Palmenberg, 1989).

This modification by myristoylation is co-translational and is carried out by a host cell N-myristyltransferase (Tower *et al.*, 1988). Myristoylation has been implicated in several stages of picornaviral assembly. Examination of mutants deficient in myristoylation have indicated that the myristate moiety is required for the stable assembly of pentamers in PV (Ansardi *et al.*, 1992; Moscufo and Chow, 1992). The determination of the three-dimensional structures of PV serotypes have revealed that the myristic acid groups cluster on the interior of the virion near the base of the five-fold axes.

Located directly above the myristic acid groups is the β-annulus structure formed by the N-terminal extensions of VP3 allowing association between the two (Filman *et al.*, 1989; Hogle *et al.*, 1985; Lentz *et al.*, 1997). A carboxylate oxygen of the myristic acid moiety has been shown to hydrogen bond to the side chain oxygen of the threonine residue at VP4 position 28 (PV numbering) from an adjacent five-fold related protomer (Lentz *et al.*, 1987). This interaction has been seen in a number of *Picornavirus* structures, and mutagenesis studies have suggested that this threonine residue plays an important role in PV assembly and infectivity (Moscufo and Chow, 1992). Other studies have also shown the myristoylation of VP0 to be essential for virus infectivity (Krausslich *et al.*, 1990; Marc *et al.*, 1989; 1990;1991). Mutant viruses which contained altered myristoylation signals at the N-terminus of VP4 could undergo one round of replication in transfected cells, but could not produce infectious virus particles. Mutants of PV which contained alterations of the alanine residue at VP4 position 2, were shown to exhibit normal levels of myristoylation, but decreased levels of infectivity (Moscufo *et al.*, 1991). These results suggested that both the myristoylation signal and the amino terminus of VP4, play a role in virus infectivity, perhaps at the stage of uncoating. Myristoylation is essential in both virus assembly and infectivity, however, the manner in which it functions remains uncertain.

1.3.3. Maturation cleavage. The final cleavage event of picornaviral polyprotein processing, i.e. the cleavage of VP0 to VP4 and VP2, is required for the production of infectious particles. The maturation cleavage is not catalyzed by any of the viral proteolytic activities yet identified and is considered to be a self-cleaving process. Cleavage occurs upon encapsidation of RNA during the final stages of virion morphogenisis at an N-S dipeptide and occurs within all 60 subunits simultaneously. Production of 1A and 1B is believed to stabilize the capsid structure.

One proposed mechanism (although unsubstantiated experimentally) is that a serine residue of 1B and aspartate and asparagine residues located nearby, form an analogous conformation to a serine protease active site with the proton-accepting role of the catalytic histidine fulfilled by the viral RNA (Fout *et al.*, 1984). *In vitro* experiments to test this theory were undertaken by Arnold *et al.* (1987). The potential involvement of

viral RNA as the proton-abstracting component in the cleavage reaction was upheld as it was found that the addition of diamino compounds resulted in VP0 cleavage.

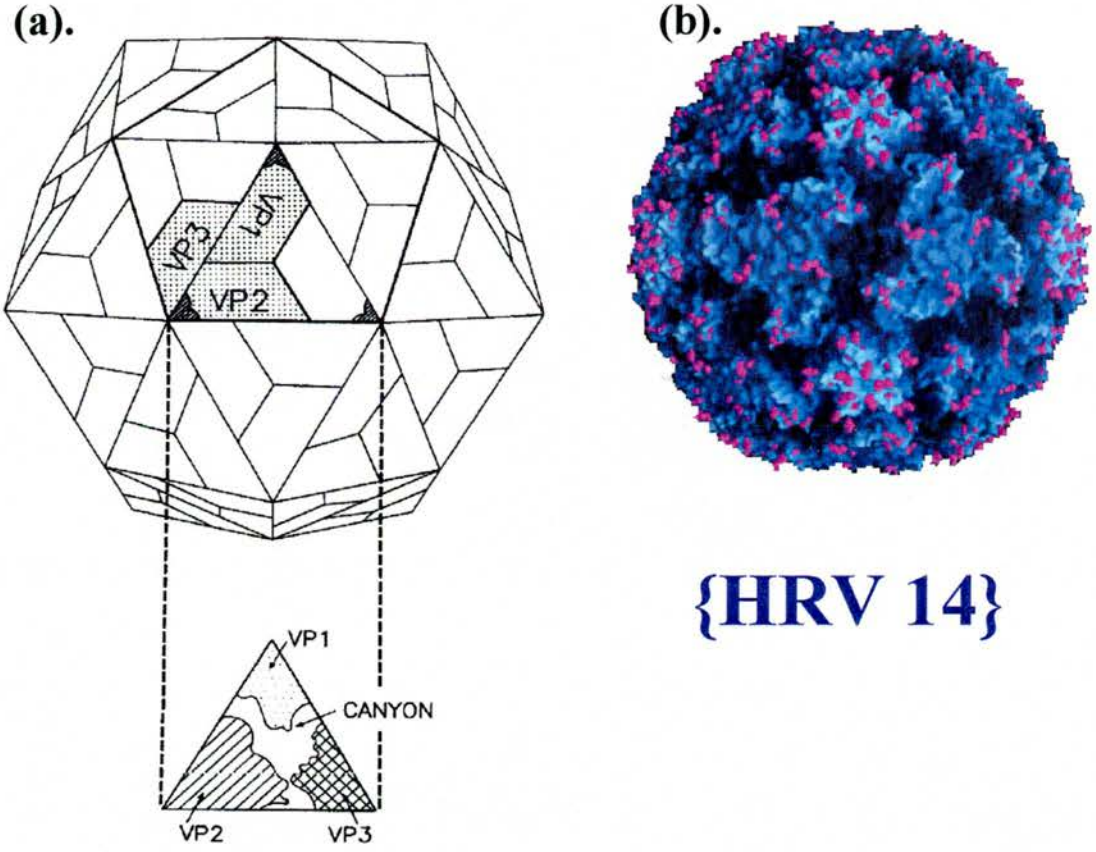

Figure 1.2. *(a). Pseudoequivalent packing arrangement of VP1, VP2, and VP3 domains in the 60-subunit picornaviral shell. Each of the three proteins has a similar folding pattern. Hatched arrowheads locate a "prow", which enables each protein to pack tightly at the three- or fivefold symmetry axes. VP4 is buried deep inside the particle at the base of the protomer and is not an integral component of the framework making up the shell. (b). Atomic structure of Human rhinovirus 14 showing the location of the antigenic sites (pink).*

1.4. Non-structural Proteins.

1.4.1. The Leader (L) Protein. The L protein is a non-structural protein positioned at the 5′ end of the ORF (see Fig. 1.0.) and is a specific feature of the *Cardio-* and *Aphthovirus* genomes (Kazachkov *et al.*, 1982; Forss *et al.*, 1984). An L protein has also been reported in the genome of *Equine rhinovirus-2* (now *Equine rhinitis B virus* (ERBV); (Li *et al.*, 1996; Wutz *et al.*, 1996). However, the structure and function of this protein varies between these genera.

The FMDV L protein was suggested to belong to the papain family of cysteine proteinases by sequence similarity (Gorbalenya *et al.*, 1991), inhibitor studies (Kleina and Grubman, 1992) and site directed mutagenesis (Piccone *et al.*, 1995b; Roberts and Belsham, 1995; reviewed by Ryan and Flint, 1997). A conserved cysteine-tryptophan amino acid pair, and a histidine residue are essential for L proteinase activity in FMDV (Gorbalenya *et al.*, 1991; Piccone *et al.*, 1995b; Roberts and Belsham, 1995). These residues are also conserved within the sequences of the L proteins of ERAV and ERBV which are similar in both length and sequence to that of FMDV (Li *et al.*, 1996; Wutz *et al.*, 1996) suggesting that these L proteins also possess proteolytic activity. Structural analysis of the L proteinases of both *Equine rhinitis A virus* (ERAV) and FMDV have suggested that they have a similar overall fold to that of papain (Skern *et al.*, 1998). This was further confirmed when the crystal structure of the L proteinase of FMDV was obtained (Guarnne *et al.*, 1998).

Piccone *et al.*, (1995a) demonstrated, through the use of genetically engineered viruses, that the L gene is apparently not required for the growth of FMDV in tissue culture. This proposal was further supported upon the generation and successful amplification of defective interfering (DI) particles of FMDV deleted in the L proteinase gene during long term passage in tissue culture (Charpentier *et al.*, 1996). However, analysis of FMDV lacking the L gene *in vivo* revealed that the L gene deficient virus was avirulent relative to the wild-type (wt) virus (Brown *et al.*, 1996).

The FMDV L gene contains two potential in-frame initiation codons located 84 nts apart, which define proteins defined as Lab and Lb (Clarke *et al.*, 1985). This has been shown for all seven serotypes of FMDV (Sangar *et al.*, 1987). Although the first

AUG, the initiating codon of Lab, is not always in the optimal context for efficient initiation of translation (Kozak, 1986), both forms of the L protein can be detected both in *in vitro* translation studies, and in infected cells (Clarke *et al.*, 1985; Sangar *et al.*, 1987) and have been shown to be capable of proteinase activity (Cao *et al.*, 1995; Medina *et al.*, 1993). Like FMDV, the ERAV L protein has two potential initiation codons suggesting that a second species of L protein may also exist in this virus (Li *et al.*, 1996; Wutz *et al.*, 1996).

In contrast, the L protein encoded by the *Cardiovirus*es does not have any known proteinase function. The L protein of *Theiler's murine encephalomyelitis virus* (TMEV) has been shown to be a zinc-binding protein containing a putative zinc-binding motif conserved among the *Cardiovirus* genus (Chen *et al.*, 1995; Kong *et al.*, 1994). Removal of the L gene from the genome of TMEV has resulted in viruses with altered host ranges in cell culture (Calenoff *et al.*, 1995; Kong *et al.*, 1994) and attenuated virulence in mice (Calenoff *et al.*, 1995). Mutations introduced into the L gene of *Mengovirus* have also suggested an involvement in inhibition of host cellular protein synthesis (Zoll *et al.*, 1996), however, the method by which this occurs remains unknown.

1.4.2. The 2A Protein. The 2A protein of *Picornaviruses* differs greatly in sequence and composition across the genera (Ryan and Flint, 1997). The 2A protein ($2A^{pro}$) in members of the *Entero-* and *Rhinovirus* genera (approx. 17kD) is a cysteine proteinase which contains an active site thiol group, but exhibits significant sequence identity to the trypsin-like small serine proteases (Bazan and Fletterick, 1988; 1989; Dougherty and Semler, 1993). Sequence comparisons suggested a catalytic triad consisting of (PV numbering) His-20, Asp-8 and an active site nucleophile Cys-109 in place of a serine residue (Bazan and Fletterick, 1988) which were subsequently confirmed by site directed mutagenesis studies (Hellen *et al.*, 1991; Sommergruber *et al.*, 1989; Yu and Lloyd, 1991; 1992). The $2A^{pro}$ in these viruses plays an important role in proteolytic processing of the virus genome (figure 1.0.), and have been shown to have a role in 'shut off' of host cellular protein synthesis.

In contrast, the cardio and *Aphthoviruses* do not encode a 2A proteinase like those of the *Entero-* and *Rhinoviruses*. In *Aphthoviruses*, the 2A protein exhibits high sequence

conservation across the genus. In FMDV this small protein was generally accepted to be 16 amino acids long due to results obtained from C-terminal degradation of the capsid protein VP1 (Bachrach *et al.*, 1973; Kurtz *et al.*, 1981) and N-terminal sequencing of the 2B protein (Robertson *et al.*, 1985). However the presence of an amino acid pair Q/X, a potential $3C^{pro}$ cleavage site, located two residues upstream from the generally accepted VP1/2A junction in all FMDV serotypes sequenced to date has lead to speculation whether this is actually the case (Donnelly *et al.*, 1997). Cleavage at this Q/X junction would increase the length of the length of the 2A protein to 18 amino acids. The *Cardiovirus* 2A protein (~15kDa) is comparable in size to those of the entero and *Rhinoviruses*, however sequence similarity is not observed.

Across this genus, only the C-terminal region of the 2A protein is highly conserved and exhibits a high degree of sequence identity with the 2A protein of members of the *Aphthovirus* genus. The 2A/2B cleavage site (-NPG ⇓ P-) is completely conserved across both genera. The C-terminal region of the *Cardiovirus* 2A is also involved in the primary cleavage event of the polyprotein which occurs at the 2A/2B junction (Batson and Rundell, 1991; Donnelly *et al.*, 1997; Hahn and Palmenberg, 1996; Donnelly *et al.*, 2001a, b).

The exact function of the *Cardiovirus* 2A protein remains to be elucidated. Recent mutational analysis of this protein in *Mengovirus* suggested that, unlike those of the entero and *Rhinoviruses*, *Mengovirus* 2A is not involved in shut-off of host cellular protein synthesis but may play a functional role in either virus translation or replication (Zoll *et al.*, 1998). Shut-off appears to be due to cleavage of the CBC. This cleavage is carried out by the viral protease $2A^{pro}$.

1.4.3. The 2B and 2C proteins. The 2B and 2C proteins are located within the P2 non-structural region of the *Picornavirus* polyprotein. Proteolytic processing of this region yields either 2B and 2C or precursor protein 2BC. The 2C protein has been associated with a number of functions. It has been shown to possess ATPase and GTPase activities, demonstrating that this protein is a phosphatase with an affinity for nucleic acids. In *Poliovirus* this protein has been shown to have a role in RNA binding involving two regions of the protein (Rodriguez and Carrasco, 1995). The proteins 2B and 2C, and the

precursor protein 2BC, have been largely implicated in viral replication (Aldabe *et al.*, 1996; Doedens and Kirkegaard, 1995; Van Kuppeveld *et al.*, 1997a, b). However, these proteins also have been suggested to have roles in RNA encapsidation and virus release.

1.4.4. The 3A Protein. The 3A protein is located at the N-terminus of the P3 non-structural region of the polyprotein (Figure 1.0.). The C-terminal 22 amino acids of the *Poliovirus* 3A protein constitutes a hydrophobic domain and it is postulated that it is through this region that the 3AB precursor protein is anchored on cytoplasmic smooth membranes where active RNA replication occurs (Lama and Carrasco, 1995; Semler *et al.*, 1982). This hydrophobic domain is highly conserved across closely related *Picornaviruses* such as the *Poliovirus* serotypes, the *Coxsackieviruses* and *Human Rhinoviruses* (Giachetti and Semler, 1990). Both 3A and 3AB have roles in viral replication.

1.4.5. The 3B protein (VPg). The *Picornavirus* genome, unlike conventional eukaryotic mRNAs, is not capped at its 5′ termini but is covalently linked to a small virus encoded protein, termed **VPg** (Barton and Flanegan, 1997, Lee *et al.*, 1977; Nomoto *et al.*, 1977 a, b) via a O^4-(5′- uridylyl) tyrosine phosphodiester bond (Ambros and Baltimore, 1978; Rothberg *et al.*, 1978) at a tyrosine residue at position 3. This tyrosine residue is conserved across picornaviral VPg proteins sequenced to date. The coding region of VPg, or polypeptide 3B, is located in the P3 non-structural region of the viral genome, and is flanked by genes for polypeptide 3A and the viral proteinase 3C (Figure 1.0.). Genomes of all *Picornaviruses* encode VPg polypeptides, ranging from 20-27 amino acids in length.

1.4.6. The 3C protein. The autocatalytic cleavage of the L proteinase or the release of P1 from the growing peptide chain by the 2A proteinase are only the first steps in *Picornaviral* processing. Most subsequent or secondary cleavages are effected by the viral 3C proteinase ($3C^{pro}$), the central enzyme in the cleavage cascade. $3C^{pro}$ catalyzes a specific and complicated series of monomolecular and bimolecular scissions within its own polyprotein. In FMDV however, at least one secondary cleavage is carried out by

another viral protease, the amino terminal leader (L) protein. The eventual result of the secondary cleavage cascade is release of all mature viral proteins necessary for establishment and completion of a successful infectious cycle.

Sequence alignments have defined two lineages with respect to active site residues in *Picornavirus* $3C^{pro}$ (Ryan and Flint, 1997). Lineage 'A' consists of members of the *Entero-* and *Rhinovirus* genera which contain a glutamate residue at position 71 (PV numbering). Lineage 'B' includes those sequences which contain an aspartate residue at an equivalent position to Glu-71 (PV), and includes members of the *Cardio-*, *Aphtho-*, *Hepato-*, *Parechoviruses* and ERBV.

X-ray crystallographic structures have been resolved for the 3C proteases of HRV14 (Matthews *et al.*, 1994), HRV2 and *Hepatitis A virus* (HAV), (Allaire *et al.*, 1994) which showed a 12-strand β-sheet secondary structure conformation together with a bilobal tertiary structure similar to the trypsin-like serine proteases. These studies confirmed the proposal (based on sequence alignments) that *Picornavirus* 3C proteases represent a novel superfamily of serine-like proteases (Allaire *et al.*, 1994; Bazan and Fletterick, 1988; Gorbalenya *et al.*, 1989; Matthews *et al.*, 1994).

The determination of atomic structures of the 3C proteases have raised questions regarding the catalytic mechanisms surrounding $3C^{pro}$ and its putative active site residues. Analysis of the HAV $3C^{pro}$ structure revealed that Asp-84 (HAV numbering) does not form a member of the catalytic triad (Allaire *et al.*, 1994; Bergmann *et al.*, 1997). Instead the catalytic site was suggested to consist of a diad formed by Cys-172 and His-44. Site directed mutagenesis of proposed HAV $3C^{pro}$ active site residues His-44, Asp-98 and Cys-172 confirmed such predictions (Gosert *et al.*, 1997).

1.4.7. The 3D Protein – an RNA-dependent RNA polymerase. Comparisons of non-structural proteins from different *Picornaviruses* generally show that they are more conserved than the capsid proteins. Of the non-structural proteins, the most conserved is the 3D polymerase protein. The *Picornavirus* 3D polypeptide is approximately 52kDa in size, exhibits RNA-dependent RNA-polymerase activity and is responsible for the synthesis of all viral RNA (Flanegan and Baltimore, 1977; Lindquist *et al.*, 1974). Replication of the picornaviral RNA genome cannot commence until translation of the

$3D^{pol}$ is completed. This enzyme is the template- and primer- dependent RNA polymerase which catalyzes the elongation of nascent RNA strands (Flanegan and Baltimore, 1977; 1979; Lindquist *et al.*, 1994; Van Dyke and Flanegan, 1980). The enzyme $3D^{pol}$ shows little specificity in its ability to discriminate between templates and can copy appropriately primed synthetic, cellular and plant RNAs (Tuschall *et al.*, 1982).

1.5. Polyprotein Processing. As already stated above, the *Picornavirus* is an RNA virus, which expresses its genome by the synthesis and subsequent cleavage of a precursor polyprotein. This stratagem allows the activation of subsets of proteins with different biochemical functions from the same precursor protein. The resulting processing cascade is a tightly controlled pathway. The full-length *Picornavirus* precursor protein is never produced since the initial processing events invariably occur while the peptides are still nascent on the ribosome. Primary processing events within the viral polyprotein are co-translational, intramolecular cleavages. Distinct processing sites and catalytic mechanisms are used by the various genera. The most thoroughly studied reactions are those of the *Poliovirus* (PV) 2A (cleaving the nascent polyprotein at the P1-P2 junction) and 3C proteinases (figs. 1.3. & 1.4. respectively). 'Secondary' processing events are post-translational, intermolecular cleavages, the majority of which are carried out by viral protease $3C^{pro}$.

1.5.1. Entero-, Rhinovirus Primary 1D / 2A Processing. Rapid co-translational scission of the PV polyprotein occurs at [Y, T, H, F, A, V]-G dipeptide pairs that mark the junction of the P1 and P2 region. The cleavage is catalysed by amino acid sequences of the 2A protein as soon as the required elements are synthesized by a ribosome (Sommergruber *et al.*, 1989;Toyoda *et al.*, 1986). Release of 2A from the polyprotein is not a prerequisite for this activity because processing occurs before the sequences of the 3C protease (responsible for 2A-2B cleavage) have been translated. Thus the primary scission is thought to be monomolecular.

When tested in cell free extracts, however, purified 2A is also capable of *trans* (bimolecular) reactions on synthetic substrates that mimic the P1-P2 junction, or natural substrates derived from defined, cloned portions of the polyprotein that likewise

encompass this region. Antibodies directed against 2A block these *in vitro* reactions, confirming the identity of the reactive agent (Toyoda *et al.*, 1986).

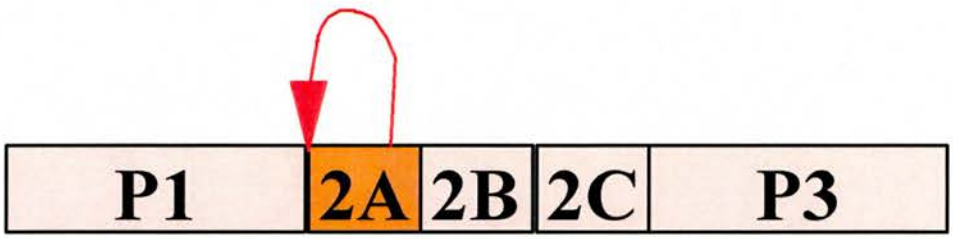

Figure 1.3. *Primary cleavage event effected by $2A^{pro}$, at the P1-P2 junction.*

1.5.2. Secondary Processing Events. Subsequent or secondary processing events are mostly effected by $3C^{pro}$, or a $3C^{pro}$ polypeptide precursor, i.e. the central enzymes in the cleavage cascade.

The 3C protease is highly homologous throughout the *Picornaviridae* albeit that each 3C protease has a strong preference for homologous substrates. The 3C protease catalyses cleavage of P1, P2 and P3 in a cascade of cleavage events. The precise order in which these cleavage events take place has not yet been fully determined.

In *Cardioviruses*, all 3C-containing precursors, i.e. 3ABCD, 3ABC, 3CD and 3C are capable of cleaving the P1 precursor (Parks *et al.*, 1989). The processing of *Rhino-* and *Enterovirus* P1 precursors requires $3CD^{pro}$ rather than $3C^{pro}$ for efficient cleavage of the VP2-VP3 junction (Jore *et al.*, 1988; Ypma-Wong *et al.*, 1988).

Both *Cardio-* and *Aphthoviruses* possess a leader protein, and this protein must be removed from the rest of the polyprotein for particle biogenesis. In *Cardioviruses*, scission at the L-P1 junction is effected by $3C^{pro}$, but in *Aphthoviruses* it has been determined that the L protease has an intrinsic catalytic activity and self processes its release at the L-1A junction (Strebel and Beck, 1986).

The multiple activities of P3 precursors intimate that 3C and its zymogens should be viewed as a family of protease species rather than a single entity. It is possible that by apportioning cleavage responsibilities to different enzyme forms, *Picornaviruses* can prudently and efficiently modulate the processing cascade to release the desired proteins at the required times throughout the infectious cycle (Palmenberg, 1990).

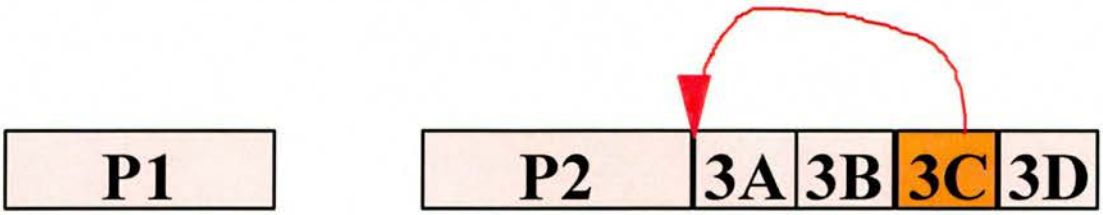

Figure 1.4. *Primary cleavage event effected by* $3C^{pro}$.

1.6. The use of defective interfering (DI) particles, complementation, and replicons in order to study gene function. Naturally-occurring RNA genomes of *Poliovirus* which contain in-frame deletions in the P1 capsid protein-encoding region have been described (Cole and Baltimore, 1973; Cole *et al.*, 1971; Kuge *et al.*, 1986). These are termed defective-interfering (DI) particles since they interfere with the production of plaque-forming particles. DI genomes are capable of replication and can be encapsidated by capsid proteins provided *in trans* by a helper virus. Encapsidation studies of *Poliovirus* genomes deficient in capsid-coding sequences have been frequently documented stating *trans*-encapsidation as the mechanism by which DI particles are propagated, as a technique to test the specificity of packaging, and as a tool to propagate *Poliovirus*-derived RNAs that contain exogenous sequences. *Poliovirus* genomes can be trans-encapsidated by capsids of the same serotype provided by helper viruses, by other serotypes of *Poliovirus*, and by capsid proteins expressed by other virus vector systems such as *Vaccinia virus* (see below).

The inclusion of a foreign marker gene, e.g. a chloramphenicol acetyltransferase (CAT) gene into a *Poliovirus* genome allows its replication and encapsidation to be easily monitored using a simple enzyme assay. As already stated above, such *Poliovirus* replicons require the presence of a helper virus for their successful propagation and thus are similar to defective interfering (DI) viruses.

In the study of Barclay *et al.*, (1998) it was shown that in genomes containing the CAT gene, all but the last two amino-acids of the P1 virus capsid region of the *Poliovirus* genome could be removed without destroying viability, indeed the smallest replicon Barclay's team created was significantly smaller than any naturally occurring DI particle

reported to date and yet the replicon still managed to retain the ability to replicate and be encapsidated by structural proteins provided by helper virus *in trans*.

Next, Barclay investigated the efficiency with which the replicons were encapsidated by using a direct immunostaining technique that allowed individual cells infected with either a replicon or a helper virus to be identified. The results she obtained were compared to the frequencies of trans-encapsidation of *Polioviruses* and *Coxsackieviruses* B4 using a two-stage neutralization assay. *Poliovirus* types 1, 2, and 3, but not *Coxsackievirus* B4, *Coxsackievirus* A21, or *Rhinovirus 14*, provided efficient trans-encapsidation of *Poliovirus* type 3, or type 3 derived replicons. These results suggest the operation of a specific encapsidation process, and that it does not involve RNA sequences within the region of the genome encoding the capsid proteins. *Poliovirus* positive-sense RNAs are specifically packaged in infected cells: cellular mRNAs, rRNAs, and tRNAs, and negative sense *Poliovirus* RNAs are excluded from the capsids (Nomoto *et al.*, 1977; Novak and Kirkegaard, 1991). Sensitive trans-encapsidation assays have shown that replicating RNA genomes derived from *Poliovirus* type 1, can be encapsidated by virion proteins encoded by any of the three *Poliovirus* serotypes but not by capsid proteins from the related *Picornaviruses*, *Coxsackievirus* A21 or B3, or *Enterovirus* 70 (Porter *et al.*, 1998).

What determines the specificity of *Poliovirus* RNA packaging? Several published observations are consistent with the hypothesis that only newly replicated *Poliovirus* positive RNA strands are encapsidated.

Nugent and co-workers (1999), proposed that there is a functional coupling between replication and packaging of *Poliovirus* replicon RNA. In this study monkey kidney cells that constitutively expressed T7 RNA polymerase were used in order to synthesize *Poliovirus* RNA genomes that contained deletions in the capsid-coding regions. These replicons were encapsidated *in trans* by superinfecting *Polioviruses*. When superinfecting *Poliovirus* resistant to the antiviral compound guanidine was used, the RNA replication of the replicon RNAs could be inhibited independently of the RNA replication of the guanidine-resistant helper virus. Inhibiting the replication of the replicon RNA was also found to profoundly inhibit its trans-encapsidation even though the capsid proteins present in the cells could efficiently encapsidate the helper virus. The

authors proposed that the observed coupling between RNA replication and RNA packaging could account for the specificity of *Poliovirus* RNA packaging in infected cells and the observed effects of mutations in the coding regions of nonstructural proteins on virion morphogenesis. It was also suggested that this coupling results from direct interactions between the RNA replication machinery and the capsid proteins.

The coupling of RNA packaging to RNA replication and of RNA replication to translation (Novak and Kirkegaard, 1994) could serve as mechanisms for late proof reading of *Poliovirus* RNA, allowing only those RNA genomes capable of translating a full complement of functional RNA replication proteins to be propagated. There is some evidence that the *Picornavirus* internal ribosome entry site (IRES) may be involved in both the specificity and the initiation of encapsidation. The 5´NCR contains the IRES, however previous studies have described *Poliovirus* genomes in which the IRES for *Encephalomyocarditis virus* (EMCV) is positioned between the P1 and P2-P3 open reading frames of the *Poliovirus* genome. Although these dicistronic *Poliovirus* genomes were replication competent, most exhibited evidence of genetic instability, and the EMCV IRES was deleted upon serial passage. One possibility for this instability of the genome may be that the dicistronic genome is at least 108% larger than the wild type (ω*t*) *Poliovirus* genome, which could reduce the efficiency of encapsidation.

In order to investigate this, Johansen and Morrow (2000) constructed dicistronic replicons by substituting the EMCV IRES and the gene encoding luciferase in place of the *Poliovirus* P1 region; the resulting dicistronic replicons are smaller than the ω*t* *Poliovirus* genome. One dicistronic replicon was constructed in which the *Poliovirus* 5′ NCR was fused to the gene encoding luciferase, followed by the complete EMCV IRES fused to the P2-P3 region of the *Poliovirus* genome (Fig. 1.5.).

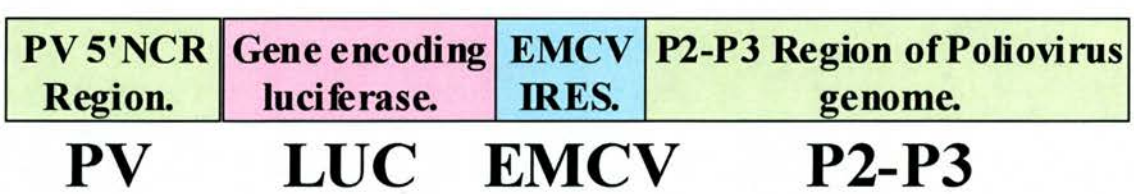

Figure 1.5. *Replicon PV-LUC-EMCV-P2-P3.*

A second dicistronic replicon was constructed with the first 108nts of the *Poliovirus* genome fused to the EMCV IRES, followed by the gene encoding luciferase and the *Poliovirus* IRES fused to the remaining P2-P3 region of the *Poliovirus* genome (Fig. 1.6.).

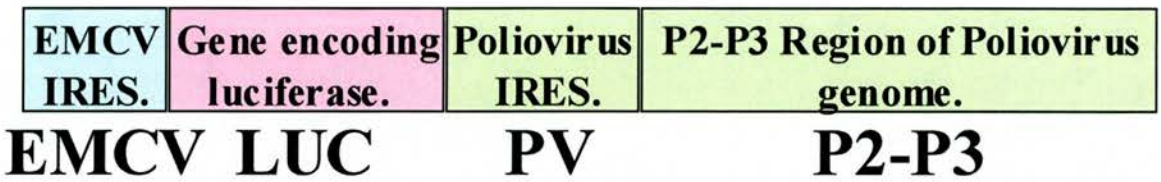

Figure 1.6. *Replicon EMCV-LUC-PV-P2-P3.*

Both dicistronic replicons expressed abundant luciferase following transfection of *in vitro* transcribed RNA into HeLa cells at 30, 33, or 37°C. In order to analyze encapsidation of the dicistronic replicons, Johansen and Morrow used a system in which the capsid protein (P1) is provided in trans from a recombinant *Vaccinia virus* (VV-P1). PV-LUC-EMCV-P2-P3 was found to be unstable upon serial passage in the presence of VV-P1, with deletions of the EMCV IRES region detected even during the initial transfection at 37°C. Following serial passage in the presence of VV-P1 at 33 or 30°C, deleted genomes were detected in which the luciferase gene was fused with the P2-P3 genes of the *Poliovirus* genome so as to maintain the translational reading frame. In contrast, EMCV-LUC-PV-P2-P3 was genetically stable during passage with VV-P1 at 33 or 30°C.

Next, the encapsidation efficiency of EMCV-LUC-PV-P2-P3 was compared to that of monocistronic replicons encoding luciferase with either a *Poliovirus* or EMCV IRES. After four serial passages with VV-P1 it was found that EMCV-LUC-PV-P2-P3 was encapsidated 46.6% more efficiently than the monocistronic replicon; EMCV-LUC-P2-P3, however, the other monocistronic replicon PV-LUC-P2-P3, was found to be encapsidated 33.3% more efficiently than EMCV-LUC-PV-P2-P3. These results suggest a genetic predisposition for *Poliovirus* genomes to contain a single *Poliovirus* IRES region (Johansen and Morrow, 2000).

Since previous studies have established that little sequence homology exists between the EMCV and the PV IRES elements, and the work by Johansen and Morrow, as already stated, indicates that the *Poliovirus* genome favours a single *Poliovirus* IRES region in order to achieve the highest level of encapsidation efficiency, I feel these data may suggest a role for the *Poliovirus* IRES in the encapsidation of the *Poliovirus* genome, possibly due to some interaction between the IRES and the P1 structural capsid proteins.

1.7. T7 RNA polymerase (T7 RNA POL). The T7 RNA polymerase is an extremely active enzyme that is encoded in the DNA of bacteriophage T7. T7 RNA polymerase is a single subunit DNA-dependent, RNA polymerase which transcribes DNA beginning with a specific 23-bp promoter called the T7 late promoter. T7 RNA polymerase requires a DNA template with the appropriate T7 phage promoter, but it does not require a primer (as do DNA polymerases). Because of T7 RNA POLs promoter specificity, it is very useful for cloning purposes as it will only transcribe DNA downstream of the specific phage promoter.

1.7.1. Expression of T7 RNA Polymerase Encoded by a Recombinant Vaccinia virus. The prototypical member of the *Orthopox-virus* family *Vaccinia virus* (VV), is a large double-stranded DNA virus encoding for approximately 200 structural and replicative viral proteins (reviewed by Moss, 1996). VV is a useful vector for insertion of foreign DNA into cells. It can infect a wide range of host cells in culture, and even cell lines which do not allow completion of the viral replication cycle (and which are therefore not lysed by the virus) may be infected and may allow expression of viral early genes.

Incorporation of the gene encoding bacteriophage T7 RNA polymerase into the VV genome produced an exceptionally useful cloning tool as transfection of genes proximal to a T7 promoter into cells infected by the T7 RNA POL modified VV, allows increased levels of expression of an extremely wide range of T7 promoter driven plasmid constructs.

The merits of the VV-T7 expression system were initially tempered due to the high level production of VV proteins and ultimately the production of the virus itself,

however, DNA replication in VV has since been shown to consist of two discrete phases, a synthesis phase which relies upon early gene expression during which input DNA is converted into replicative intermediates, followed by a processing or resolution stage, which relies on late gene products (DeLange, 1989; Merchlinsky and Moss, 1989). Thus, a VV which is conditionally defective in viral late gene expression, and is modified to express bacteriophage T7 RNA polymerase has been developed (Eckert and Merchlinsky, 1999). The hybrid virus (vtsT7) expresses high levels of proteins from genes adjacent to a T7 promoter in the absence of normal VV late gene production.

1.7.2. T7 RNA Polymerase – Atomic Structure. Crystallization studies have provided evidence for a unified two metal ion catalytic mechanism of polymerases (Brautigam and Steitz, 1998). Two invariant acidic amino acid residues are positioned at the catalytic centre of all polymerase structures. Mutations of these invariant residues lead to strongly impaired polymerase activity (Date *et al.*, 1991) and the ternary complex crystal structures show that they are involved in co-ordinating the two catalytic metal ions (Doublie *et al.*, 1998). T7 RNA polymerase is the only DNA-dependent RNA polymerase that has been crystallized (Jeruzalmi and Steitz, 1998).

The structure resembles a right hand with the active site positioned in the palm (see figure 1.7. below). As in other polymerase structures two acidic residues (Asp^{537} and Asp^{812}) are positioned near the catalytic centre and mutational studies have shown that they are important for catalysis (Bonner *et al.*, 1994). Moreover, electron paramagnetic resonance experiments on mutated T7 RNA polymerase have demonstrated that they are involved in metal ion binding (Woody *et al.*, 1996). The C-terminus of T7 RNA polymerase is positioned near to the active site and mutational analyses have shown that both the length and the sequence of the C-terminal –Phe-Ala-Phe-Ala-OH^{883} at the 'heel of the hand' is important for polymerase activity (Gardner *et al.*, 1997).

Work by Anderson and Christiansen (Anderson and Christiansen, 1998), examined whether the C-terminal carboxy group is important for magnesium ion-dependent catalysis by T7 RNA polymerase. Introduction of a methyl ester or decarboxylation of the C-terminal carboxy group was achieved with an intein-based protein expression system and an elongation rate assay was developed to test the effects

of the modifications. Anderson and Christiansen's (1998) results showed that T7 RNA polymerases with a modified C-terminal carboxy group exhibited a magnesium ion-dependent decrease in catalytic activity.

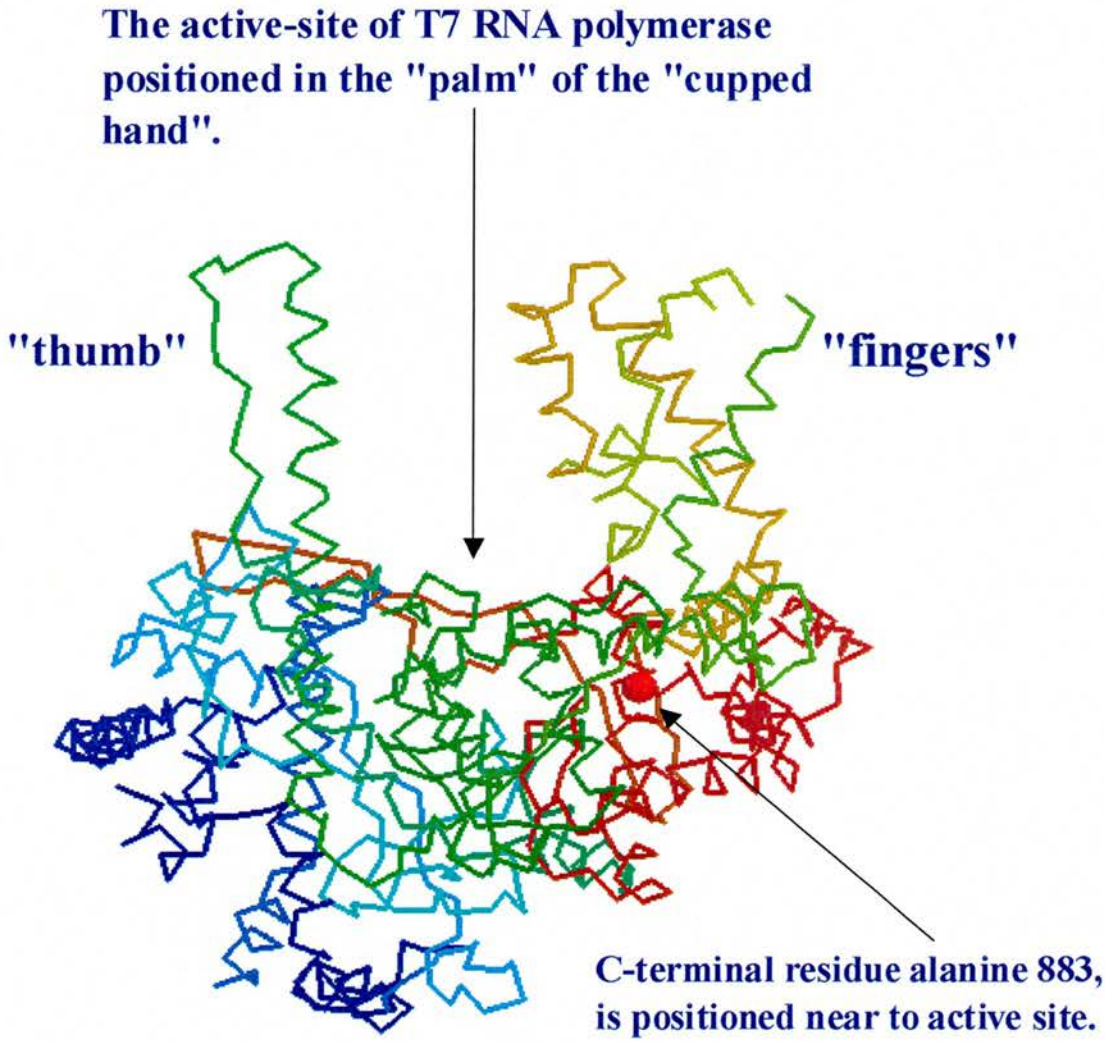

Figure 1.7. *The molecular structure of T7 RNA polymerase resembles a cupped right hand, with the active-site positioned in the palm (structure above taken from, Sousa et al., 1993). The C-terminal residue alanine, highlighted above as a red sphere, is positioned near to the active site and is an important factor in the catalytic activity of the enzyme (Anderson and Christiansen, 1998).*

1.8. Project aims and objectives. The aim of this project was to create and characterize plasmid constructs encoding recombinant *Human Rhinovirus 85* (HRV85) genomes in order to study the replication, recombination and encapsidation properties of HRV85 (see figure 1.8. below).

HRV85.

Complete genome of *Human Rhinovirus 85* (kind gift of Prof. G. Stanway).

pJL1.

Plasmid pJL1 was constructed to facilitate production and analysis of plasmid pJL3.

pJL2.

Plasmid pJL2 was constructed to facilitate production and analysis of plasmid pJL3.

pJL3.

Plasmid pJL3 was constructed in order to analyze $2A^{pro}$ cleavage capabilities at its own N-terminus when the sequences encoding $2A^{pro}$ were fused the gene encoding T7 RNA POL, as opposed to the P1 region of the HRV85 genome.

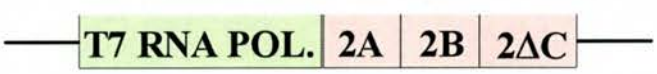

pJMP1del.

Plasmid pJMP1del was constructed in order to analyze the replication capabilities of an HRV85 genome devoid of its entire P1 encoding sequence.

pHRV85-T7.

Plasmid pHRV85-T7 was constructed in order to analyze the replication and encapsidation properties of an HRV85 genome where the P1 encoding sequences were replaced by sequences encoding T7 RNA polymerase. As already mentioned in sections 1.7. and 1.7.1, due to the fact that T7 RNA POL will only transcribe DNA downstream of the T7 late promoter, it has proved an extremely useful cloning tool. If, therefore, the gene encoding this RNA polymerase could be expressed under the direction of recombinant HRV85 genome HRV85-T7, it would prove invaluable to the further characterization of the HRV85 replication process, i.e. expression of T7 RNA POL directed by the HRV85 genome itself will enable (using T7-late-promoter driven expression vectors) the co-expression of virus (or host-cell) proteins, or, transcription of RNA sequences 'only in cells where HRV85 genomic RNA replication is occurring', thereby circumventing many of the problems associated with other methods of co-expression /co-transcription.

pHRV85R.

Plasmid pHRV85R was constructed in order to serve as a negative control for the nucleic acid hybridization analysis of RNA replication.

Figure 1.8. *Plasmid constructs and recombinant HRV85 genomes constructed for this project.*

2.0. Materials and Methods.

2.1. Materials. RNAse A, T4 DNA ligase, T4 DNA polymerase, 1kb DNA ladder, TAQ DNA polymerase, protein size markers, all restriction enzymes (REs) and their buffers (including multicore buffer) were obtained from Promega. Oligonucleotides were obtained from Oswel. Transformations, mini- and maxi-preparations of plasmid DNA were carried out using *E. coli* strain JM-109 high efficiency competent cells from Promega. PCR was carried out using the Perkin Elmer Gene Amp PCR System 2400. Agarose gels were visualized using the Gel Doc 2000 UV transilluminator from BIO RAD.

2.1.1. Solutions:

Destain
20% [v/v]methanol,
10% [v/v] acetic acid

LB
1% [w/v] bacto-tryptone,
0.5% [w/v] bacto-yeast extract,
1% [w/v] NaCl, pH 7.0

TAE
0.04 M tris-acetate,
0.001 M EDTA (pH 8.0).

Phenol/Chloroform
50% phenol
50% chloroform
overlaid with 0.001 M Tris/HCl.

2×SDS-PAGE loading buffer
124 mM Tris/HCl (pH6.8)
4% SDS
0.2% Bromophenol blue
20% Glycerol
10% β-mercaptoethanol

Agarose gel loading buffer
5 % [v/v] glycerol
0.005 % [w/v] bromophenol blue

2.2. Methods

2.2.1. Restriction enzyme digestions. All plasmid DNA RE digestions were carried out under the conditions specified by the supplier. In general, 1μg of DNA was digested with 1 unit of enzyme in a total volume of 20μl, containing 2μl of ×10 restriction buffer at 37°C unless otherwise specified.

2.2.2. Agarose-gel electrophoresis. Flatbed agarose gels, of concentration 0.7 – 2% [w/v] were prepared with 1× TAE which contained ethidium bromide at a final concentration of 0.5μg/ml. DNA samples were applied to the gel in agarose gel loading buffer. Electrophoresis was carried out at 100-180V in 1× TAE containing 0.5μg/ml ethidium bromide. Following electrophoresis the bands were visualised by illumination from the UV transilliuminator mentioned above.

2.2.3. Transformation of E. coli JM109 high efficiency competent cells (Promega). The cells were removed from storage in a –70°C freezer and thawed on ice for approximately 5 minutes. 10μl of ligation reaction was added to a 200μl aliquot of cells and incubated on ice for 30 minutes. The cells were subsequently heat-shocked at 42°C for 70 seconds, then placed on ice immediately for at least 2 minutes prior to plating out onto LB agar plates containing the appropriate antibiotic.

2.2.4. Purification of DNA fragments from agarose. The desired DNA band was run into 1% low-melting point (LMP) agarose, the band of DNA was excised from the LMP agarose and placed in a 1.5ml microcentrifuge tube. The sample was heated to 70°C in order to melt the agarose. The DNA was isolated from the agarose using the Wizard® Preps DNA Purification system (Promega). Briefly, a Wizard® minicolumn was attached to a syringe barrel. The melted agarose was mixed with 1ml of Wizard® DNA purification resin for 20 seconds and then pushed through the minicolumn. The minicolumn was washed with 2ml of 80% isopropanol. The column was dried by centrifugation for 2 minutes at 10,000g. The bound DNA was eluted from the

minicolumn by the addition of 50µl of dH_2O, incubation for 1 minute, and finally, centrifugation at 10,000g for 20 seconds.

2.2.5. Phenol/Chloroform extraction of DNA. An equal volume of phenol/chloroform [v/v] was added to the DNA sample, this was vortexed and centrifuged at 14,000g for 5 minutes. The upper aqueous layer was transferred to a clean tube. The above procedure was repeated until the interface between the upper aqueous layer (DNA sample) and the lower phenol/chloroform layer was clear. The upper aqueous layer was transferred to a sterile tube and the DNA was precipitated by the addition of 2.5 volumes of ethanol and 0.05 volume of 2M sodium acetate. The sample was stored at –70°C for 40 minutes. The DNA was then pelleted by centrifugation at 14,000g for 30 minutes. The ethanol and sodium acetate was decanted off, and the pelleted DNA sample was allowed to air dry for 5 minutes before being resuspended in 100µl of dH_20.

2.2.6. DNA preparations. Mini-, or maxi-preparations of plasmid DNA were isolated depending on the quality and quantity of DNA required. Maxi-preparations were required for DNA used in transcription and translation analysis.

2.2.7. Small-scale preparation of plasmid DNA using the Wizard® SV™miniprep kit (Promega). Minipreparations of plasmid DNA were purified using a Promega Wizard® SV™miniprep kit and protocol as per manufacturers instructions.

2.2.8. Large-scale preparation of plasmid DNA using the QIAfilter Plasmid Maxi-kit (Qiagen). Maxi-preparations of plasmid DNA were purified using a Qiagen® Plasmid Maxi-kit and protocol, as per manufacturers instructions (Qiagen).

2.2.9. Polymerase Chain Reaction (PCR). The PCR was used to amplify regions of DNA for cloning and also to introduce specific mutations within a gene. A typical reaction was performed in a 100µl volume and contained 20ng of template DNA, 100pm of each primer, 0.25mM of each dNTP, 2.5mM $MgCl_2$, 2 units of TAQ DNA polymerase, and 10µl of ×10 TAQ polymerase reaction buffer (50mM KCl, 10mM Tris. HCl (pH

9.0), 0.1% [v/v] Triton X-100, 1.5mM $MgCl_2$). Amplification of DNA was carried out in a thermal-cycler using the following parameters: 95°C for 1 minute, to denature the DNA; 50^0C for 1 minute, to allow primers to anneal to template DNA (The annealing temperature of the reaction was varied according to the particular base composition of the primers involved); 72^0C for 1 minute for every thousand base pairs to be amplified, to allow the TAQ DNA polymerase to extend from each primer. The amplification was carried out for 25-30 cycles, and finally, the reaction was held at 72^0C for 15 minutes in order to ensure that the majority of final product was full length double stranded DNA.

2.2.10. Nucleotide dideoxy sequencing of recombinant DNA clones. Alex Houston performed automated sequencing on a Perkin Elmer ABI Prism™ DNA sequencer. Data provided by this system was generally found to be accurate within ~650 residues of the primer binding site. Sequencing primers were designed for the T7 late promoter, internal regions of *Human Rhinovirus 85*, and the T7 RNA polymerase gene (see table 2.1.). A sample containing 500ng of plasmid DNA and 4-5 pmol of the appropriate oligonucleotide primer was submitted for sequencing. The sequencing data was viewed using Editview software from Applied Biosystems.

T7 Promoter primer (20mer)	5′-d(TAATACGACTCACTATAGGG)-3′
I.T7. sequencing primer (18mer)	5′-d(CAAGGTGTGAAGAGCCCC)-3′
T7-2A1.sequencing primer (18mer)	5′-d(CGCGGCAAGCGCCCGACA)-3′
T7-2A2. sequencing primer (18mer)	5′-d(TGGCATCTCTCCGATGTT)-3′
T7-2A3. sequencing primer (18mer)	5′-d(TGTCAATGTTCAACCCGC)-3′
T7-2A4. sequencing primer (18mer)	5′-d(ACCGTGACCGATGAGAAC)-3′
T7-2A5. sequencing primer (18mer)	5′-d(CTCCTAACTTTGTACACA)-3′

Table 2.1. *Nucleotide sequences of oligonucleotide sequencing primers used in automated DNA sequencing. The T7 promoter primer, was used to sequence all plasmid constructs where gene(s) of interest were placed proximal to the T7 late promoter, i.e. pHRV85-T7, pJMP1del, pJL3, pHRV85R. Due to the accuracy of the sequencing system being limited to ~650nts downstream of the primer binding site, six primers (I.T7, T7-2A1, T7-2A2, T7-2A3, T7-2A4 and T7-2A5) were used to sequence the entire recombinant region of pHRV85-T7, i.e. [IRES-T7 RNA POL-2A]. Primer I.T7. binds to a region 141nts upstream of the HRV85 IRES 3′ terminus and so was also used to sequence the IRES-P2 junction of pJMP1del.*

2.2.11. Ligation of vector and insert DNA. Ligation reactions were generally carried out in a final volume of 25µl. The reaction mix contained 1µl T4 DNA ligase, 0.5µg of vector DNA, and insert DNA at concentrations of 2-fold, 5-fold, or 10-fold molar ratios in T4 DNA ligase buffer (50mM Tris-HCl (pH 7.5), 10mM $MgCl_2$, 10mM dithiothreitol, 1mM ATP, 25µg/ml BSA). The reactions were incubated overnight at 4°C.

2.2.12. Coupled Transcription and Translation (TnT) reactions. Proteins were expressed *in vitro* using coupled transcription/translation kits (Promega). Proteins were expressed in both wheatgerm extract and rabbit reticulocyte lysate systems according to the manufacturer's instructions (Promega). The proteins were radio-labeled with ^{35}S methionine (Amersham). The reactions were incubated at 30°C for 90 minutes, then stopped by the addition of an equal volume of 2× SDS-PAGE protein loading buffer. The reactions were analyzed in 5µl aliquots, by denaturing poyacrylamide gel electrophoresis (SDS-PAGE).

2.2.13. Denaturing polyacrylamide gel electrophoresis (SDS-PAGE). The gels were constructed with a 4% polyacrylamide stacking gel and a 10% polyacrylamide resolving gel. The gel was run using a Hoefer mini-gel apparatus. The resolving gel was poured between the plates, overlaid with 1ml of water saturated iso-butanol, and allowed to set for approximately 30 minutes. The iso-butanol was poured off and the apparatus was rinsed with water prior to the addition of the stacking gel, with the combs in place. The stacking gel was allowed to set and the apparatus was transferred to the electrophoresis tank. Sample, in SDS-PAGE loading buffer, and protein size markers were applied to the wells of the gel, under Tris-glycine buffer. The electrophoresis was carried out at a constant current of 20mA through the stacking gel and 40mA through the resolving gel, until the Bromophenol blue dye reached the bottom of the gel. The plates of the apparatus were separated and the gel was transferred into a Coomassie blue staining solution. The gel was incubated in the staining solution for 30 minutes, after which the stain was poured off and replaced with destain. The gel was incubated in the destain for 10-15 minutes, the destain was then poured off and replaced with fresh destain. The replacement of the destain with 'fresh' destain was repeated several times. The gel was then transferred onto filter paper, covered with cling film and dried on a gel dryer for 1 hour. The radioactive samples on the gel were visualized using the FUJIX Bio-imaging analyzer, BAS1000 MacBas system. This system uses a Fuji imaging plate, which consists of an image-sensing layer composed of fine photo-reactive phosphor crystals. Briefly, when exposed, by close contact with a radio-labeled sample in a cassette, the imaging plate accumulates and stores the radioactive energy. The exposed imaging plate is inserted into a computer-linked imaging plate reader, which scans the imaging plate with a He-Ne laser beam. Luminescence is emitted in proportion to the recorded radiation intensity. The luminescence is detected by a photomultiplier tube and converted to electrical signals, which are then displayed on a computer terminal.

3.0. Results.

3.1. Introduction. This section provides details of methods and strategies used to create, investigate and characterize the plasmid constructs and recombinant HRV85 genomes introduced in figure 1.8. of section 1.8.

3.2. Construction of plasmid pJL3. The polyprotein product of the HRV85 genome is normally cleaved at the P1-P2 junction by the 2A protease ($2A^{pro}$) during translation so that the full-length protein is never formed. Therefore, rather than proceeding directly to the insertion of the gene for T7 RNA polymerase (T7 RNA POL.) into a P1 deficient cDNA (infectious copy) of HRV85, it was desirable to ascertain whether the primary cleavage event by $2A^{pro}$ at its own N-terminus, would still occur if $2A^{pro}$ was proximal (fused) to the 3′ terminal sequences of the gene encoding T7 RNA POL, as opposed to those of the P1 region.

In order to aid analysis of the translational consequences of fusing the gene encoding T7 RNA POL to the 5′ terminus of sequences encoding the P2 region of HRV85, plasmids pJL1, pJL2 and pJL3 were constructed (see figure 3.1.). Plasmid pJL3 contained the required T7 RNA POL - $2A^{pro}$ fusion, plasmids pJL1 and pJL2 were used to provide translational protein products in order to aid identification (during analysis by SDS-PAGE) of protein products produced by the translation of pJL3. HRV85 possesses a unique *Apa*1 (GGGCCC) RE site in the cDNA encoding the 5′ terminus of HRV85-$2A^{pro}$, and a unique *Eco*RV (GATATC) site a further 1144 bases downstream.

This data permitted the use of these two REs to remove region; [2A.2B.2ΔC] from the cDNA of HRV85. Vector pGEM®5Zf(+/-) (Promega), was also cut with *Apa*1 and *Eco*RV, which, following agarose gel purification of both vector and [2A.2B.2ΔC] fragment, permitted the ligation of [2A.2B.2ΔC], into pGEM®5Zf(+/-) to create plasmid pJL1 (see figure 3.1.).

For the purposes of this experiment, it was required that the T7 RNA POL gene possess an *Apa*1 RE site at its 3′ terminus and a *Bam*H1 (GGATCC) RE site at its 5′ terminus in order to; (a) permit ligation to the unique *Apa*1 site situated at the 5′ terminus

of fragment; [2A.2B.2ΔC] and (b) permit ligation into designated vector pGEM11Zf(+/-), thereby creating plasmid pJL2. These sites were added to T7 RNA POL by forward and reverse primers used in the PCR amplification of the gene. The polylinker in vector pGEM11Zf(+/-) contains the RE sites *Bam*H1, *Apa*1 and *Not*1 (GCGGCCGC), respectively. In plasmid pJL2, the gene for T7 RNA POL is situated between *Bam*H1 and *Apa*1. Figure 3.1. shows that in plasmid pJL1, the [2A.2B.2ΔC] fragment is situated between RE sites for *Apa*1 and *Not*1.

This data dictates that it was then a relatively simple matter to digest both pJL1 and pJL2 with *Apa*1 and *Not*1, agarose gel purify the released [2A.2B.2ΔC] fragment and the restricted plasmid, then ligate [2A.2B.2ΔC] into pJL2 in order to create pJL3.

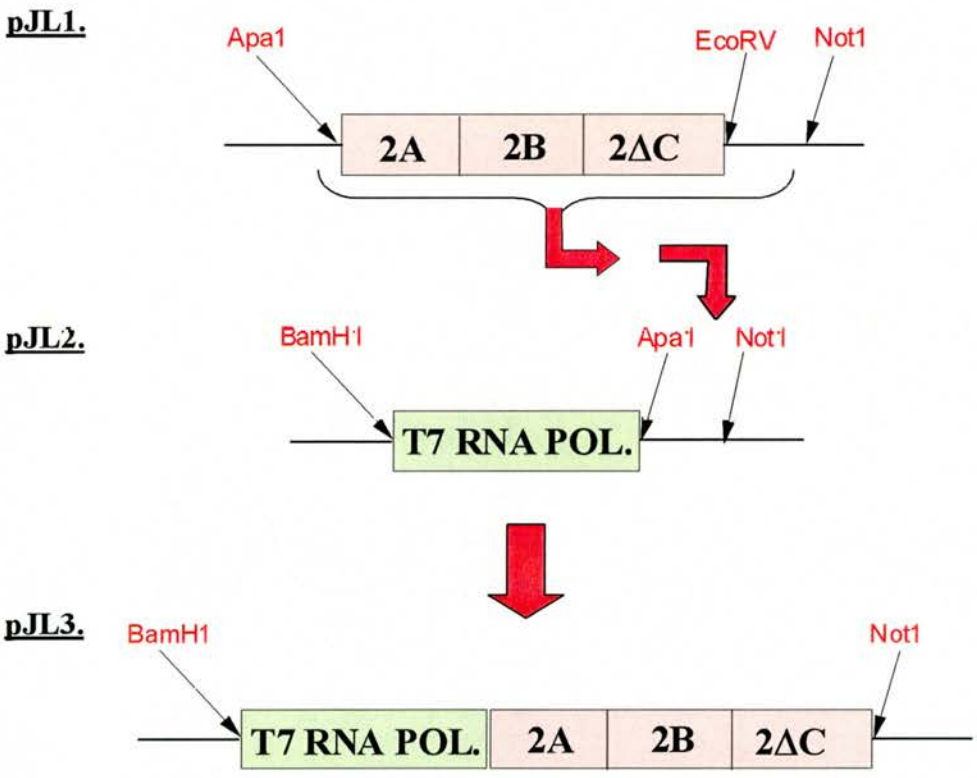

Figure 3.1. *Method used to construct plasmid pJL3 in order to investigate the properties of a fusion between T7 RNA POL. and the P2 region of HRV85.*

3.3. Translation of pJL1, pJL2 and pJL3 In vitro, by wheatgerm extract (WGE) and rabbit reticulocyte lysate (RRL) coupled transcription and translation (TnT) reactions.

Plasmids pJL1, pJL2 and pJL3 were used to program both WGE and RRL *in vitro* coupled transcription and translation (TnT) systems (see figure 3.2; (a) and (b) respectively) in order to verify whether or not HRV85 $2A^{Pro}$ would indeed cleave at the T7 RNA POL.-2A junction during the translation process as in *ωt* HRV85. The protein products were radiolabelled with ^{35}S-methionine, analyzed by SDS-PAGE and visualized by autoradiography. In order to aid identification of the translation products, i.e. to verify whether or not $2A^{pro}$ N-terminus cleavage had indeed taken place, the translation products of plasmids pJL1 and pJL2 were run in adjacent lanes on the gel.

The data displayed in figure 3.2. indicates that $2A^{pro}$ did in fact manage to retain its ability to cleave at its own N-terminus, however, the cleavage witnessed appears to be at a much lower level than is witnessed in *ωt* HRV85.

In translation studies using simple plasmid constructs containing sequences encoding HRV14-$2A^{pro}$ fused to those encoding green fluorescent protein (GFP), Cowton (2000) also found that, while $2A^{pro}$ translated *In vitro* did manage to retain much of its self-processing abilities, the cleavage efficiency was markedly lower than that observed in HRV14 infected cells.

One possible explanation for the reduced cleavage efficiency of the 2A proteinase when used in *in vitro* transcription/translation systems, may come from the structure of the proteinase itself, i.e. the *Entero-* and *Rhinovirus* $2A^{pro}$ contains a tightly bound zinc ion (see figure 3.3.). Studies on the proteolytic mechanism suggested that the zinc ion is not involved in the proteolyitic activity of the protease, but that it has an important structural role and is vital for folding of the protein (Sommergruber *et al.*, 1994b; Voss *et al.*, 1995). The pre-treatment of RRL with the chelating agent EGTA (Ethylene glycol-bis (β-aminoethyl ether) N,N,N',N',- Tetraacetic acid) in order to remove excess calcium ions, would also act to deplete the compliment of zinc ions present (pers. Comm. L. Sheppeard, Sigma-Aldrich). It is therefore possible that the addition of excess Zn^{2+} to the system may rescue the efficiency of the proteolytic activity.

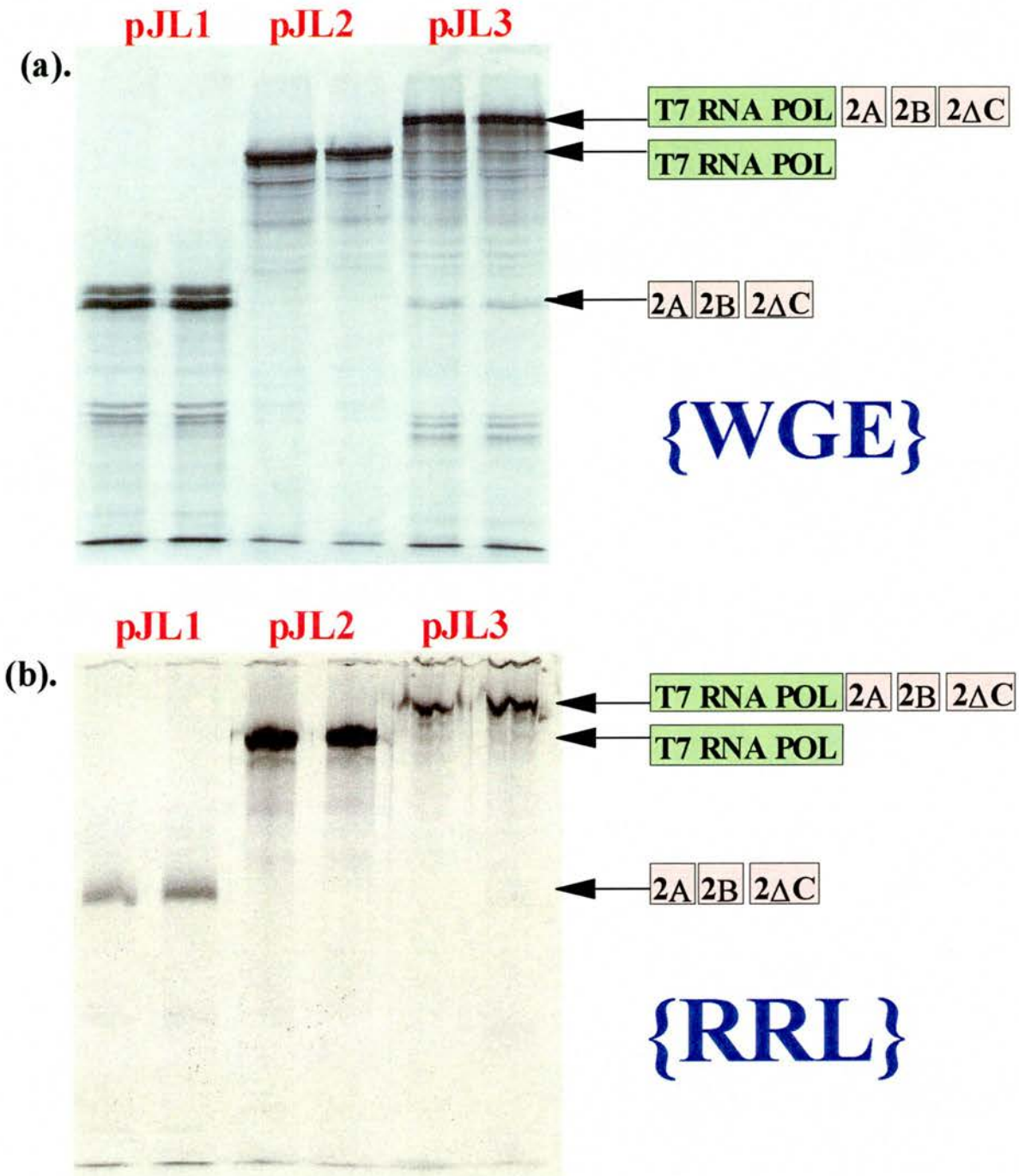

Figure 3.2. *Denaturing-PAGE gels of* ***(a).****WGE, and* ***(b).****RRL, TnT reactions featuring duplicate samples of the protein products of plasmids; pJL1, pJL2 and pJL3. The lanes containing the translation products of pJL3 show bands corresponding to both T7 RNA POL and HRV85-P2 proteins seen in adjacent lanes, indicating that some (albeit low-level) cleavage by the HRV85-2A^{pro} at its own N-terminus has indeed occurred.*

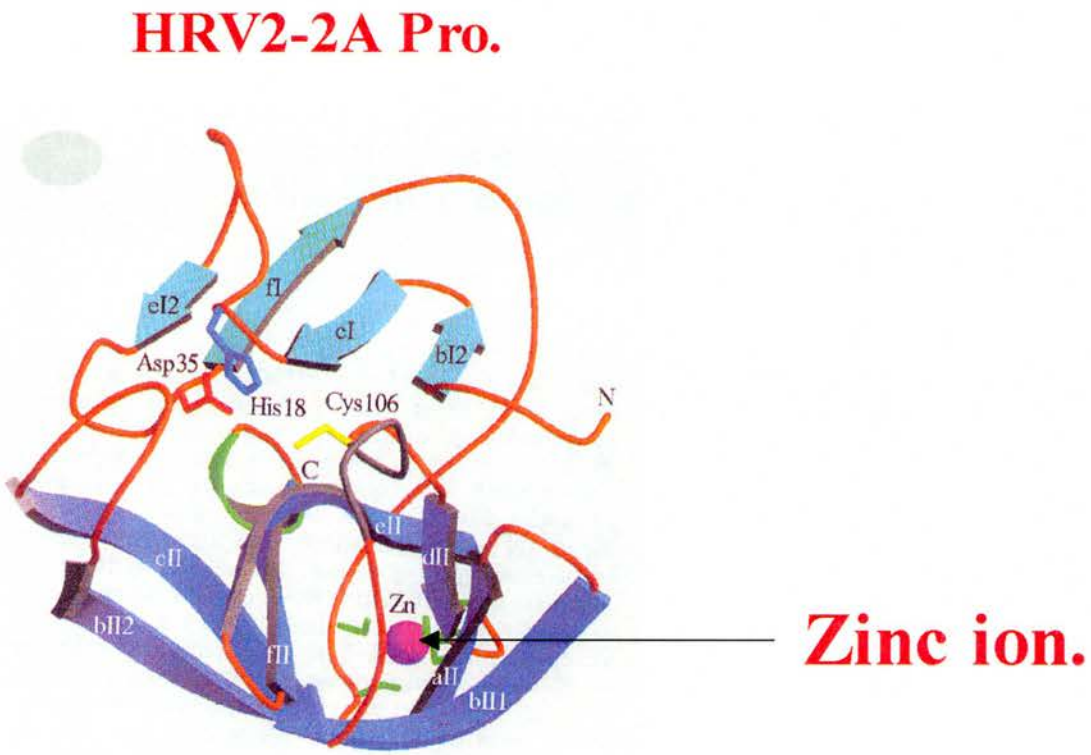

Figure 3.3. *Ribbon diagram of the overall structure of HRV2-2A^{pro} (taken from Peterson et al., 1999). The fold of HRV2-2A^{pro} has been closely related to that of the chymotrypsin-related proteinases (Bazan and Fletterick, 1988; Gorbalenya et al., 1989). Streptomyces griseus proteinase B (SGPB) has been preferred as a representative structure of a minimal chymotrypsin-like proteinase fold (Read et al., 1983) and here the strands of the HRV2-2A^{pro} are labeled according to the topology of SGPB. β strands of the N–terminal domain (light blue, Roman numeral I) and C-terminal domain (dark blue, Roman numeral II) are indicated. Members of the catalytic triad, the zinc ion (purple sphere) and the zinc-binding site are shown.*

3.4. Construction of plasmid pHRV85-T7. In plasmid pHRV85-T7, the P1 structural region of HRV85 cDNA (2577bp), was deleted and replaced by sequences encoding T7 RNA polymerase (2652bp), a difference of 75nts (see figure 3.4.).

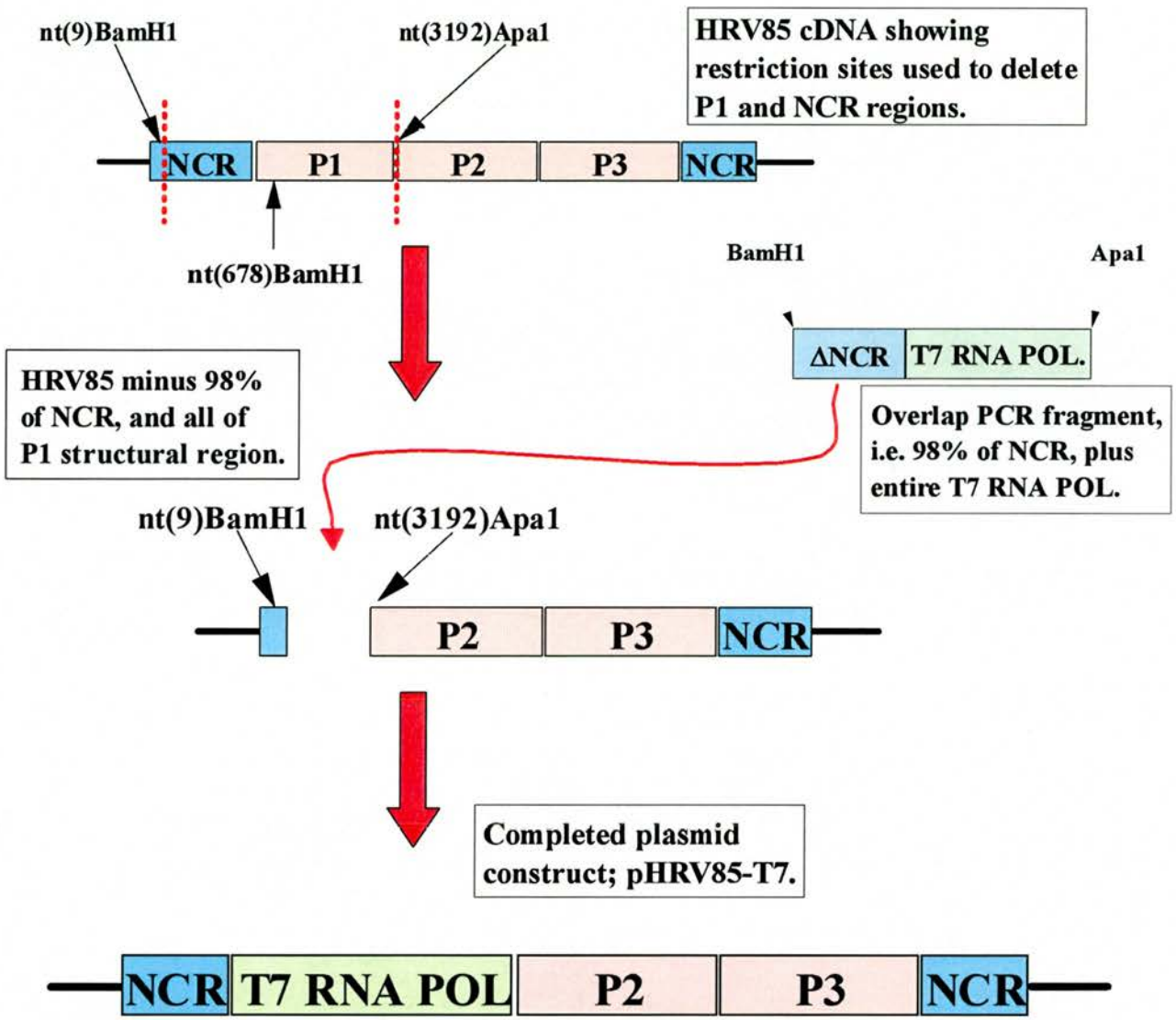

Figure 3.4. *Schematic describing the rudimentary strategy used to assemble plasmid pHRV85-T7.*

The strategy elected to construct pHRV85-T7 had three stages. Stage one was to perform a double restriction upon HRV85 cDNA with REs *Apa*I and *Bam*HI, which, in effect, removed 98% of the 5′ NCR (which contains the IRES structure), and also the entire sequence encoding the P1 structural region. As mentioned above, HRV85 has a

unique, endogenous, *Apa*1 site at the P1-P2 junction (site of $2A^{pro}$). The genomic cDNA possesses two *Bam*H1 RE sites, one at nine bases downstream of the start point of the 5′ NCR, and a second a further 669 bases downstream of the first site. This second *Bam*H1 site was however irrelevant as it resided within the P1 region and was therefore removed by the *Bam*HI/*Apa*I double digestion.

The initial plan for the second stage of the strategy was to PCR amplify both the section of the 5′ NCR (figure 3.5.) removed by the double restriction mentioned above, and also the gene encoding T7 RNA POL (figure 3.6.), then join the two PCR fragments together using an overlap (OL) PCR procedure (figure 3.7.).

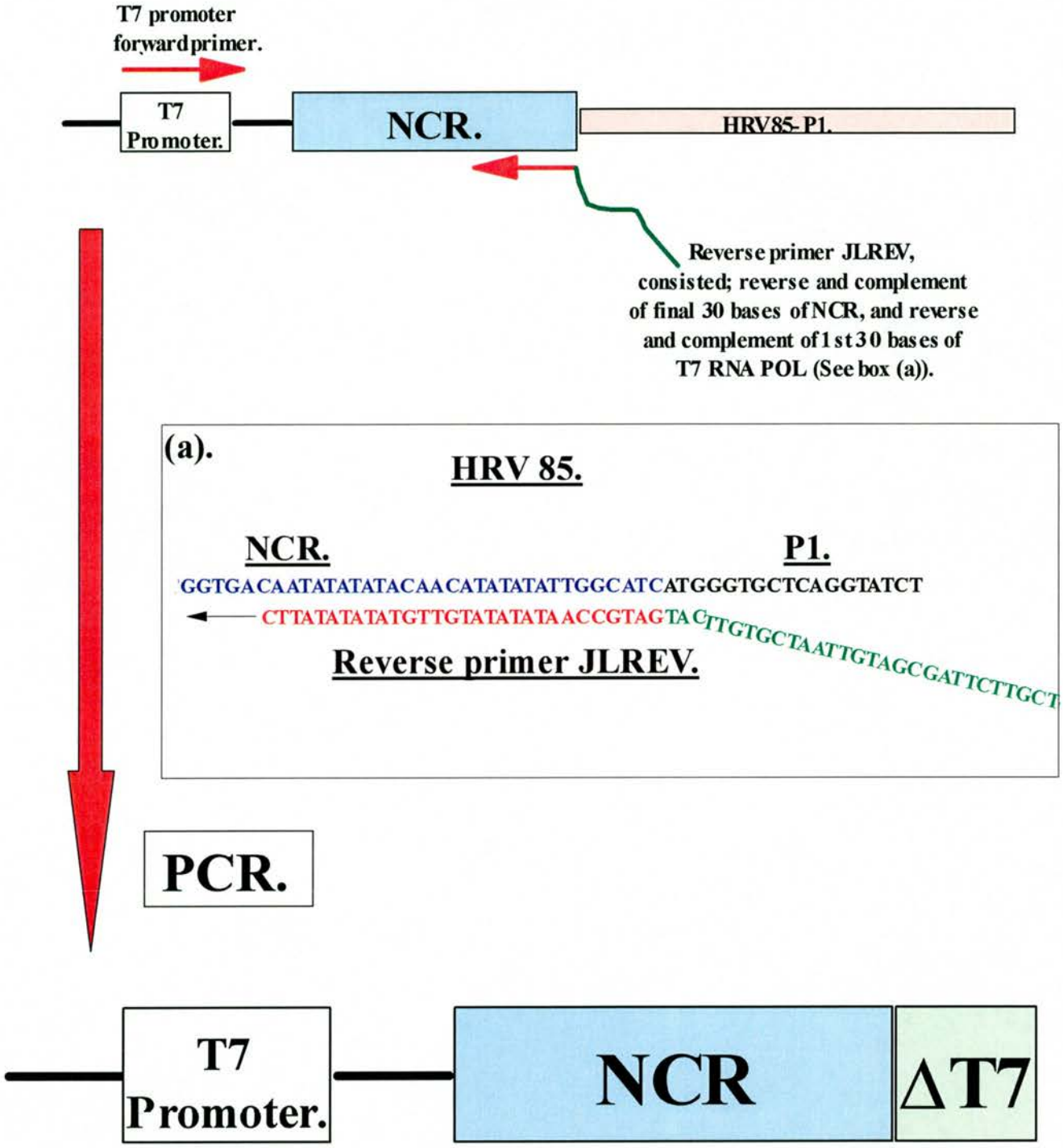

Figure 3.5. *Initial strategy attempted to PCR amplify the 5′ template used in the OL-PCR.*

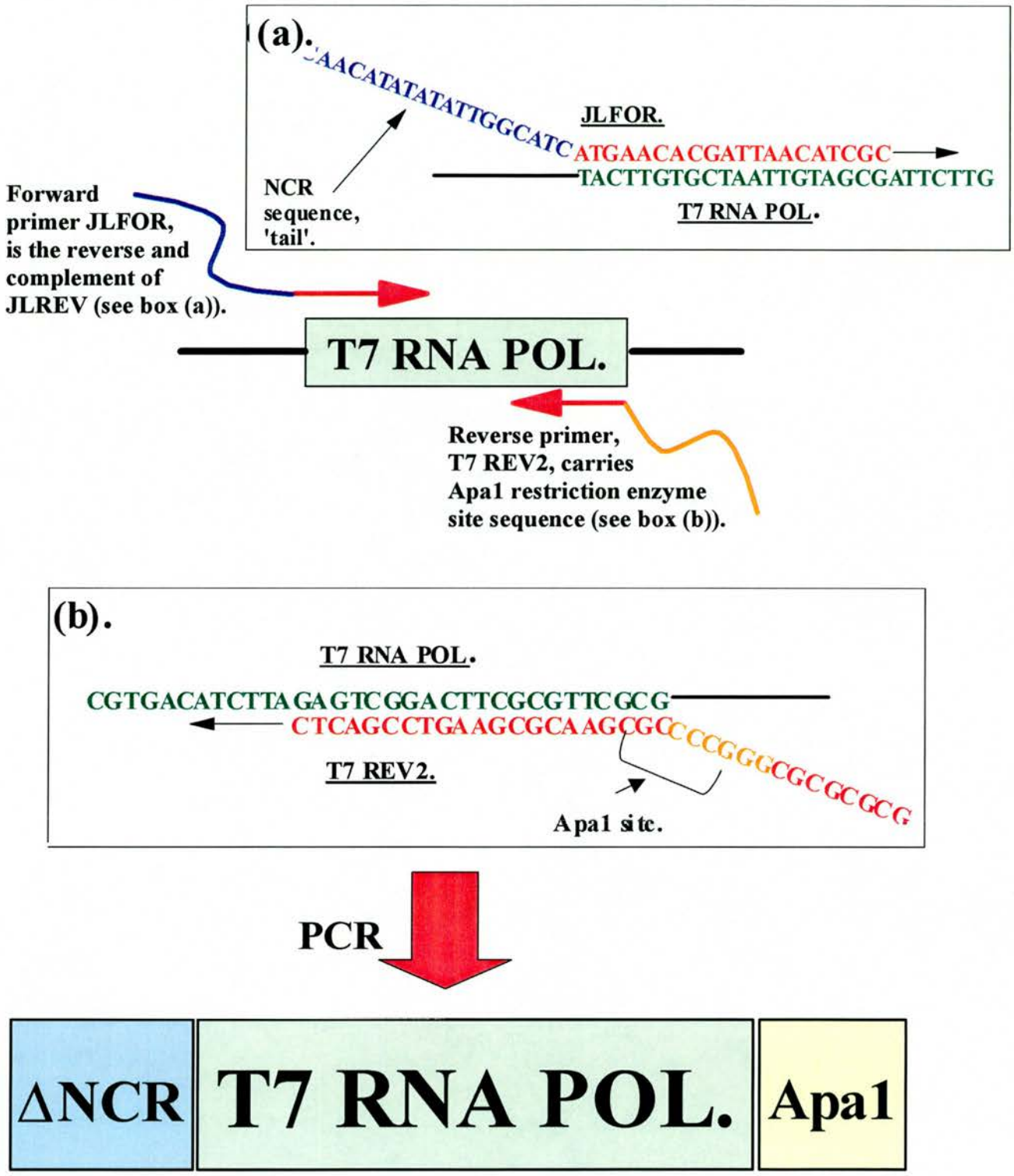

Figure 3.6. *Primary strategy attempted to PCR amplify the 3′ template used in OL-PCR.*

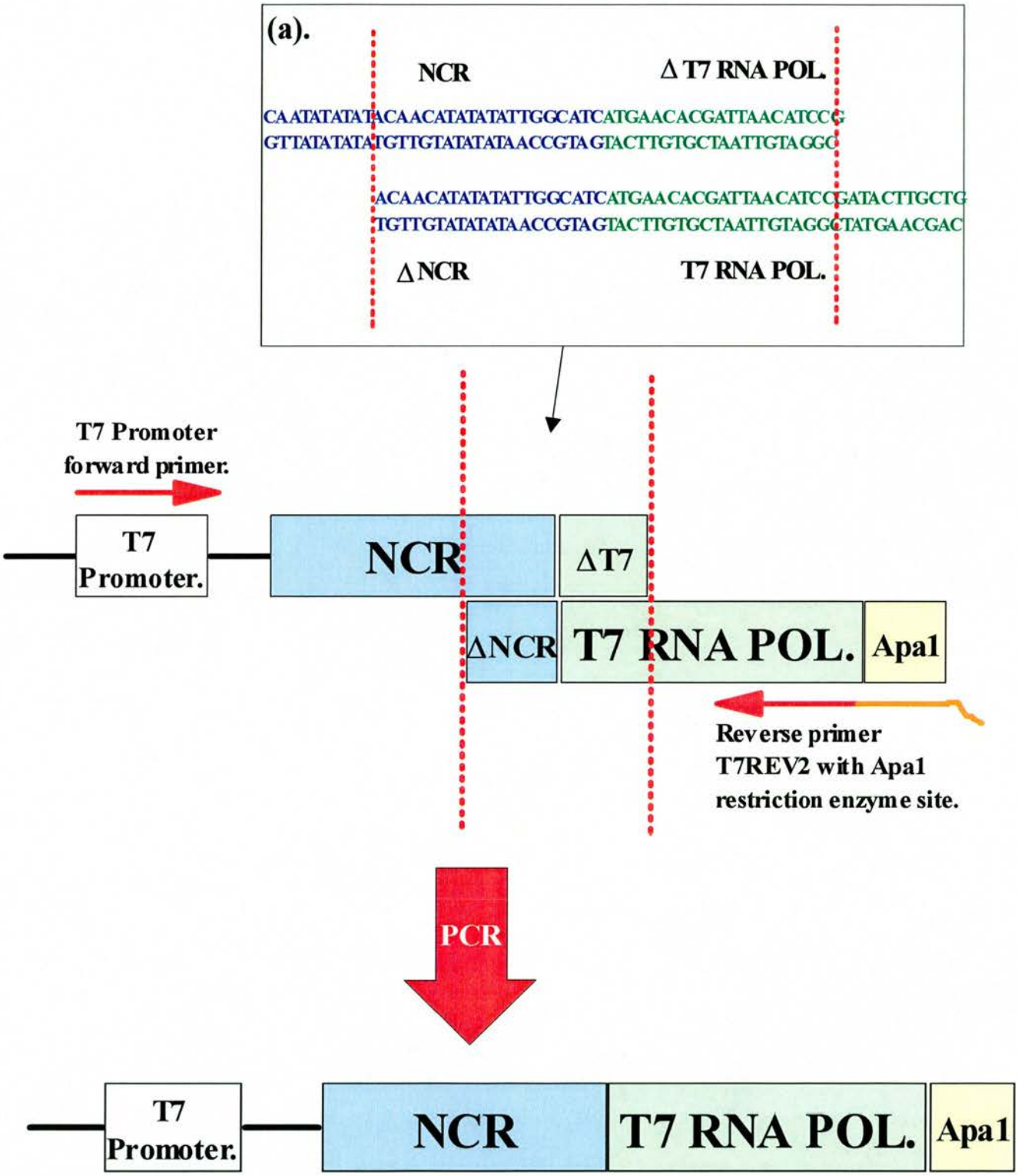

Figure 3.7. *Schematic of the first strategy employed in an attempt to fuse the HRV85-NCR to T7 RNA POL.*

It was also required that the 3′ end of the OL construct possess an *Apa*I RE site, and the 5′ end of the construct possess a *Bam*HI RE site, to permit re-ligation of the construct back into the doubly-digested HRV85 cDNA from stage one. In order to produce the [T7 promoter, NCR, ΔT7] PCR fragment seen in figure 3.5., reverse primer JLREV was designed. JLREV comprised; the reverse and complement of the 3′ terminal 30nts of HRV85-5′NCR, with a 30nt 'tail', consisting of the reverse and complement of the 5′ terminal 30nts of T7 RNA POL (Fig. 3.5.). Therefore, a PCR with HRV85 cDNA as the template, and using reverse primer JLREV in conjunction with the T7 promoter forward primer (seen in Fig. 3.5.), would produce an HRV85-5′NCR fragment with sequences encoding T7 RNA POL N-terminus residues extending from its 3′ sequences.

The [ΔNCR,T7 RNA POL,*Apa*I] PCR fragment would be produced with a virtually identical strategy. Production of this fragment required the design of two new primers; Forward primer JLFOR, and reverse primer T7REV2. Primer JLFOR was the reverse and complement of JLREV, i.e. it was designed to transcribe the T7 RNA POL gene, while concurrently 'tacking-on' a 30nt 'tail' of 5′-HRV85-5′NCR sequence to the 5' end of the T7 RNA POL sequences (Fig. 3.6.). Reverse primer T7REV2 was merely the reverse and complement of the final twenty-one 3′ nts of the T7 RNA POL gene, with an added *Apa*1 RE site, 3′ tail. Using the T7 RNA POL gene as the template, a PCR run with primers JLFOR and T7REV2, would result in a PCR fragment that consisted of the gene encoding T7 RNA POL, with the 3′ 30nts of HRV85-NCR fused to its 5' end, and an *Apa*1 RE site extending the 3' end.

The above protocol, for the construction of OL-PCR fragments [T7promoter,NCR,ΔT7], and [ΔNCR,T7 RNA POL,*Apa*I], while in theory seeming fairly straight forward, turned out in practice to be quite problematic.

Initial attempts to produce the [ΔNCR,T7 RNA POL,*Apa*1] PCR fragment seen in figure 3.6., seemed successful, producing a clear discrete band of the correct size (~2688bp) when run out on agarose gel (see figure 3.8. below).

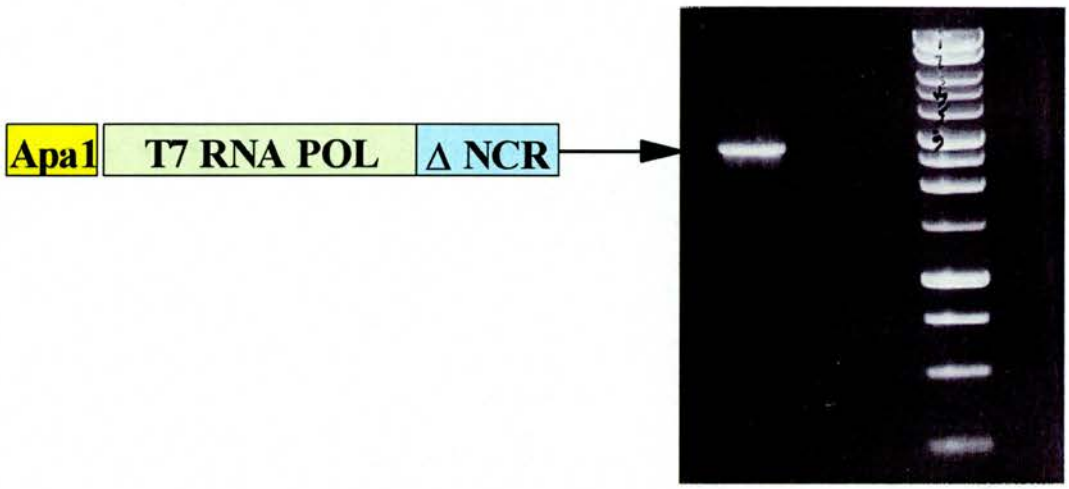

Figure 3.8. *Photograph of an agarose gel displaying what appeared to be the successfully constructed and 'correct' [ΔNCR, T7 RNA POL, Apa1] (~2688bp) PCR fragment.*

A PCR fragment corresponding to [T7 promoter, NCR, ΔT7] (shown in figure 3.5.), was not produced, however, despite many attempts to optimize the PCR protocol. The first and most obvious step, was to replace any of the PCR components which could possibly be, either out of date, or perhaps contaminated, e.g. Taq polymerase, dNTPs, primers etc. As this measure still produced no perceptible success, efforts were then prosecuted to achieve an optimum magnesium concentration and annealing temperature for the reaction. An annealing temperature gradient was applied starting at 40^0C, and rising in 1^0C increments to 65^0C. Concomitantly, a magnesium titration was performed, each PCR differing by 0.5mM $MgCl_2$, starting at 1.5mM $MgCl_2$, and rising to 8.0mM. Multiple combinations of the above steps were explored with no success.

The only apparent avenue left for exploration was to re-address the design of the reverse primer JLREV due to the T7 promoter forward primer being a well-known quantity. As the 5' NCR of HRV85 contains the IRES, which has a complex folded RNA secondary structure, I examined the sequence of reverse primer JLREV to look for any self-complementarity. Upon analyzing the sequence of primer JLREV using DNAMAN®

to perform a search for self-complementarity, I was disappointed to note that almost the entire NCR sector of the primer formed a stem-loop structure (see figure 3.9.).

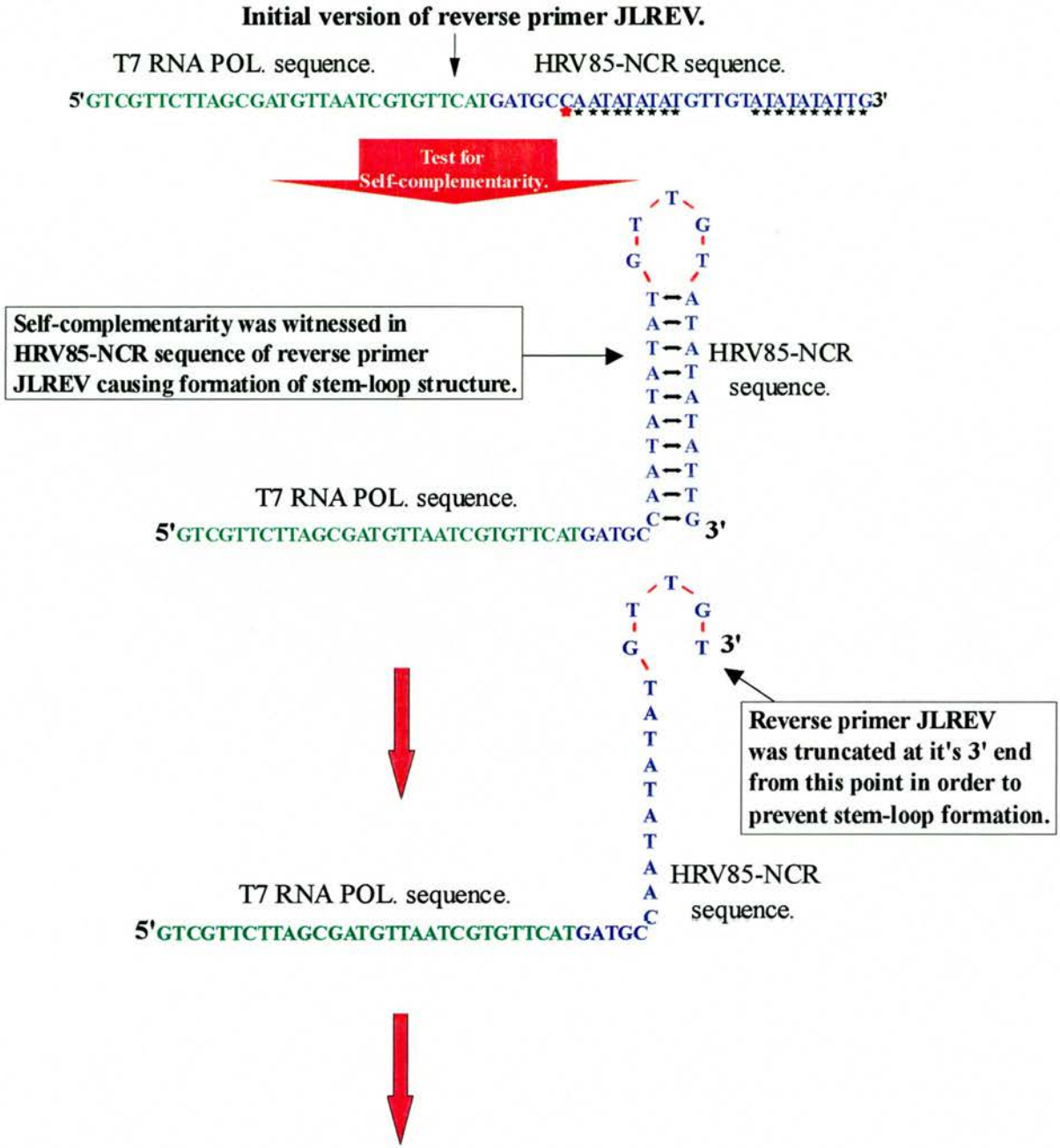

New truncated reverse primer JLREV.

5'GTCGTTCTTAGCGATGTTAATCGTGTTCATGATGCCAATATATATGTTGT3'

Figure 3.9. *Schematic describing the 10nt reduction made to the 3'end of reverse primer JLREV in order to avert formation of the stem-loop structure which was preventing its successful priming to the complementary NCR sequence of HRV85.*

This appeared to explain why no amount of PCR protocol 'fine-tuning' produced any perceptible improvement, i.e. the primer was unable to bind to the complementary sequences of HRV85-NCR cDNA due to the extent of self-annealing by the primer.

All stocks of JLREV were immediately discarded, and a 'new' JLREV was designed in which the section of the primer which was NCR sequence was truncated by 10nts at its 3' end and so was unable to self base-pair (Fig. 3.9.). After the redesign of primer JLREV, the PCR worked perfectly, producing a clear, discrete band of the predicted size (~650bp) when visualized on an agarose gel adjacent to PCR fragment [T7 promoter, NCR] which was used as a visual control size marker (see figure 3.10.).

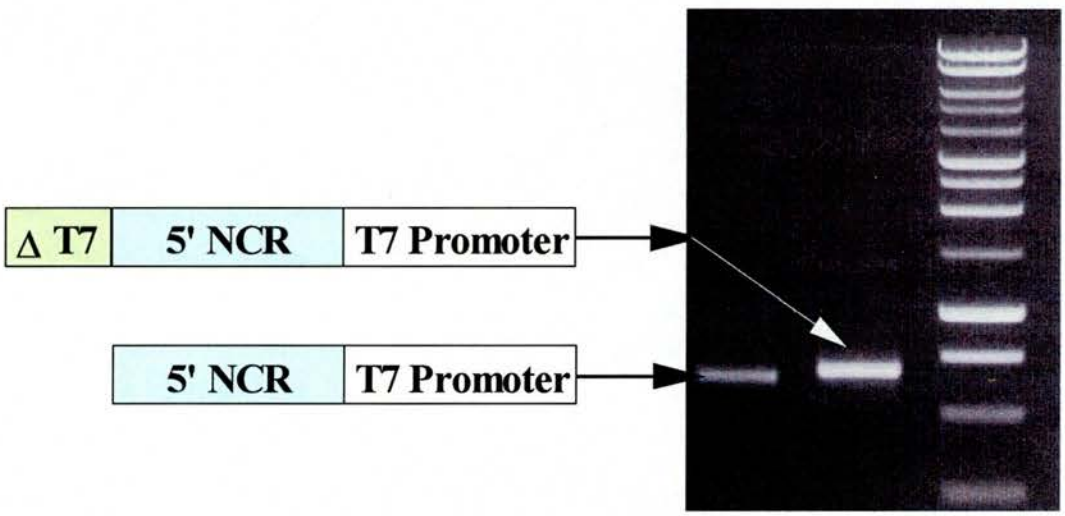

Figure 3.10. *Photograph displaying successfully amplified [T7 promoter, 5'NCR, ΔT7] PCR fragment run on agarose gel adjacent to a [T7 promoter, 5'NCR] PCR fragment which was used as a visual control size marker.*

Armed with both OL-PCR fragments, i.e. [T7promoter, NCR, ΔT7] and [ΔNCR, T7 RNA POL, *Apa*I], I proceeded directly to the OL-PCR procedure shown in figure 3.7., which would join together the 5'NCR of HRV85 to the gene encoding T7 RNA polymerase, i.e. [T7 promoter, NCR,T7 RNA POL, *Apa*I]. Using the two newly created PCR fragments as the DNA templates, the T7 promoter forward primer and T7 REV2 as the reverse primer, the OL reaction would seem quite straightforward.

Unfortunately, upon running a standard PCR as a preliminary attempt, and then visualizing the result on an agarose gel, it was apparent that there was now a severe problem to overcome with this stage of the strategy as can be seen in figure 3.11.

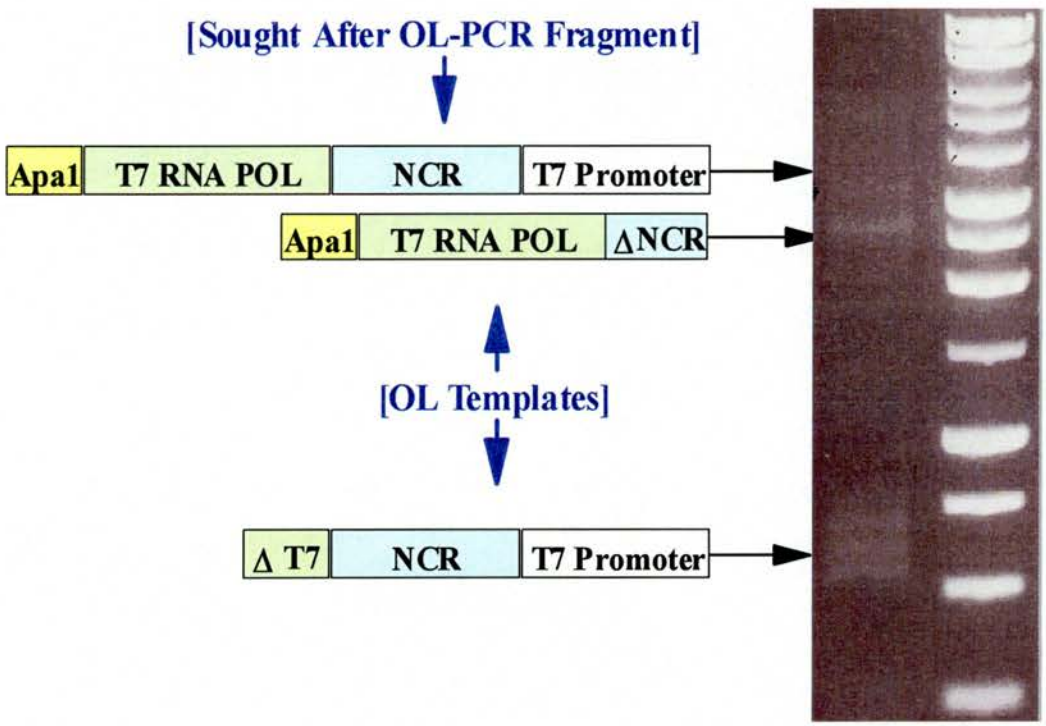

Figure 3.11. *Unsuccessful attempt to produce OL-PCR fragment [T7promoter, NCR, T7 RNA POL, Apa1], using PCR fragments; [T7promoter, NCR, ΔT7] and [ΔNCR, T7 RNA POL, Apa1] as templates.*

Although the gel (above) showed faint bands corresponding to the PCR fragment templates used in the reaction, there was virtually no evidence of the hoped-for PCR OL (fusion) of the two fragments.

I had started another round of annealing temperature gradients and magnesium titrations in an effort optimize this stage of the strategy, when, during talks with Martin Ryan, we realized that to some extent we had been building on sand, in that the same problem which had prevented the first version of reverse primer JLREV from priming to the 5'NCR of the HRV85 cDNA would be stopping the [ΔNCR, T7 RNA POL, *Apa*I] PCR fragment from priming to the [T7 promoter, NCR, ΔT7] PCR fragment, i.e. the 30nts of NCR sequence added onto the 5' end of T7 RNA POL by the forward primer JLFOR was forming a stem-loop structure and was therefore unable to bind to the complementary NCR sequence of the [T7 promoter, NCR, ΔT7] fragment, which would also be forming a stem-loop structure in its NCR sequences (see figure 3.12.).

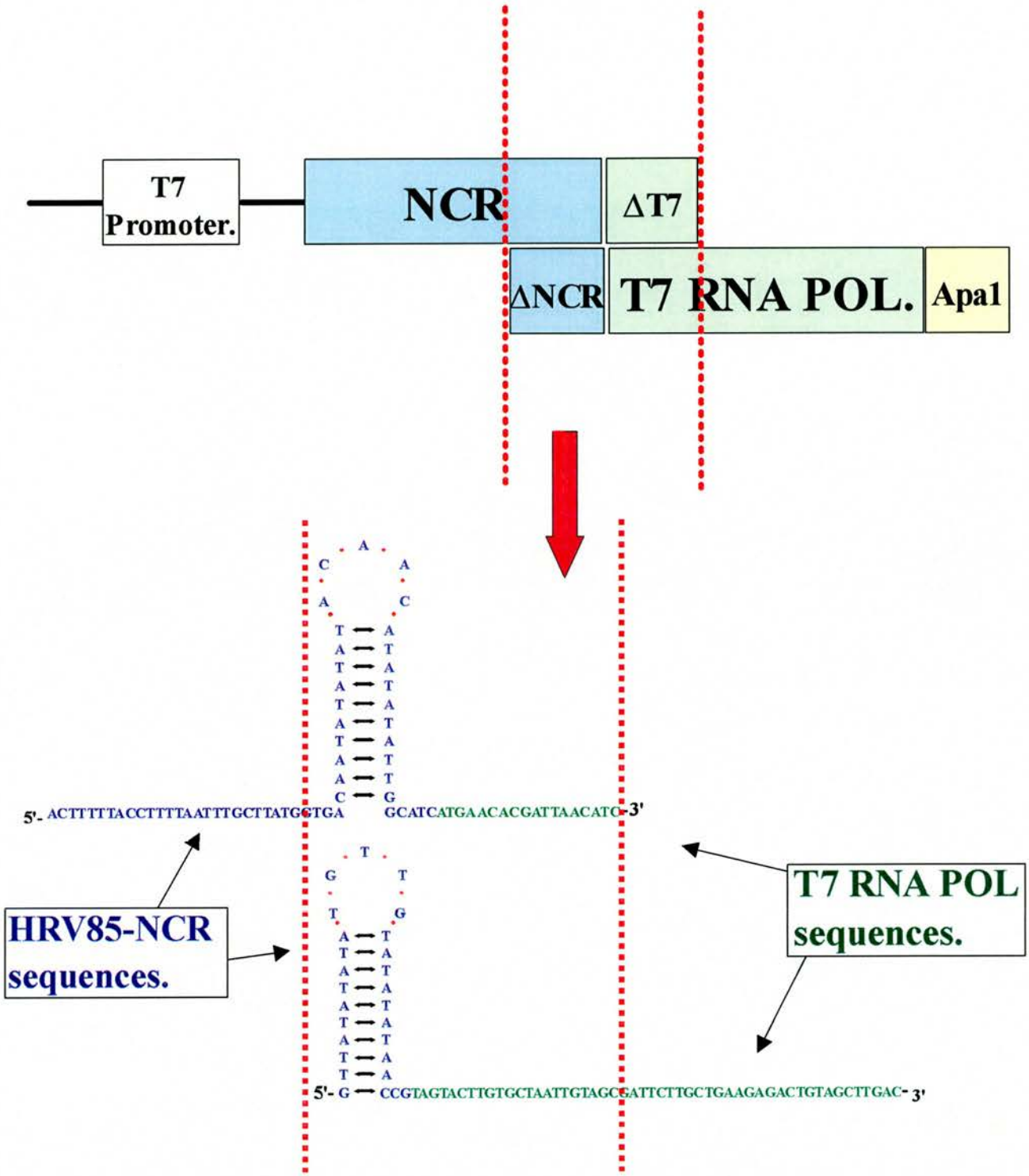

Figure 3.12. *Schematic displaying reason for failure of 1st over-lap PCR strategy, i.e. high level self-complementarity in the final 30nts of HRV85-5'NCR cDNA was causing formation of stem-loop structures, and thereby preventing adequate base-pairing of complementary sequences in the two PCR fragments.*

To circumvent this problem, I altered the OL-PCR protocol from that shown in figure 3.7., i.e.

- Both PCR fragment [ΔNCR,T7 RNA POL,*Apa*I] and the T7 promoter forward primer were discarded.
- PCR fragment [T7promoter,NCR,ΔT7], now took on the role of forward primer.
- Unmodified T7 RNA POL gene sequence was introduced as PCR template.
- T7REV2 was retained as the overall reverse primer (see figure 3.13. below).

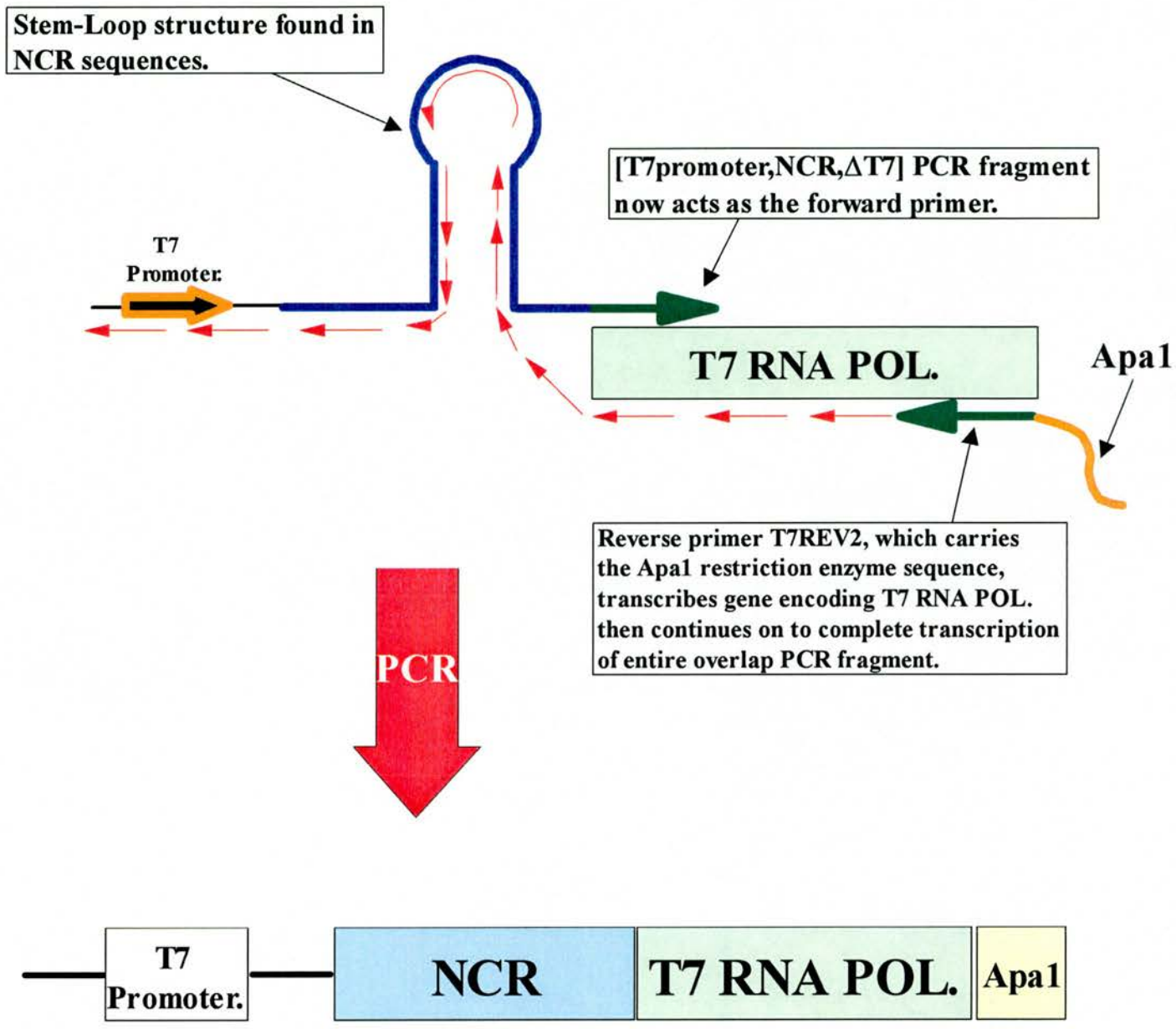

Figure 3.13. *Schematic describing the final 'successful' OL-PCR protocol used to produce a cDNA construct where the gene encoding T7 RNA polymerase and carrying an Apa1 restriction enzyme site, is fused to the 3'end of the HRV85-NCR.*

Using the newly modified OL-PCR protocol (figure 3.13.), I proceeded to run the reaction under standard PCR conditions. Once the reaction was complete, I attempted to visualize the product on an agarose gel (Fig. 3.14.) in a lane adjacent to one containing

PCR fragment [ΔNCR, T7 RNA POL, *Apa*I] (2688bp) which would serve as a 'rough' visual size-marker (an added precaution due to the relevance of fragment [T7promoter, NCR, T7 RNA POL, *Apa*I] to the construction of plasmid pHRV85-T7). As can be seen in figure 3.14., the newly modified OL-PCR protocol was successful, producing the desired OL-PCR fragment [T7promoter, NCR, T7 RNA POL, *Apa*I] (3300bp), the size marker (control) PCR fragment [ΔNCR, T7 RNA POL, *Apa*I] providing further confirmation as to the exact size of [T7promoter, NCR, T7 RNA POL, *Apa*I] by appearing approx. 612bp smaller than the OL-PCR fragment.

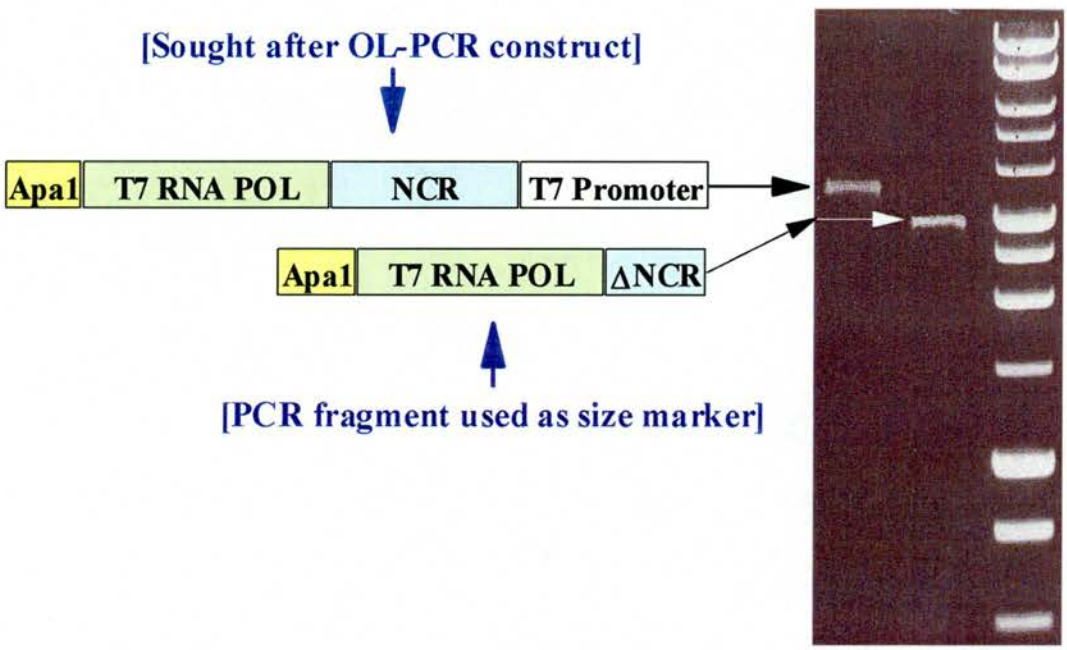

Figure 3.14. *Photograph of an agarose gel displaying the successfully assembled OL construct [T7promoter, NCR, T7 RNA POL, Apa1] (3300bp), run adjacent to a lane containing size marker (control) PCR fragment [ΔNCR, T7 RNA POL, Apa1] (2688bp). As can be seen from the gel, the sought after OL construct appears to be the desired 612bp larger than the control fragment.*

The third and final stage of the strategy, was to complete construction of plasmid pHRV85-T7. This proved to be a relatively simple matter, in that, as we recall from above (Fig.3.4.), the first stage of the strategy to create pHRV85-T7 was to doubly

restrict HRV85 cDNA with the REs *Apa*I and *Bam*HI (deleting 98% of the 5′ NCR and also the entire sequence encoding the P1 structural region).

Therefore, by performing an identical *Bam*HI/*Apa*I RE double digestion upon the newly created OL-PCR fragment [T7promoter, NCR, T7 RNA POL, *Apa*I] and producing restriction fragment [*Bam*HI, ΔNCR, T7 RNA POL, *Apa*I], it was a straightforward procedure to agarose gel purify and ligate the restriction fragment into the *Bam*H1/*Apa*1 restricted HRV85 cDNA, thereby completing assembly of plasmid pHRV85-T7 (see figure 3.15.).

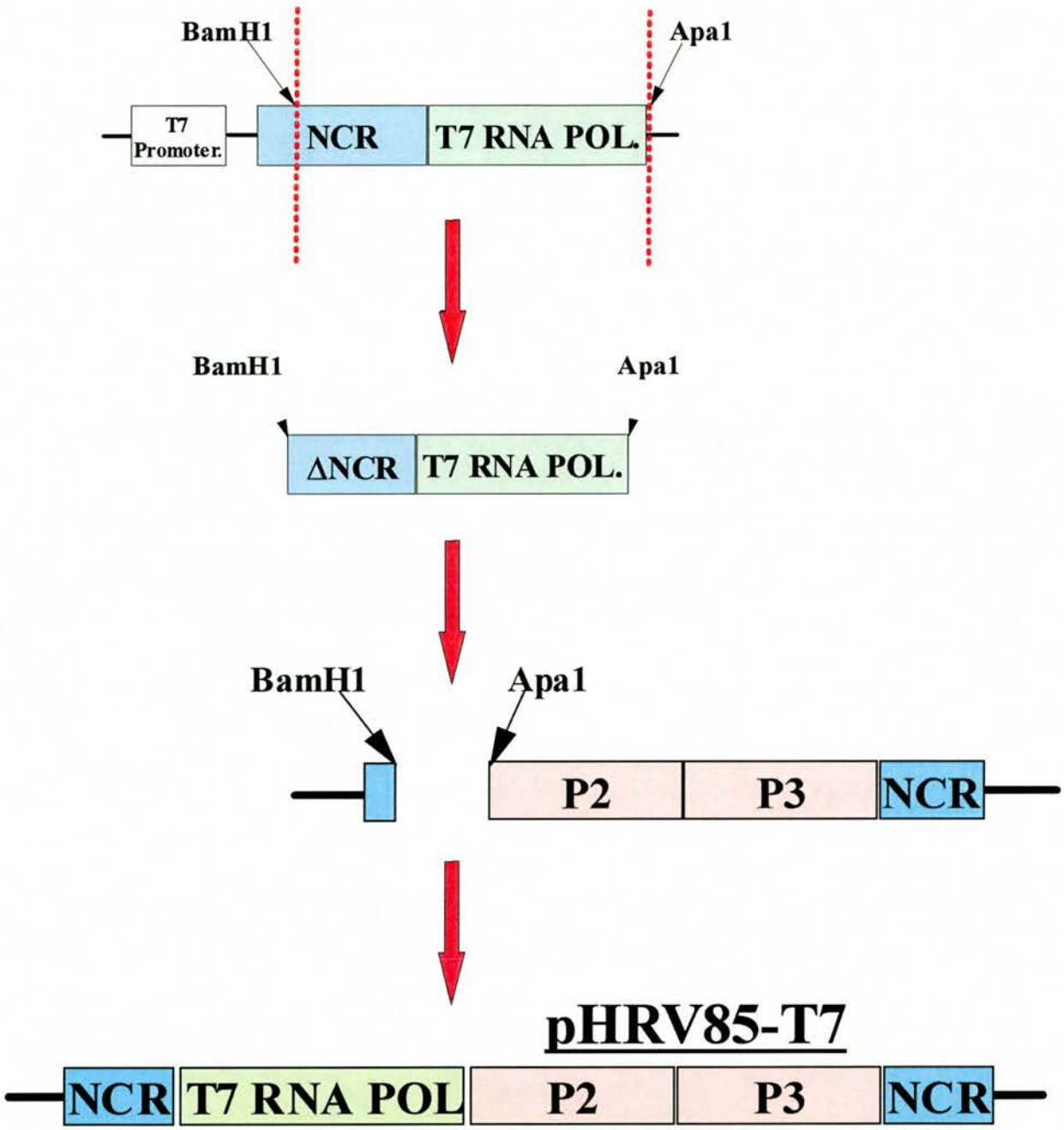

Figure 3.15. *BamH1/Apa1 double restriction of OL-PCR fragment [T7promoter,NCR,T7 RNA POL,Apa1], and ligation of the restricted fragment into similarly restricted HRV85 cDNA to create plasmid pHRV85-T7.*

3.5. Construction of plasmid pJMP1del. Plasmid pJMP1del was constructed in order to ascertain whether HRV85 cDNA would still be replication competent following removal of sequences encoding its entire P1 structural region.

Although creation of plasmid pJMP1del did not require quite as complex a strategy as that used to produce plasmid pHRV85-T7, the procedure was virtually identical, forgoing only the OL-PCR process used to fuse HRV85-5′NCR sequences to those encoding T7 RNA POL. Analogous to reverse primer T7REV2 described above, which was used in the production of pHRV85-T7, a new reverse primer (85P1del) was designed with additional sequences comprising an *Apa*I RE site, and which would prime to the 5′ NCR of HRV85, while at the same time adding an *Apa*I restriction site 'tail' to its 3′ end during the PCR (Fig. 3.16.). Reverse primer 85P1del was used in conjunction with the T7 promoter forward primer to produce PCR fragment P1del, i.e. [T7promoter, 5′NCR, *Apa*I]. P1del was then agarose gel purified before being doubly restricted with enzymes *Bam*H1 and *Apa*1.

The assembly of plasmid pJMP1del was then brought to fruition when restriction fragment [*Bam*H1, ΔNCR, *Apa*I] was agarose gel purified before being ligated into *Bam*HI/*Apa*I restricted HRV85 cDNA in a manner identical to that used to assemble pHRV85-T7 (compare figures 3.15. and 3.16.).

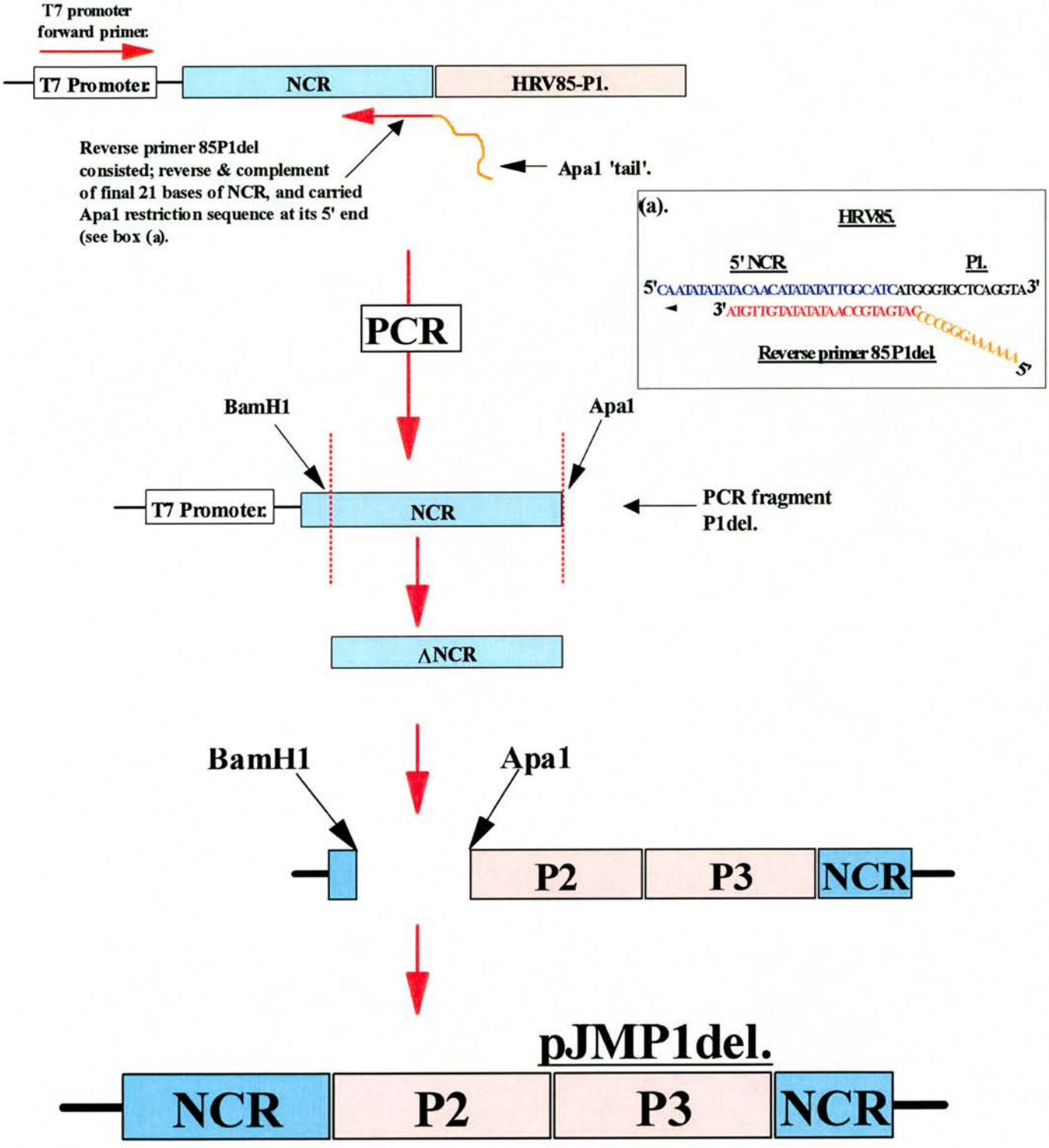

Figure 3.16. *Strategy used to create and assemble plasmid pJMP1del.*

3.6. Construction of plasmid pHRV85R. Plasmid pHRV85R consists of full length HRV85 cDNA minus a 669nt deletion encompassing 98.5% of the 5′ NCR region and 64nts from the 5′ terminus of the P1 structural region. This deletion renders the genome replication-incompetent due to the removal of the IRES structure which resides within the deleted sequences.

pHRV85R was created to serve as a negative control for the nucleic acid hybridization analysis of RNA replication since an HRV85 specific probe would hybridize to the input cDNA in the absence of any RNA replication.

As was mentioned above in section 3.3, HRV85 cDNA possesses two *Bam*HI RE sites, one at 9nts downstream of the 5′ terminus of the HRV85-5'NCR, and a second a further 669nts downstream of the first site. Therefore, by simply digesting HRV85 cDNA with RE *Bam*H1, isolating, agarose gel purifying, then re-ligating the larger restriction fragment, i.e. the plasmid containing HRV85 minus the 669nts [*Bam*HI, Δ5′NCR, ΔP1, *Bam*HI], I was able to remove a restriction fragment which contained most of the 5′ NCR, and also sequences encoding the N-terminal region of P1, thereby creating the desired virtually full length HRV85 cDNA which would not be replication competent (see figure 3.17.) – to act as a negative control in replication studies.

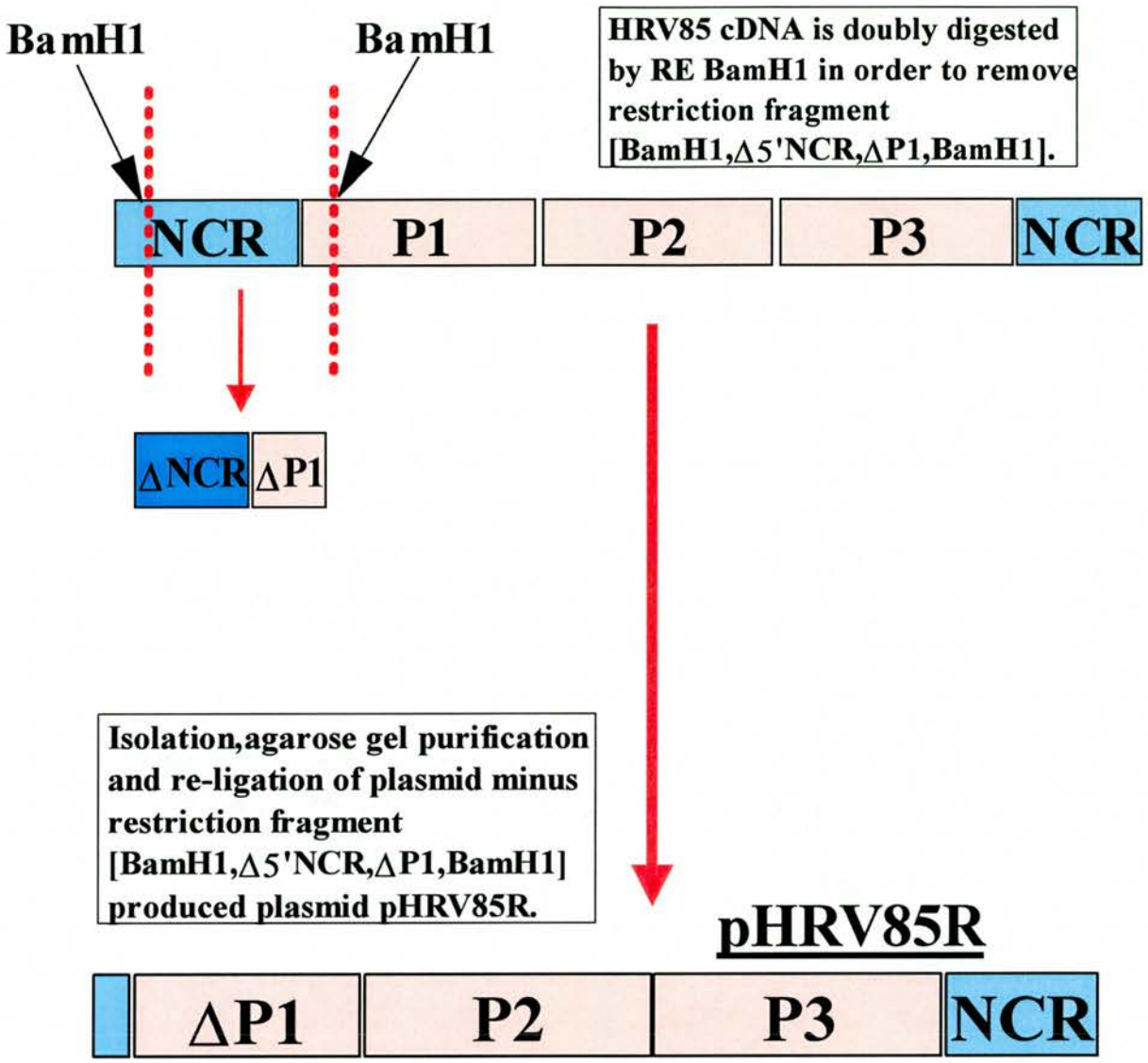

Figure 3.17. *Schematic showing the strategy used to create plasmid pHRV85R.*

4.0. Discussion.

4.1. The HRV85 genome encoding for the T7 RNA polymerase. The Ryan laboratory is primarily concerned with characterization studies of *Picornavirus* replication. One of the projects currently pursued by the laboratory, is expression of specific virus (or host cell) proteins and RNA tracts in the environment of replicating viral RNA in order to observe the effect(s) introducing these molecules may have upon the picornaviral replication process.

The ability to control the expression of these and other molecules would be greatly enhanced by the presence within infected cells of T7 RNA polymerase (T7 RNA POL) in order to drive their transcription. T7 RNA POL expressed by the HRV85 genome itself will allow co-expression of the above mentioned molecules solely in cells where RNA replication is in progress while concomitantly avoiding many of the problems associated with other methods of co-expression / co-transcription.

In order to pursue this objective, I have replaced sequences encoding the entire P1 capsid protein region (2577bp) with the gene for T7 RNA POL (2652bp), producing a recombinant genome 75nts larger than the wt.

As mentioned in section 3.4., my preliminary scheme (Fig. 3.4.) for insertion of the gene encoding T7 RNA POL into the HRV85-P1 'slot', initially seemed relatively straight forward, i.e.;

- Delete the HRV85 cDNA encoding the entire P1 region and 98% of the 5′NCR proximal to it.
- PCR amplify a cDNA fragment constituting the HRV85-5′NCR sequences.
- PCR amplify the gene encoding T7 RNA POL.
- Unite the two PCR fragments (5′NCR + T7 RNA POL = [5′NCR,T7 RNA POL]) using an OL-PCR strategy (Fig. 3.7.).
- Tailor (restrict) the newly fashioned OL-PCR construct, then insert the fragment into the HRV85-(Δ5′NCR-P1 deficient) cDNA to create an HRV85 cDNA genome where the gene for T7 RNA POL exists in place of a P1 region, i.e. [5′NCR,T7 RNA POL,P2,P3,3′NCR].

All appeared to proceed well until it came time to pursue the OL-PCR segment of the above protocol. The requirements (regarding the 5′NCR and T7 RNA POL PCR fragments) for the OL-PCR strategy (seen in figure 3.7.) demanded that;

(a) The 5′NCR PCR fragment possess (at its 3′ end) 30nts from the 5′ end of the T7 RNA POL gene, i.e. [T7promoter,NCR,ΔT7].

(b) The PCR fragment encoding T7 RNA POL should, (at its 5′ end) have 30nts from the 3′ end of the HRV85-5′NCR, and (at its 3′ end) sequences encoding an *Apa*1 RE site, i.e. [ΔNCR,T7 RNA POL,*Apa*1].

To this end, four primers were employed;

1. **T7 promoter forward primer.** A primer used frequently for cloning purposes as the forward primer for the transcription of recombinant plasmids.
2. **T7REV2.** A primer produced by the Ryan laboratory for previous studies (Cowton, 2000), which, while being a reverse primer involved in the transcription of the T7 RNA POL gene, also carried an *Apa*1 RE sequence at its 3′ end, thereby producing [T7 RNA POL,*Apa*1] PCR fragments.
3. **JLFOR.** Designed for this protocol (Fig. 3.6.), forward primer JLFOR comprised the final thirty nt at the 3′ end of the HRV85-5′NCR fused to the initial 30nts at the 5′ end of the T7 RNA POL gene, and was designed (when used with primer T7REV2, and the T7 RNA POL gene as template) to produce PCR fragment [ΔNCR,T7 RNA POL,*Apa*1].
4. **JLREV.** Also designed for this protocol (Fig. 3.5.), this reverse primer was the reverse and complement of forward primer JLFOR and was designed with the intention that when employed in a PCR with the T7 promoter forward primer and using unmodified HRV85 cDNA as template, JLREV would generate PCR fragment [T7promoter,NCR,ΔT7].

As is detailed in section 3.4., PCR fragment [ΔNCR,T7 RNA POL,*Apa*1] was yielded at virtually the first attempt using a standard PCR environment (Fig. 3.8.), while fragment [T7promoter,NCR,ΔT7], despite the large variety PCR environments attempted, could not be produced. After a reappraisal of the situation, and an obligatory removal,

replacement or alteration of any PCR component which could possibly inhibit the reaction, primer JLREV began to emerge as the most likely source of the problem.

Given that primer JLFOR appeared to be working (Fig. 3.8.), and therefore must be annealing to the initial 30nts at the 5′ end of the template (T7 RNA POL gene), and that primer JLREV was the reverse and compliment of JLFOR, it was reasonable to presume that a design fault may exist in the HRV85-5′NCR sector of the primer sequences.

The 5′ NCR of HRV is known to contain three independent domains (see figure 4.1. below), i.e.;

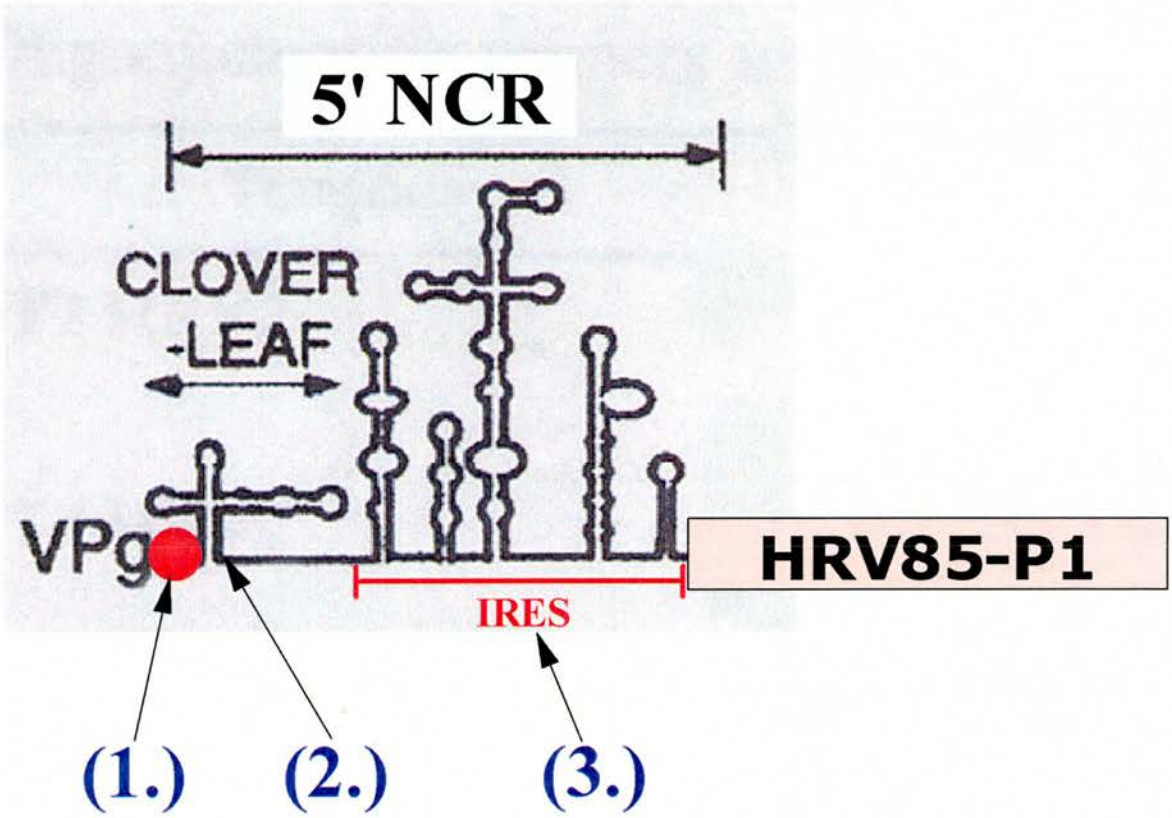

Figure 4.1. *Schematic displaying the three independent functional elements contained within the sequences of the HRV2 5′ NCR. (1.) 5′ terminal protein VPg (3B). (2.) Cloverleaf-like RNA secondary structure. (3.) IRES.*

1. The terminal protein VPg, which is involved in the initiation of minus-strand synthesis during replication (Paul *et al.*, 1998).

2. A cloverleaf-like RNA secondary structure containing about 100 nt which is involved both in plus-strand RNA synthesis (Andino *et al.*, 1990; Andino *et al.*, 1993; Harris *et al.*, 1994; Xiang *et al.*, 1995) and in the process of switching from translation to replication (Gamarnik and Andino, 1988).
3. The large and complex RNA secondary structure, the IRES, which has a primary function of controlling translation (Borman and Jackson, 1992; Jang et al., 1988; Pelletier and Sonnenberg, 1988), but mutations in this structure also appear to have deleterious effects on RNA replication (Borman and Jackson, 1994; Shiroki et al., 1995).

Looking at figure 4.1. we see that the RNA secondary structure proximal to the 3′ end of the 5′NCR of HRV85 is the complexly folded IRES. This data, when coupled with the relatively lengthy form of JLREV ([thirty 5′NCR nts] + [thirty T7RNA POL nts]), led me to perform a search (using DNAMAN®) for sequence self-complimentarity in primer JLREV. The astonishing response provided by DNAMAN® was that virtually the entire NCR sequence (~85%) of primer JLREV was forming a single stem-loop structure (see Fig. 3.9.) – including the critical 3'-terminal base. This information provided a reasonably unambiguous answer to the question of why PCR fragment [T7promoter,NCR,ΔT7] was proving so difficult to produce, i.e. during the annealing stage of the PCR, primer JLREV could not prime to the complementary sequences of HRV85-5′NCR cDNA due to the extent of self-annealing by the primer.

Upon close inspection of a JLREV sequence printout, it appeared that a 10nt truncation at the 3′ end of the primer should eliminate its ability to self base-pair. All remaining stocks of the flawed JLREV were immediately discarded, and a new truncated form of primer JLREV was designed where the 3′ terminal 10nts were deleted (Fig. 3.9.).

As a preliminary attempt, I applied the new truncated JLREV to a PCR of similar environment to that used to successfully produce PCR fragment [ΔNCR, T7 RNA POL, *Apa*1]. The new primer worked perfectly, producing a distinct PCR fragment of the desired size (see figure 3.10.).

Following this success, I proceeded directly to the OL-PCR described in figure 3.7, and with a view to gauge what modifications if any the PCR might require, I ran a

relatively standard reaction. When the results from the PCR were visualized on an agarose gel (seen in figure 3.11.), it was evident that a serious flaw still existed within the protocol as there was no perceptible sign of the sought after OL-PCR fragment [T7 promoter, NCR, T7 RNA POL, *Apa*1] (~3300bp). This was a very discouraging turn of events as (provided there had been no error while performing the PCR protocol) no product at all hinted that another serious obstacle to the success of the reaction had materialized.

Realizing however, that PCRs are often extremely sensitive to even the subtlest protocol modification, my preliminary strategy to discover and eliminate the new obstacle, was to the repeat the methodology initially employed to attempt to determine that reverse primer JLREV was foiling production of PCR fragment [T7 promoter, NCR, ΔT7], i.e. remove, replace or alter any component of the PCR protocol which could possibly have a detrimental influence upon the reaction. This approach however, was proceeding with little or no success until, during discussions with Martin Ryan we noted that one area where this latest obstruction resembled the previous problem (production of fragment [T7 promoter, NCR, ΔT7]), was that virtually no alteration to the PCR environment (however extreme) had any positive effect upon the result. This tenuous similarity between the two problems led to closer examination of all primers and PCR products to-date, which, in turn, led to the realization that I had overlooked the obvious.

As already stated above, the initial form of reverse primer JLREV had failed to bind to complementary sequences on HRV85-5′NCR due to extensive self-complementarity within the primer causing formation of a stem-loop structure. Functionality of the primer was only rescued upon deletion of the terminal 10nts from the 3′ end.

Forward primer JLFOR (along with reverse primer T7REV2 and template gene T7 RNA POL) was used to produce PCR fragment [ΔNCR, T7 RNA POL, *Apa*1]. Due to primer JLFOR being the reverse and complement of the initial non-truncated version of reverse primer JLREV, it possessed the same flaw as the reverse primer, i.e. JLFOR, along with reverse primer T7REV2, had produced a PCR fragment ([ΔNCR, T7 RNA POL, *Apa*1]), which was unable to bind to the complementary sequences of PCR

fragment [T7promoter, NCR, ΔT7], due to extensive self-annealing and stem-loop formation within the NCR sequences of both fragments.

The possible solution to this latest barrier came in the form of two alternatives; (a). Truncate the 5′ terminal NCR sequences of forward primer JLFOR in a manner identical to that used to reinstate the functionality of reverse primer JLREV. Re-PCR amplify fragment [ΔNCR, T7 RNA POL, *Apa*1] using the new truncated JLFOR, then re-try the OL-PCR strategy seen in figure 3.7.

(b). Modify the OL strategy seen in Fig. 3.7., i.e. use PCR fragment [T7promoter, NCR, ΔT7] as the forward primer, with unmodified T7 RNA POL gene as the PCR template. Retain reverse primer T7REV2 as it carried the essential *Apa I* RE site (see figure 3.13.).

The later option (b) was chosen as, comparison of the diagrams shown in figures 3.7. and 3.13, which visually portray the two alternatives (a) and (b) respectively, reveals that, in effect, option (b) was merely a more efficient derivative of option (a). I consequently ran an OL-PCR under standard conditions using the modified protocol seen in figure 3.13. and was rewarded with the desired OL-PCR fragment [T7promoter, NCR, T7 RNA POL, *Apa*I] (3300bp) which was visualized on agarose gel (see figure 3.14.).

From this point, it was a relatively straight forward procedure to restrict the newly created OL-PCR construct with REs *Bam*H1 and *Apa*1, then insert the fragment into the previously fashioned HRV85-(Δ5′NCR-P1 deleted) cDNA to produce HRV85 cDNA in which the P1 capsid coding region (2577bp) had been replaced by the gene encoding T7 RNA POL (2652bp) (see figure 3.15.).

4.2. cis–Acting Replication Elements (CREs). All *Picornaviruses* show a strong similarity in their gene organization and in the mechanism by which they replicate their genomes (Rueckert, 1996), indeed, the replicative (nonstructural) proteins encoded by these viruses contain several conserved domains, suggesting that these proteins, in concert with host cell components, support similar mechanisms for replication of the viral RNA (Hodgman, 1988).

Viral RNA replication takes place in the cytoplasm of the infected host cell on membranous vesicles (Bienz *et al.*, 1992; Koliais and Dimmock, 1974; Yin and Knight, 1972), and the enzyme primarily responsible for RNA synthesis is the viral RNA-dependent RNA polymerase $3D^{pol}$, which is both primer and template dependent (Flanegan and Baltimore, 1977; Gerber *et al.*, 2001; Koliais and Dimmock, 1974; Yin and Knight, 1972). The parental RNA is first transcribed into a minus strand, which in turn is used as a template for the production of the progeny plus strands. Finally, the progeny viral RNA is encapsidated and released from the host cell.

While the basic steps of the viral genome replication are well documented, much remains unknown about the intricacies of these processes and in particular, about the precise functions of the *cis*-acting RNA structures contained within the picornaviral genome (Agol *et al.*, 1999). Indeed, one of the most important unanswered questions about minus strand synthesis is, how does $3D^{pol}$ recognize and select only its own RNA as template among the many polyadenylated mRNAs present in the host cell? (Paul *et al.*, 1998).

Until fairly recently, the 5′ and 3′ NCR termini of picornaviral genomes were considered to posses all of the *cis*-acting signal(s) required by the viral RNA replicase to initiate transcription, indeed, the 3′ NCR had been elected the origin of replication (*oriR*) for minus strand RNA synthesis (Pilipenko *et al.*, 1996), however, subsequent studies cast doubt over this hypothesis, i.e. it was found that deletion of the entire 3′ NCR region of *Poliovirus* type-1 Mahoney [PV1(M)] did not fully eliminate RNA replication (Todd *et al.*, 1997). Contemporary data has brought to light the existence of *cis*-acting replication elements (CREs) essential to minus-strand synthesis, within both the structural and non-structural coding regions of a number of *Picornavirus* serotypes.

In 1995, McKnight and Lemon, intrigued by studies at the time where *Poliovirus* P1 capsid-coding sequences were replaced by RNA encoding heterologous proteins without compromise of viral RNA replication (Andino *et al.*, 1993; Choi *et al.*, 1991 ; Percy *et al.*, 1992), constructed HRV14 replicons with reporter protein sequences (β-galactosidase or luciferase), where segments of the P1 region were removed in-frame from the genome. They found that HRV14 mutants with deletions involving the 5′ 1,498nts of the P1 region replicated efficiently, while those with deletions involving the

3′ 1,079nts of the region did not. Reintroduction of the 3′-P1 sequences was found to reinstate replication competency. Capsid proteins provided in *trans* by helper virus failed to rescue the replicon with the 3′-P1 sequence deletion, but were able to package the replicon upon reinstatement of the deleted 3′-P1 sequences. This led to the conclusion that a ~1-kb sector (nt 2117- nt 3196) at the 3′ end of the P1 structural region of HRV14 contained a previously unrecognized *cis*-acting function essential to efficient replication of HRV14 RNA (McKnight and Lemon, 1996).

In a later study McKnight and Lemon (1998) showed that a CRE indispensable to HRV14 genome replication mapped to a 96nt sequence located within RNA encoding the amino terminal segment of the capsid protein VP1 (McKnight and Lemon, 1998). McKnight and Lemon also demonstrated that the CREs function was dependent upon formation of a stable stem-loop structure within the positive-strand RNA (McKnight and Lemon, 1998). Analogous elements have since been found in the VP2 coding sequences of *Mengovirus* and *Theiler's virus* (Lubert *et al.*, 1999), the $2C^{ATPase}$ coding sequence of *Poliovirus* (Goodfellow *et al.*, 2000), and within the sequence encoding $2A^{pro}$ of HRV2 (Gerber *et al.*, 2001).

The internally located CREs of these *Picornaviruses* were all found to consist of a simple hairpin-loop structure, but possessed widely varying nucleotide sequences, (Goodfellow *et al.*, 2000; Lubert *et al.*, 1999; McKnight and Lemon, 1998; Paul *et al.*, 2000; Rieder *et al.*, 2000) except for a conserved AAACA motif in the loop (Paul *et al.*, 2000; Rieder *et al.*, 2000).

Replication of the *Picornavirus* positive-stranded RNA genome begins by the synthesis of the complementary minus strand. Minus-strand synthesis is initiated by the covalent attachment of uridine-monophosphate (UMP) to the terminal protein VPg, yielding products VPgpU and VpgpUpU, the precursors of VPg-linked poly-U, the 5′ end of minus-strand RNA (Paul *et al.*, 1998). It has recently been shown in PV1(M), that it is the first two A's of the conserved CRE motif $A_1A_2A_3CA$ (located within the sequences encoding viral protein 2C), and not the poly (A) tail, which serves as the primary template for the *in vitro* synthesis of VPgpU and VpgpUpU (Paul *et al.*, 2000; Rieder *et al.*, 2000).

4.2.1. Possible impact of CRE upon the aims of this project. The fact that the entire P1 structural region of plasmid pJMP1del (Fig. 3.16) was deleted, and in the case of pHRV85-T7 (Fig. 3.15) replaced, means that the possible presence and hence location of an internally positioned HRV85 CRE, has potentially great bearing upon this project, i.e. if, as in the case of HRV14, the HRV85 CRE was found to be resident in the P1 structural region (McKnight and Lemon, 1998), pJMP1del and pHRV85-T7 would not possess replication competency. However, the recent data (mentioned above) identifying the presence of a CRE within the $2A^{pro}$ coding region of HRV2 (Gerber *et al.*, 2001) has provided some reason to anticipate that pJMP1del and pHRV85-T7 will indeed be replication competent. Sequence analysis recently performed by the Ryan laboratory has indicated three sites within the P2 coding region, where the aforementioned AAACA motif is conserved amongst HRVs – other than HRV14. Additional data produced by the Ryan laboratory from RNA folds and covariance analyses has indicated one potential HRV85 CRE site identical to that published by Gerber *et al.*, 2001.

If, however, it transpires that both pJMP1del and pHRV85-T7 are not replication competent, it would clearly be a strong indication that the HRV85 CRE does indeed reside within the sequences encoding the P1 structural region. In this eventuality, it is reasonable to suppose that the HRV85 CRE could be mapped by systematic reinsertion of a series of P1 sequences into pJMP1del. Once located, the sequences containing the CRE could be specifically incorporated to return replication competency to the modified genomes.

4.3. Future studies. The availability of newly constructed recombinant HRV85 plasmids; pHRV85-T7 (Fig. 3.15.) and pJMP1del (Fig. 3.16.), now permits the following lines of enquiry:

1. Examine the replicative, translational and encapsidation capabilities of these constructs (the entire HRV85-T7 cDNA recombinant genome is currently in the process of being transferred into an SP6 polymerase-driven transcription vector in order to avoid the 'autogene' effect of a construct generating T7 RNA POL, being driven by a T7 promoter and therefore giving rise to transcription 'imitating' RNA replication).

2. Study the expression and enzymic activity of T7 RNA POL directed by the HRV85 genome.

4.3.1. Replication and translation studies. The preliminary issue to be resolved is; are recombinant plasmids pHRV85-T7 and pJMP1del replication competent? And if not? Why not?

One feature that both pHRV85-T7 and pJMP1del share is that neither plasmid possesses a P1 capsid coding region. Therefore, if both pHRV85-T7 and pJMP1del are found to be replication incompetent, it would suggest that an essential *cis*-acting replication element, discussed in section 4.2, may be resident in the deleted or replaced sequences. If this were found to be the case, the method by which the CRE may be mapped and re-integrated into the plasmids in order to reinstate replication competency is summarized in section 4.2.1.

pHRV85-T7 and pJMP1del will be analyzed by transfection of the plasmids into HeLa cells, and dot-blot hybridization of cell extracts at different time points, using a probe to detect negative sense HRV85 sequences. Background hybridization from the input cDNA / transcript RNA will be monitored by the comparison of a negative control (replication incompetent pHRV85R (Fig. 3.17.)), with; full-length infectious HRV85 cDNA (positive-control), pJMP1del and pHRV85-T7.

Translation and polyprotein processing will be analyzed by *in vitro* coupled transcription/translation systems (rabbit reticulocyte lysates / wheatgerm extracts), and SDS PAGE analysis. The polyprotein processing event which will come under the majority of scrutiny will be the ability of $2A^{pro}$ (or lack of it) to cleave at its own N-terminus in plasmid pHRV85-T7. The junction between T7 RNA POL and $2A^{pro}$ was designed to permit (if required) the making of minimal changes to the C-terminus of T7 RNA POL. The ααs upstream of the cleavage site may need alteration by site-directed mutagenesis in order to maximize cleavage, although it should be noted that $2A^{pro}$ primary cleavage at the P1-P2 junction of the polyprotein (in *cis*) has been shown to be insensitive to mutations around the cleavage site, only branched side-chain αα at the P1 position inhibiting cleavage (reviewed in Ryan and Flint (1997).

4.3.2. T7 RNA POL expression. A reporter plasmid encoding either luciferase, enhanced green fluorescent protein (eGFP), or cyan fluorescent protein (CFP) (conditional on which type of analysis performed), under the control of the T7 promoter, will be co-transfected along with plasmid pHRV85-T7 (SP6 polymerase driven transcription) in order to monitor T7 RNA POL expression levels.

4.3.3. Encapsidation capabilities. *Poliovirus* genomes with the majority of the P1 capsid coding region deleted have been encapsidated by *wt* helper virus (Barclay *et al.*, 1998). Therefore, it is not unrealistic to presume that the P1 sequence deletion or replacement genomes of pJMP1del and pHRV85-T7 respectively, may similarly be encapsidated. Trans-encapsidation experiments will be executed using HRV85 as the helper virus. A construct encoding the IRES-P1 region of HRV85 under the control of the T7 promoter, would be co-transfected in conjunction with pHRV85-T7 in order to gauge the yield of particles containing the recombinant genome.

References.

Acharya, R., E. Fry, D. Stuart, G. Fox, D. Rowlands, and F. Brown. 1989. The three-dimensional structure of foot-and-mouth disease virus at 2.9 A resolution. Nature **337:**709-16.

Agol, V. I. 1991. The 5'-untranslated region of picornaviral genomes. Adv Virus Res **40:**103-80.

Agol, V. I., A. V. Paul, and E. Wimmer. 1999. Paradoxes of the replication of picornaviral genomes. Virus Res **62:**129-47.

Aldabe, R., A. Barco, and L. Carrasco. 1996. Membrane permeabilization by poliovirus proteins 2B and 2BC. J Biol Chem **271:**23134-7.

Allaire, M., M. M. Chernaia, B. A. Malcolm, and M. N. James. 1994. Picornaviral 3C cysteine proteinases have a fold similar to chymotrypsin-like serine proteinases. Nature **369:**72-6.

Alvey, J. C., E. E. Wyckoff, S. F. Yu, R. Lloyd, and E. Ehrenfeld. 1991. cis- and trans-cleavage activities of poliovirus 2A protease expressed in Escherichia coli. J Virol **65:**6077-83.

Ambros, V., and D. Baltimore. 1978. Protein is linked to the 5' end of poliovirus RNA by a phosphodiester linkage to tyrosine. J Biol Chem **253:**5263-6.

Ambros, V., R. F. Pettersson, and D. Baltimore. 1978. An enzymatic activity in uninfected cells that cleaves the linkage between poliovirion RNA and the 5' terminal protein. Cell **15:**1439-46.

Anderson, A. H., B. S. Sorensen, K. Christiansen, J. Q. Svejstrup, K. Lund, and O. Westergaard. 1991. Studies of the topoisomerase II-mediated cleavage and religation reactions by use of a suicidal double-stranded DNA substrate. J Biol Chem **266:**9203-10.

Andino, R., G. E. Rieckhof, P. L. Achacoso, and D. Baltimore. 1993. Poliovirus RNA synthesis utilizes an RNP complex formed around the 5'-end of viral RNA. Embo J **12:**3587-98.

Andino, R., G. E. Rieckhof, and D. Baltimore. 1990. A functional ribonucleoprotein complex forms around the 5' end of poliovirus RNA. Cell **63:**369-80.

Andino, R., G. E. Rieckhof, D. Trono, and D. Baltimore. 1990. Substitutions in the protease (3Cpro) gene of poliovirus can suppress a mutation in the 5' noncoding region. J Virol **64:**607-12.

Ansardi, D. C., D. C. Porter, and C. D. Morrow. 1992. Myristoylation of poliovirus capsid precursor P1 is required for assembly of subviral particles. J Virol **66:**4556-63.

Bachrach, H. L., and W. R. Hess. 1973. Animal picornaviruses with a single major species of capsid protein. Biochem Biophys Res Commun **55:**141-9.

Bachrach, H. L., J. B. Swaney, and G. F. Vande Woude. 1973. Isolation of the structural polypeptides of foot-and-mouth disease virus and analysis of their C-terminal sequences. Virology **52:**520-8.

Barclay, W., Q. Li, G. Hutchinson, D. Moon, A. Richardson, N. Percy, J. W. Almond, and D. J. Evans. 1998. Encapsidation studies of poliovirus subgenomic replicons. J Gen Virol **79:**1725-34.

Barton, D. J., and J. B. Flanegan. 1997. Synchronous replication of poliovirus RNA: initiation of negative-strand RNA synthesis requires the guanidine-inhibited activity of protein 2C. J Virol **71:**8482-9.

Batson, S., and K. Rundell. 1991. Proteolysis at the 2A/2B junction in Theiler's murine encephalomyelitis virus. Virology **181:**764-7.

Bazan, J. F., and R. J. Fletterick. 1988. Viral cysteine proteases are homologous to the trypsin-like family of serine proteases: structural and functional implications. Proc Natl Acad Sci U S A **85:**7872-6.

Bazan, J. F., and R. J. Fletterick. 1989. Comparative analysis of viral cysteine protease structural models. FEBS Lett **249:**5-7.

Bergmann, E. M., S. C. Mosimann, M. M. Chernaia, B. A. Malcolm, and M. N. James. 1997. The refined crystal structure of the 3C gene product from hepatitis A virus: specific proteinase activity and RNA recognition. J Virol **71:**2436-48.

Bienz, K., D. Egger, T. Pfister, and M. Troxler. 1992. Structural and functional characterization of the poliovirus replication complex. J Virol **66:**2740-7.

Blair, W. S., S. S. Hwang, M. F. Ypma-Wong, and B. L. Semler. 1990. A mutant poliovirus containing a novel proteolytic cleavage site in VP3 is altered in viral maturation. J Virol **64:**1784-93.

Blondel, B., R. Crainic, O. Fichot, G. Dufraisse, A. Candrea, D. Diamond, M. Girard, and F. Horaud. 1986. Mutations conferring resistance to neutralization with monoclonal antibodies in type 1 poliovirus can be located outside or inside the antibody-binding site. J Virol **57:**81-90.

Bonner, G., E. M. Lafer, and R. Sousa. 1994. Characterization of a set of T7 RNA polymerase active site mutants. J Biol Chem **269:**25120-8.

Bonner, G., E. M. Lafer, and R. Sousa. 1994. The thumb subdomain of T7 RNA polymerase functions to stabilize the ternary complex during processive transcription. J Biol Chem **269:**25129-36.

Borman, A., and R. J. Jackson. 1992. Initiation of translation of human rhinovirus RNA: mapping the internal ribosome entry site. Virology **188:**685-96.

Borman, A. M., F. G. Deliat, and K. M. Kean. 1994. Sequences within the poliovirus internal ribosome entry segment control viral RNA synthesis. Embo J **13:**3149-57.

Brautigam, C. A., and T. A. Steitz. 1998. Structural principles for the inhibition of the 3'-5' exonuclease activity of Escherichia coli DNA polymerase I by phosphorothioates. J Mol Biol **277:**363-77.

Brautigam, C. A., and T. A. Steitz. 1998. Structural and functional insights provided by crystal structures of DNA polymerases and their substrate complexes. Curr Opin Struct Biol **8:**54-63.

Brown, M. A., and J. P. Nadler. 1996. Infections in HIV-Infected Patients With Malignancy. Cancer Control **3:**544-551.

Calenoff, M. A., C. S. Badshah, M. C. Dal Canto, H. L. Lipton, and M. K. Rundell. 1995. The leader polypeptide of Theiler's virus is essential for neurovirulence but not for virus growth in BHK cells. J Virol **69:**5544-9.

Cao, J., R. A. Vescio, M. B. Rettig, C. H. Hong, A. Kim, J. C. Lee, A. K. Lichtenstein, and J. R. Berenson. 1995. A CD10-positive subset of malignant cells is identified in multiple myeloma using PCR with patient-specific immunoglobulin gene primers. Leukemia **9:**1948-53.

Carroll, A. R., D. J. Rowlands, and B. E. Clarke. 1984. The complete nucleotide sequence of the RNA coding for the primary translation product of foot and mouth disease virus. Nucleic Acids Res **12:**2461-72.

Charpentier, N., M. Davila, E. Domingo, and C. Escarmis. 1996. Long-term, large-population passage of aphthovirus can generate and amplify defective noninterfering particles deleted in the leader protease gene. Virology **223:**10-8.

Chen, H. H., W. P. Kong, and R. P. Roos. 1995. The leader peptide of Theiler's murine encephalomyelitis virus is a zinc-binding protein. J Virol **69:**8076-8.

Choi, W. S., R. Pal-Ghosh, and C. D. Morrow. 1991. Expression of human immunodeficiency virus type 1 (HIV-1) gag, pol, and env proteins from chimeric HIV-1-poliovirus minireplicons. J Virol **65:**2875-83.

Chow, C. B., K. Y. Chan, A. Tam, L. C. Ho, W. Y. Ho, and W. K. Chang. 1987. Outbreak of echo virus type 11 infection in newborn infants in a maternity ward: clinical presentation. J Trop Pediatr **33:**305-8.

Chumakov, K. M., and V. I. Agol. 1976. Poly(C) sequence is located near the 5'-end of encephalomyocarditis virus RNA. Biochem Biophys Res Commun **71:**551-7.

Clarke, B. E., D. V. Sangar, J. N. Burroughs, S. E. Newton, A. R. Carroll, and D. J. Rowlands. 1985. Two initiation sites for foot-and-mouth disease virus polyprotein in vivo. J Gen Virol **66:**2615-26.

Cole, C. N., and D. Baltimore. 1973. Defective interfering particles of poliovirus. IV. Mechanisms of enrichment. J Virol **12:**1414-26.

Cole, C. N., and D. Baltimore. 1973. Defective interfering particles of poliovirus. 3. Interference and enrichment. J Mol Biol **76:**345-61.

Cole, C. N., and D. Baltimore. 1973. Defective interfering particles of poliovirus. II. Nature of the defect. J Mol Biol **76:**325-43.

Colonno, R. J., J. H. Condra, S. Mizutani, P. L. Callahan, M. E. Davies, and M. A. Murcko. 1988. Evidence for the direct involvement of the rhinovirus canyon in receptor binding. Proc Natl Acad Sci U S A **85:**5449-53.

Date, T., S. Yamamoto, K. Tanihara, Y. Nishimoto, and A. Matsukage. 1991. Aspartic acid residues at positions 190 and 192 of rat DNA polymerase beta are involved in primer binding. Biochemistry **30:**5286-92.

DeLange, A. M. 1989. Identification of temperature-sensitive mutants of vaccinia virus that are defective in conversion of concatemeric replicative intermediates to the mature linear DNA genome. J Virol **63:**2437-44.

Diamond, D. C., B. A. Jameson, J. Bonin, M. Kohara, S. Abe, H. Itoh, T. Komatsu, M. Arita, S. Kuge, A. Nomoto, and et al. 1985. Antigenic variation and resistance to neutralization in poliovirus type 1. Science **229:**1090-3.

Doedens, J. R., and K. Kirkegaard. 1995. Inhibition of cellular protein secretion by poliovirus proteins 2B and 3A. Embo J **14:**894-907.

Donnelly, M. L., D. Gani, M. Flint, S. Monaghan, and M. D. Ryan. 1997. The cleavage activities of aphthovirus and cardiovirus 2A proteins. J Gen Virol **78:**13-21.

Doublie, S., and T. Ellenberger. 1998. The mechanism of action of T7 DNA polymerase. Curr Opin Struct Biol **8:**704-12.

Doublie, S., S. Tabor, A. M. Long, C. C. Richardson, and T. Ellenberger. 1998. Crystal structure of a bacteriophage T7 DNA replication complex at 2.2 A resolution. Nature **391:**251-8.

Dougherty, W. G., and B. L. Semler. 1993. Expression of virus-encoded proteinases: functional and structural similarities with cellular enzymes. Microbiol Rev **57:**781-822.

Duechler, M., T. Skern, D. Blaas, B. Berger, W. Sommergruber, and E. Kuechler. 1989. Human rhinovirus serotype 2: in vitro synthesis of an infectious RNA. Virology **168:**159-61.

Duke, G. M., and A. C. Palmenberg. 1989. Cloning and synthesis of infectious cardiovirus RNAs containing short, discrete poly(C) tracts. J Virol **63:**1822-6.

Eckert, D., and M. Merchlinsky. 1999. Vaccinia virus-bacteriophage T7 expression vector for complementation analysis of late gene processes. J Gen Virol **80:**1463-9.

Filman, D. J., R. Syed, M. Chow, A. J. Macadam, P. D. Minor, and J. M. Hogle. 1989. Structural factors that control conformational transitions and serotype specificity in type 3 poliovirus. Embo J **8:**1567-79.

Flanegan, J. B., and D. Baltimore. 1977. Poliovirus-specific primer-dependent RNA polymerase able to copy poly(A). Proc Natl Acad Sci U S A **74:**3677-80.

Flanegan, J. B., and D. Baltimore. 1979. Poliovirus polyuridylic acid polymerase and RNA replicase have the same viral polypeptide. J Virol **29:**352-60.

Forss, S., K. Strebel, E. Beck, and H. Schaller. 1984. Nucleotide sequence and genome organization of foot-and-mouth disease virus. Nucleic Acids Res **12:**6587-601.

Fout, G. S., K. C. Medappa, J. E. Mapoles, and R. R. Rueckert. 1984. Radiochemical determination of polyamines in poliovirus and human rhinovirus 14. J Biol Chem **259:**3639-43.

Fu, J. L., S. Stein, L. Rosenstein, T. Bodwell, M. Routbort, B. L. Semler, and R. P. Roos. 1990. Neurovirulence determinants of genetically engineered Theiler viruses. Proc Natl Acad Sci U S A **87:**4125-9.

Gardner, L. P., K. A. Mookhtiar, and J. E. Coleman. 1997. Initiation, elongation, and processivity of carboxyl-terminal mutants of T7 RNA polymerase. Biochemistry **36:**2908-18.

Gerber, K., E. Wimmer, and A. V. Paul. 2001. Biochemical and genetic studies of the initiation of human rhinovirus 2 RNA replication: identification of a cis-replicating element in the coding sequence of 2A(pro). J Virol **75:**10979-90.

Gerber, K., E. Wimmer, and A. V. Paul. 2001. Biochemical and genetic studies of the initiation of human rhinovirus 2 RNA replication: purification and enzymatic analysis of the RNA-dependent RNA polymerase 3D(pol). J Virol **75:**10969-78.

Goodfellow, I., Y. Chaudhry, A. Richardson, J. Meredith, J. W. Almond, W. Barclay, and D. J. Evans. 2000. Identification of a cis-acting replication element within the poliovirus coding region. J Virol **74:**4590-600.

Gorbalenya, A. E., V. M. Blinov, A. P. Donchenko, and E. V. Koonin. 1989. An NTP-binding motif is the most conserved sequence in a highly diverged monophyletic group of proteins involved in positive strand RNA viral replication. J Mol Evol **28:**256-68.

Gorbalenya, A. E., A. P. Donchenko, V. M. Blinov, and E. V. Koonin. 1989. Cysteine proteases of positive strand RNA viruses and chymotrypsin-like serine proteases. A distinct protein superfamily with a common structural fold. FEBS Lett **243:**103-14.

Gorbalenya, A. E., and E. V. Koonin. 1989. Viral proteins containing the purine NTP-binding sequence pattern. Nucleic Acids Res **17:**8413-40.

Gorbalenya, A. E., E. V. Koonin, A. P. Donchenko, and V. M. Blinov. 1989. Two related superfamilies of putative helicases involved in replication, recombination, repair and expression of DNA and RNA genomes. Nucleic Acids Res **17:**4713-30.

Gorbalenya, A. E., E. V. Koonin, and M. M. Lai. 1991. Putative papain-related thiol proteases of positive-strand RNA viruses. Identification of rubi- and aphthovirus proteases and delineation of a novel conserved domain associated with proteases of rubi-, alpha- and coronaviruses. FEBS Lett **288:**201-5.

Gorbalenya, A. E., E. V. Koonin, and M. M. Lai. 1991. Putative papain-related thiol proteases of positive-strand RNA viruses. Identification of rubi- and aphthovirus proteases and delineation of a novel conserved domain associated with proteases of rubi-, alpha- and coronaviruses. FEBS Lett **288:**201-5.

Gosert, R., G. Dollenmaier, and M. Weitz. 1997. Identification of active-site residues in protease 3C of hepatitis A virus by site-directed mutagenesis. J Virol **71:**3062-8.

Greve, J. M., G. Davis, A. M. Meyer, C. P. Forte, S. C. Yost, C. W. Marlor, M. E. Kamarck, and A. McClelland. 1989. The major human rhinovirus receptor is ICAM-1. Cell **56:**839-47.

Hahn, H., and A. C. Palmenberg. 1996. Mutational analysis of the encephalomyocarditis virus primary cleavage. J Virol **70:**6870-5.

Harris, K. S., W. Xiang, L. Alexander, W. S. Lane, A. V. Paul, and E. Wimmer. 1994. Interaction of poliovirus polypeptide 3CDpro with the 5' and 3' termini of the poliovirus genome. Identification of viral and cellular cofactors needed for efficient binding. J Biol Chem **269:**27004-14.

Heinz, B. A., R. R. Rueckert, D. A. Shepard, F. J. Dutko, M. A. McKinlay, M. Fancher, M. G. Rossmann, J. Badger, and T. J. Smith. 1989. Genetic and molecular analyses of spontaneous mutants of human rhinovirus 14 that are resistant to an antiviral compound. J Virol **63:**2476-85.

Hellen, C. U., M. Facke, H. G. Krausslich, C. K. Lee, and E. Wimmer. 1991. Characterization of poliovirus 2A proteinase by mutational analysis: residues required for autocatalytic activity are essential for induction of cleavage of eukaryotic initiation factor 4F polypeptide p220. J Virol **65:**4226-31.

Hodgman, T. C. 1988. A new superfamily of replicative proteins. Nature **333:**22-3.

Hogle, J. M., M. Chow, and D. J. Filman. 1985. Three-dimensional structure of poliovirus at 2.9 A resolution. Science **229:**1358-65.

Hogle, J. M., M. Chow, and D. J. Filman. 1985. Three-dimensional structure of poliovirus at 2.9 A resolution. Science **229:**1358-65.

Jang, S. K., H. G. Krausslich, M. J. Nicklin, G. M. Duke, A. C. Palmenberg, and E. Wimmer. 1988. A segment of the 5' nontranslated region of encephalomyocarditis virus RNA directs internal entry of ribosomes during in vitro translation. J Virol **62:**2636-43.

Jeruzalmi, D., and T. A. Steitz. 1998. Structure of T7 RNA polymerase complexed to the transcriptional inhibitor T7 lysozyme. Embo J **17:**4101-13.

Johansen, L. K., and C. D. Morrow. 2000. Inherent instability of poliovirus genomes containing two internal ribosome entry site (IRES) elements supports a role for the IRES in encapsidation. J Virol **74:**8335-42.

Johansen, L. K., and C. D. Morrow. 2000. The RNA encompassing the internal ribosome entry site in the poliovirus 5' nontranslated region enhances the encapsidation of genomic RNA. Virology **273:**391-9.

Jore, J., B. De Geus, R. J. Jackson, P. H. Pouwels, and B. E. Enger-Valk. 1988. Poliovirus protein 3CD is the active protease for processing of the precursor protein P1 in vitro. J Gen Virol **69:**1627-36.

Kazachkov Yu, A., T. V. Chernovskaya, E. Siyanova, V. Svitkin Yu, T. Ugarova, and V. I. Agol. 1982. Leader polypeptides encoded in the 5'-region of the encephalomyocarditis virus genome. FEBS Lett **141:**153-6.

Kitamura, N., B. L. Semler, P. G. Rothberg, G. R. Larsen, C. J. Adler, A. J. Dorner, E. A. Emini, R. Hanecak, J. J. Lee, S. van der Werf, C. W. Anderson, and E. Wimmer. 1981. Primary structure, gene organization and polypeptide expression of poliovirus RNA. Nature **291:**547-53.

Kleina, L. G., and M. J. Grubman. 1992. Antiviral effects of a thiol protease inhibitor on foot-and-mouth disease virus. J Virol **66:**7168-75.

Koliais, S. I., and N. J. Dimmock. 1974. Rhinovirus RNA polymerase: products and kinetics of appearance in human diploid cells. J Virol **14:**1035-9.

Kong, I. C., J. S. Hubbard, and W. J. Jones. 1994. Metal-induced inhibition of anaerobic metabolism of volatile fatty acids and hydrogen. Appl Microbiol Biotechnol **42:**396-402.

Kozak, M. 1986. Influences of mRNA secondary structure on initiation by eukaryotic ribosomes. Proc Natl Acad Sci U S A **83:**2850-4.

Krausslich, H. G., C. Holscher, Q. Reuer, J. Harber, and E. Wimmer. 1990. Myristoylation of the poliovirus polyprotein is required for proteolytic processing of the capsid and for viral infectivity. J Virol **64:**2433-6.

Kuge, S., I. Saito, and A. Nomoto. 1986. Primary structure of poliovirus defective-interfering particle genomes and possible generation mechanisms of the particles. J Mol Biol **192:**473-87.

Kurtz, D. T., and C. F. Nicodemus. 1981. Cloning of alpha 2u globulin cDNA using a high efficiency technique for the cloning of trace messenger RNAs. Gene **13:**145-52.

Lama, J., and L. Carrasco. 1995. Mutations in the hydrophobic domain of poliovirus protein 3AB abrogate its permeabilizing activity. FEBS Lett **367:**5-11.

Lawson, M. A., B. Dasmahapatra, and B. L. Semler. 1990. Species-specific substrate interaction of picornavirus 3C proteinase suballelic exchange mutants. J Biol Chem **265:**15920-31.

Lawson, M. A., and B. L. Semler. 1990. Picornavirus protein processing--enzymes, substrates, and genetic regulation. Curr Top Microbiol Immunol **161:**49-87.

Lawson, T. G., L. L. Smith, A. C. Palmenberg, and R. E. Thach. 1989. Inducible expression of encephalomyocarditis virus 3C protease activity in stably transformed mouse cell lines. J Virol **63:**5013-22.

Lee, Y. F., A. Nomoto, B. M. Detjen, and E. Wimmer. 1977. A protein covalently linked to poliovirus genome RNA. Proc Natl Acad Sci U S A **74:**59-63.

Lentz, K. N., A. D. Smith, S. C. Geisler, S. Cox, P. Buontempo, A. Skelton, J. DeMartino, E. Rozhon, J. Schwartz, V. Girijavallabhan, J. O'Connell, and E. Arnold. 1997. Structure of poliovirus type 2 Lansing complexed with antiviral agent SCH48973: comparison of the structural and biological properties of three poliovirus serotypes. Structure **5:**961-78.

Li, F., G. F. Browning, M. J. Studdert, and B. S. Crabb. 1996. Equine rhinovirus 1 is more closely related to foot-and-mouth disease virus than to other picornaviruses. Proc Natl Acad Sci U S A **93:**990-5.

Lobert, P. E., N. Escriou, J. Ruelle, and T. Michiels. 1999. A coding RNA sequence acts as a replication signal in cardioviruses. Proc Natl Acad Sci U S A **96:**11560-5.

Lykke-Andersen, J., and J. Christiansen. 1998. The C-terminal carboxy group of T7 RNA polymerase ensures efficient magnesium ion-dependent catalysis. Nucleic Acids Res **26:**5630-5.

Marc, D., G. Drugeon, A. L. Haenni, M. Girard, and S. van der Werf. 1989. Role of myristoylation of poliovirus capsid protein VP4 as determined by site-directed mutagenesis of its N-terminal sequence. Embo J **8:**2661-8.

Marc, D., M. Girard, and S. van der Werf. 1991. A Gly1 to Ala substitution in poliovirus capsid protein VP0 blocks its myristoylation and prevents viral assembly. J Gen Virol **72:**1151-7.

Marc, D., G. Masson, M. Girard, and S. van der Werf. 1990. Lack of myristoylation of poliovirus capsid polypeptide VP0 prevents the formation of virions or results in the assembly of noninfectious virus particles. J Virol **64:**4099-107.

Matthews, D. A., W. W. Smith, R. A. Ferre, B. Condon, G. Budahazi, W. Sisson, J. E. Villafranca, C. A. Janson, H. E. McElroy, C. L. Gribskov, and et al. 1994. Structure of human rhinovirus 3C protease reveals a trypsin-like polypeptide fold, RNA-binding site, and means for cleaving precursor polyprotein. Cell **77:**761-71.

McKnight, K. L., and S. M. Lemon. 1996. Capsid coding sequence is required for efficient replication of human rhinovirus 14 RNA. J Virol **70:**1941-52.

McKnight, K. L., and S. M. Lemon. 1998. The rhinovirus type 14 genome contains an internally located RNA structure that is required for viral replication. Rna **4:**1569-84.

Meerovitch, K., and N. Sonenberg. 1993. Internal initiation of Picornavirus RNA translation. Seminars in Virology **4**: 217-227.

Medina, J., G. Hueros, and P. Carbonero. 1993. Cloning of cDNA, expression, and chromosomal location of genes encoding the three types of subunits of the barley tetrameric inhibitor of insect alpha-amylase. Plant Mol Biol **23:**535-42.

Medina, M., E. Domingo, J. K. Brangwyn, and G. J. Belsham. 1993. The two species of the foot-and-mouth disease virus leader protein, expressed individually, exhibit the same activities. Virology **194:**355-9.

Melnick, J. L., V. I. Agol, H. L. Bachrach, F. Brown, P. D. Cooper, W. Fiers, S. Gard, J. H. Gear, Y. Ghendon, L. Kasza, M. LaPlaca, B. Mandel, S. McGregor, S. B. Mohanty, G. Plummer, R. R. Rueckert, F. L. Schaffer, I. Tagaya, D. A. Tyrrell, M. Voroshilova, and H. A. Wenner. 1974. Picornaviridae. Intervirology **4:**303-16.

Merchlinsky, M., and B. Moss. 1989. Nucleotide sequence required for resolution of the concatemer junction of vaccinia virus DNA. J Virol **63:**4354-61.

Merchlinsky, M., and B. Moss. 1989. Resolution of vaccinia virus DNA concatemer junctions requires late-gene expression. J Virol **63:**1595-603.

Minor, P. D., D. M. Evans, M. Ferguson, G. C. Schild, G. Westrop, and J. W. Almond. 1985. Principal and subsidiary antigenic sites of VP1 involved in the neutralization of poliovirus type 3. J Gen Virol **66:**1159-65.

Minor, P. D., M. Ferguson, D. M. Evans, J. W. Almond, and J. P. Icenogle. 1986. Antigenic structure of polioviruses of serotypes 1, 2 and 3. J Gen Virol **67:**1283-91.

Minor, P. D., M. Ferguson, D. M. Evans, J. W. Almond, and J. P. Icenogle. 1986. Antigenic structure of polioviruses of serotypes 1, 2 and 3. J Gen Virol **67:**1283-91.

Minor, P. D., M. Ferguson, K. Katrak, D. Wood, A. John, J. Howlett, G. Dunn, K. Burke, and J. W. Almond. 1990. Antigenic structure of chimeras of type 1 and type 3 poliovirus involving antigenic site 1. J Gen Virol **71:**2543-51.

Minor, P. D., G. C. Schild, J. Bootman, D. M. Evans, M. Ferguson, P. Reeve, M. Spitz, G. Stanway, A. J. Cann, R. Hauptmann, L. D. Clarke, R. C. Mountford, and J. W. Almond. 1983. Location and primary structure of a major antigenic site for poliovirus neutralization. Nature **301:**674-9.

Moscufo, N., and M. Chow. 1992. Myristate-protein interactions in poliovirus: interactions of VP4 threonine 28 contribute to the structural conformation of assembly intermediates and the stability of assembled virions. J Virol **66:**6849-57.

Moscufo, N., J. Simons, and M. Chow. 1991. Myristoylation is important at multiple stages in poliovirus assembly. J Virol **65:**2372-80.

Moss, B. 1996. Genetically engineered poxviruses for recombinant gene expression, vaccination, and safety. Proc Natl Acad Sci U S A **93:**11341-8.

Moss, G. W., J. Marshall, and E. Moczydlowski. 1996. Hypothesis for a serine proteinase-like domain at the COOH terminus of Slowpoke calcium-activated potassium channels. J Gen Physiol **108:**473-84.

Moss, G. W., J. Marshall, M. Morabito, J. R. Howe, and E. Moczydlowski. 1996. An evolutionarily conserved binding site for serine proteinase inhibitors in large conductance calcium-activated potassium channels. Biochemistry **35:**16024-35.

Nitayaphan, S., D. Omilianowski, M. M. Toth, G. D. Parks, R. R. Rueckert, A. C. Palmenberg, and R. P. Roos. 1986. Relationship of Theiler's murine encephalomyelitis viruses to the cardiovirus genus of picornaviruses. Intervirology **26:**140-8.

Nomoto, A., N. Kitamura, F. Golini, and E. Wimmer. 1977. The 5'-terminal structures of poliovirion RNA and poliovirus mRNA differ only in the genome-linked protein VPg. Proc Natl Acad Sci U S A **74:**5345-9.

Novak, J. E., and K. Kirkegaard. 1991. Improved method for detecting poliovirus negative strands used to demonstrate specificity of positive-strand encapsidation and the ratio of positive to negative strands in infected cells. J Virol **65:**3384-7.

Novak, J. E., and K. Kirkegaard. 1994. Coupling between genome translation and replication in an RNA virus. Genes Dev **8:**1726-37.

Nugent, C. I., K. L. Johnson, P. Sarnow, and K. Kirkegaard. 1999. Functional coupling between replication and packaging of poliovirus replicon RNA. J Virol **73:**427-35.

Page, P. L. 1988. Preventing transfusion of infectious blood negative for human immunodeficiency virus antibodies (anti-HIV). Ann Intern Med **109:**436.

Palmenberg, A. C. 1987. Picornaviral processing: some new ideas. J Cell Biochem **33:**191-8.

Palmenberg, A. C. 1990. Proteolytic processing of picornaviral polyprotein. Annu Rev Microbiol **44:**603-23.

Palmenberg, A. C., E. M. Kirby, M. R. Janda, N. L. Drake, G. M. Duke, K. F. Potratz, and M. S. Collett. 1984. The nucleotide and deduced amino acid sequences of the encephalomyocarditis viral polyprotein coding region. Nucleic Acids Res **12:**2969-85.

Parks, G. D., J. C. Baker, and A. C. Palmenberg. 1989. Proteolytic cleavage of encephalomyocarditis virus capsid region substrates by precursors to the 3C enzyme. J Virol **63:**1054-8.

Parks, G. D., J. C. Baker, and A. C. Palmenberg. 1989. Proteolytic cleavage of encephalomyocarditis virus capsid region substrates by precursors to the 3C enzyme. J Virol **63:**1054-8.

Paul, A. V., J. Mugavero, A. Molla, and E. Wimmer. 1998. Internal ribosomal entry site scanning of the poliovirus polyprotein: implications for proteolytic processing. Virology **250:**241-53.

Paul, A. V., E. Rieder, D. W. Kim, J. H. van Boom, and E. Wimmer. 2000. Identification of an RNA hairpin in poliovirus RNA that serves as the primary template in the in vitro uridylylation of VPg. J Virol **74:**10359-70.

Paul, A. V., J. H. van Boom, D. Filippov, and E. Wimmer. 1998. Protein-primed RNA synthesis by purified poliovirus RNA polymerase. Nature **393:**280-4.

Pelletier, J., M. E. Flynn, G. Kaplan, V. Racaniello, and N. Sonenberg. 1988. Mutational analysis of upstream AUG codons of poliovirus RNA. J Virol **62:**4486-92.

Percy, N., W. S. Barclay, M. Sullivan, and J. W. Almond. 1992. A poliovirus replicon containing the chloramphenicol acetyltransferase gene can be used to study the replication and encapsidation of poliovirus RNA. J Virol **66:**5040-6.

Percy, N., G. J. Belsham, J. K. Brangwyn, M. Sullivan, D. M. Stone, and J. W. Almond. 1992. Intracellular modifications induced by poliovirus reduce the requirement for structural motifs in the 5' noncoding region of the genome involved in internal initiation of protein synthesis. J Virol **66:**1695-701.

Peterson, J. D., S. D. Miller, and C. Waltenbaugh. 1990. Rapid biotin-avidin method for quantitation of antiviral antibody isotypes. J Virol Methods **27:**189-201.

Peterson, J. D., C. Waltenbaugh, and S. D. Miller. 1992. IgG subclass responses to Theiler's murine encephalomyelitis virus infection and immunization suggest a dominant role for Th1 cells in susceptible mouse strains. Immunology **75:**652-8.

Pevear, D. C., M. J. Fancher, P. J. Felock, M. G. Rossmann, M. S. Miller, G. Diana, A. M. Treasurywala, M. A. McKinlay, and F. J. Dutko. 1989. Conformational change in the floor of the human rhinovirus canyon blocks adsorption to HeLa cell receptors. J Virol **63:**2002-7.

Piccone, M. E., E. Rieder, P. W. Mason, and M. J. Grubman. 1995. The foot-and-mouth disease virus leader proteinase gene is not required for viral replication. J Virol **69:**5376-82.

Piccone, M. E., S. Sira, M. Zellner, and M. J. Grubman. 1995. Expression in Escherichia coli and purification of biologically active L proteinase of foot-and-mouth disease virus. Virus Res **35:**263-75.

Piccone, M. E., M. Zellner, T. F. Kumosinski, P. W. Mason, and M. J. Grubman. 1995. Identification of the active-site residues of the L proteinase of foot-and-mouth disease virus. J Virol **69:**4950-6.

Pilipenko, E. V., K. V. Poperechny, S. V. Maslova, W. J. Melchers, H. J. Slot, and V. I. Agol. 1996. Cis-element, oriR, involved in the initiation of (-) strand poliovirus RNA: a quasi-globular multi-domain RNA structure maintained by tertiary ('kissing') interactions. Embo J **15:**5428-36.

Pilipenko, E. V., K. V. Poperechny, S. V. Maslova, W. J. Melchers, H. J. Slot, and V. I. Agol. 1996. Cis-element, oriR, involved in the initiation of (-) strand poliovirus RNA: a quasi-globular multi-domain RNA structure maintained by tertiary ('kissing') interactions. Embo J **15:**5428-36.

Porter, A. G., P. Fellner, D. N. Black, D. J. Rowlands, T. J. Harris, and F. Brown. 1978. 3'-Terminal nucleotide sequences in the genome RNA of picornaviruses. Nature **276:**298-301.

Porter, D. C., D. C. Ansardi, J. Wang, S. McPherson, Z. Moldoveanu, and C. D. Morrow. 1998. Demonstration of the specificity of poliovirus encapsidation using a novel replicon which encodes enzymatically active firefly luciferase. Virology **243:**1-11.

Racaniello, V. R., and D. Baltimore. 1981. Molecular cloning of poliovirus cDNA and determination of the complete nucleotide sequence of the viral genome. Proc Natl Acad Sci U S A **78:**4887-91.

Rieder, E., A. V. Paul, D. W. Kim, J. H. van Boom, and E. Wimmer. 2000. Genetic and biochemical studies of poliovirus cis-acting replication element cre in relation to VPg uridylylation. J Virol **74:**10371-80.

Roberts, P. J., and G. J. Belsham. 1995. Identification of critical amino acids within the foot-and-mouth disease virus leader protein, a cysteine protease. Virology **213:**140-6.

Robertson, B. H., M. J. Grubman, G. N. Weddell, D. M. Moore, J. D. Welsh, T. Fischer, D. J. Dowbenko, D. G. Yansura, B. Small, and D. G. Kleid. 1985. Nucleotide and amino acid sequence coding for polypeptides of foot-and-mouth disease virus type A12. J Virol **54:**651-60.

Rodriguez, P. L., and L. Carrasco. 1995. Poliovirus protein 2C contains two regions involved in RNA binding activity. J Biol Chem **270:**10105-12.

Rodriguez, P. L., and L. Carrasco. 1995. Improved factor Xa cleavage of fusion proteins containing maltose binding protein. Biotechniques **18:**238, 241-3.

Rossmann, M. G., E. Arnold, J. W. Erickson, E. A. Frankenberger, J. P. Griffith, H. J. Hecht, J. E. Johnson, G. Kamer, M. Luo, A. G. Mosser, and et al. 1985. Structure of a human common cold virus and functional relationship to other picornaviruses. Nature **317:**145-53.

Rossmann, M. G., and J. E. Johnson. 1989. Icosahedral RNA virus structure. Annu Rev Biochem **58:**533-73.

Rothberg, P. G., T. J. Harris, A. Nomoto, and E. Wimmer. 1978. O4-(5'-uridylyl)tyrosine is the bond between the genome-linked protein and the RNA of poliovirus. Proc Natl Acad Sci U S A **75:**4868-72.

Rueckert, R.R. 1996. Picornaviridae, the viruses and their replication. In "Virology" (B.N. Fields, D.M. Knipe and P.M. Howley, Eds.), Vol. 3rd edition, pp. 609-654. Lippincott-Raven, Philadelphia.

Ryan, M. D., and M. Flint. 1997. Virus-encoded proteinases of the picornavirus super-group. J Gen Virol **78:**699-723.

Sarnow, P. 1989. Role of 3'-end sequences in infectivity of poliovirus transcripts made in vitro. J Virol **63:**467-70.

Sarnow, P., H. D. Bernstein, and D. Baltimore. 1986. A poliovirus temperature-sensitive RNA synthesis mutant located in a noncoding region of the genome. Proc Natl Acad Sci U S A **83:**571-5.

Semler, B. L., C. W. Anderson, R. Hanecak, L. F. Dorner, and E. Wimmer. 1982. A membrane-associated precursor to poliovirus VPg identified by immunoprecipitation with antibodies directed against a synthetic heptapeptide. Cell **28:**405-12.

Sherry, B., A. G. Mosser, R. J. Colonno, and R. R. Rueckert. 1986. Use of monoclonal antibodies to identify four neutralization immunogens on a common cold picornavirus, human rhinovirus 14. J Virol **57:**246-57.

Sherry, B., and R. Rueckert. 1985. Evidence for at least two dominant neutralization antigens on human rhinovirus 14. J Virol **53:**137-43.

Shiroki, K., T. Ishii, T. Aoki, M. Kobashi, S. Ohka, and A. Nomoto. 1995. A new cis-acting element for RNA replication within the 5' noncoding region of poliovirus type 1 RNA. J Virol **69:**6825-32.

Skern, T., I. Fita, and A. Guarne. 1998. A structural model of picornavirus leader proteinases based on papain and bleomycin hydrolase. J Gen Virol **79:**301-7.

Sommergruber, W., H. Ahorn, H. Klump, J. Seipelt, A. Zoephel, F. Fessl, E. Krystek, D. Blaas, E. Kuechler, H. D. Liebig, and et al. 1994. 2A proteinases of coxsackie- and rhinovirus cleave peptides derived from eIF-4 gamma via a common recognition motif. Virology **198:**741-5.

Sommergruber, W., G. Casari, F. Fessl, J. Seipelt, and T. Skern. 1994. The 2A proteinase of human rhinovirus is a zinc containing enzyme. Virology **204:**815-8.

Sommergruber, W., M. Zorn, D. Blaas, F. Fessl, P. Volkmann, I. Maurer-Fogy, P. Pallai, V. Merluzzi, M. Matteo, T. Skern, and et al. 1989. Polypeptide 2A of human rhinovirus type 2: identification as a protease and characterization by mutational analysis. Virology **169:**68-77.

Sousa, R., Y. J. Chung, J. P. Rose, and B. C. Wang. 1993. Crystal structure of bacteriophage T7 RNA polymerase at 3.3 A resolution. Nature **364:**593-9.

Spector, D. H., L. Villa-Komaroff, and D. Baltimore. 1975. Studies on the function of polyadenylic acid on poliovirus RNA. Cell **6:**41-4.

Stewart, S.R., and B.L. Semler. 1997. RNA determinants of Picornavirus cap-independent translation initiation. Seminars in Virology **8:** 242-255.

Strebel, K., and E. Beck. 1986. A second protease of foot-and-mouth disease virus. J Virol **58:**893-9.

Strebel, K., E. Beck, K. Strohmaier, and H. Schaller. 1986. Characterization of foot-and-mouth disease virus gene products with antisera against bacterially synthesized fusion proteins. J Virol **57:**983-91.

Todd, S., J. S. Towner, D. M. Brown, and B. L. Semler. 1997. Replication-competent picornaviruses with complete genomic RNA 3' noncoding region deletions. J Virol **71:**8868-74.

Tower, J., and B. Sollner-Webb. 1988. Polymerase III transcription factor B activity is reduced in extracts of growth-restricted cells. Mol Cell Biol **8:**1001-5.

Toyoda, H., M. J. Nicklin, M. G. Murray, C. W. Anderson, J. J. Dunn, F. W. Studier, and E. Wimmer. 1986. A second virus-encoded proteinase involved in proteolytic processing of poliovirus polyprotein. Cell **45:**761-70.

Tuschall, D. M., E. Hiebert, and J. B. Flanegan. 1982. Poliovirus RNA-dependent RNA polymerase synthesizes full-length copies of poliovirion RNA, cellular mRNA, and several plant virus RNAs in vitro. J Virol **44:**209-16.

Usherwood, E. J., I. C. Johnston, L. J. Lovelidge, P. Tonks, and A. A. Nash. 1995. Lymphocyte recognition elements on the VP1 protein of Theiler's virus. Immunology **85:**190-7.

Van Dyke, T. A., and J. B. Flanegan. 1980. Identification of poliovirus polypeptide P63 as a soluble RNA-dependent RNA polymerase. J Virol **35:**732-40.

van Kuppeveld, F. J., J. G. Hoenderop, R. L. Smeets, P. H. Willems, H. B. Dijkman, J. M. Galama, and W. J. Melchers. 1997. Coxsackievirus protein 2B modifies endoplasmic reticulum membrane and plasma membrane permeability and facilitates virus release. Embo J **16:**3519-32.

van Kuppeveld, F. J., P. J. van den Hurk, W. van der Vliet, J. M. Galama, and W. J. Melchers. 1997. Chimeric coxsackie B3 virus genomes that express hybrid coxsackievirus-poliovirus 2B proteins: functional dissection of structural domains involved in RNA replication. J Gen Virol **78:**1833-40.

van Kuppeveld, F. J., A. M. van Horssen, and G. J. Martens. 1997. Intracellular transport, sorting, and proteolytic processing of regulated secretory proteins does not require protein sulfation. Mol Cell Endocrinol **136:**29-35.

Voss, J., W. L. Hubbell, and H. R. Kaback. 1995. Distance determination in proteins using designed metal ion binding sites and site-directed spin labeling: application to the lactose permease of Escherichia coli. Proc Natl Acad Sci U S A **92:**12300-3.

Voss, J., L. Salwinski, H. R. Kaback, and W. L. Hubbell. 1995. A method for distance determination in proteins using a designed metal ion binding site and site-directed spin labeling: evaluation with T4 lysozyme. Proc Natl Acad Sci U S A **92:**12295-9.

Voss, T., R. Meyer, and W. Sommergruber. 1995. Spectroscopic characterization of rhinoviral protease 2A: Zn is essential for the structural integrity. Protein Sci **4:**2526-31.

Wiegers, K., and R. Dernick. 1992. Molecular basis of antigenic structures of poliovirus: implications for their evolution during morphogenesis. J Virol **66:**4597-600.

Wiegers, K., H. Uhlig, and R. Dernick. 1988. Evidence for a complex structure of neutralization antigenic site I of poliovirus type 1 Mahoney. J Virol **62:**1845-8.

Wiegers, K. J., K. Wetz, and R. Dernick. 1990. Molecular basis for linkage of a continuous and discontinuous neutralization epitope on the structural polypeptide VP2 of poliovirus type 1. J Virol **64:**1283-9.

Woody, A. Y., S. S. Eaton, P. A. Osumi-Davis, and R. W. Woody. 1996. Asp537 and Asp812 in bacteriophage T7 RNA polymerase as metal ion-binding sites studied by EPR, flow-dialysis, and transcription. Biochemistry **35:**144-52.

Wutz, G., H. Auer, N. Nowotny, B. Grosse, T. Skern, and E. Kuechler. 1996. Equine rhinovirus serotypes 1 and 2: relationship to each other and to aphthoviruses and cardioviruses. J Gen Virol **77:**1719-30.

Xiang, W., A. Cuconati, A. V. Paul, X. Cao, and E. Wimmer. 1995. Molecular dissection of the multifunctional poliovirus RNA-binding protein 3AB. Rna **1:**892-904.

Yin, F. H., and E. Knight, Jr. 1972. In vivo and in vitro synthesis of human rhinovirus type 2 ribonucleic acid. J Virol **10:**93-8.

Yogo, Y., M. H. Teng, and E. Wimmer. 1974. Poly(U) in poliovirus minus RNA is 5'-terminal. Biochem Biophys Res Commun **61:**1101-9.

Yogo, Y., and E. Wimmer. 1975. Sequence studies of poliovirus RNA. III. Polyuridylic acid and polyadenylic acid as components of the purified poliovirus replicative intermediate. J Mol Biol **92:**467-77.

Ypma-Wong, M. F., P. G. Dewalt, V. H. Johnson, J. G. Lamb, and B. L. Semler. 1988. Protein 3CD is the major poliovirus proteinase responsible for cleavage of the P1 capsid precursor. Virology **166:**265-70.

Ypma-Wong, M. F., D. J. Filman, J. M. Hogle, and B. L. Semler. 1988. Structural domains of the poliovirus polyprotein are major determinants for proteolytic cleavage at Gln-Gly pairs. J Biol Chem **263:**17846-56.

Yu, S. F., and R. E. Lloyd. 1991. Identification of essential amino acid residues in the functional activity of poliovirus 2A protease. Virology **182:**615-25.

Yu, S. F., and R. E. Lloyd. 1992. Characterization of the roles of conserved cysteine and histidine residues in poliovirus 2A protease. Virology **186:**725-35.

Zoll, J., J. M. Galama, F. J. van Kuppeveld, and W. J. Melchers. 1996. Mengovirus leader is involved in the inhibition of host cell protein synthesis. J Virol **70:**4948-52.

Zoll, J., F. J. van Kuppeveld, J. M. Galama, and W. J. Melchers. 1998. Genetic analysis of mengovirus protein 2A: its function in polyprotein processing and virus reproduction. J Gen Virol **79:**17-25.